Modeling of

Modern Excitation Control Systems

by

Conrado Orta, Jr.

B.E.(E.E.), Manhattan College
(1978)

SUBMITTED IN PARTIAL FULFILLMENT
OF THE REQUIREMENTS FOR THE
DEGREE OF

MASTER OF SCIENCE

at the

MASSACHUSETTS INSTITUTE OF TECHNOLOGY

February, 1980

Signature of Author Signature redacted
Department of Electrical Engineering
February, 1980

Certified by Signature redacted
Thesis Supervisor

Accepted by Signature redacted
Chairman, Departmental Committee on Graduate Students

Modeling of

Modern Excitation Control Systems

by

Conrado Orta, Jr.

Submitted to the Department of Electrical Engineering on February, 1980 in Partial Fullfillment of the Requirements for the Degree of Master of Science in Electrical Engineering

ABSTRACT

Excitation control systems are an important source of dynamics in power systems so their modeling is critical for the understanding of power system behavior and control. Modeling techniques are developed here for exciter-alternators with output rectifiers. These are feedback systems of nonlinear characteristics. The modeling techniques described here are specifically applied to the Alterrex* excitation control system. The mathematical model developed for this system is of such a nature as to include some of the effects neglected in past models of this device. The form of this model has been chosen so that there is a correspondence between the model structure and the actual device and so that model parameters can be obtained from a knowledge of the parameters and settings of the physical system. The model developed in this thesis is complex and represents the properties of the Alterrex excitation control system in considerable detail. The degree of complexity is greater than that which would normally be considered necessary for a transient or dynamic stability study. However, the object of this thesis is to develop an accurate model directly from the physical device. This model can then be used to study Alterrex performance in detail or as a basis for exploring simpler, lower order models.

Thesis Supervisor: Dr. Stephen D. Umans
Title: Research Associate

---

* Registered trademark of the General Electric Co.

Acknowledgement

First I would like to thank Dr. S. D. Umans for suggesting the research topic. Many of the ideas discussed in this thesis have arisen out of discussions with him and without his criticisms and suggestions this thesis would be of greatly reduced value. In addition I would also like to thank the members of the Electric Power System Engineering Laboratory at the Massachusetts Institute of Technology for their willingness to help and make useful suggestions. I am particularly grateful to Karl Wyatt, Patrick Usoro and Art Radun.

I am grateful to the Bell Telephone Laboratories for allowing me to participate in the One Year On Campus program at the Massachusetts Institute of Technology. I am also grateful to the American Electric Power Co. for providing the necessary data and information for this thesis.

To My Parents

TABLE OF CONTENTS

Page

List of Figures

Figures

Figures

List of Tables

Chapter I: INTRODUCTION

1.1 Basic Background

1.1.1 Power System Stability and Excitation Control Systems

In a world more dependent on electric energy than ever, the reliability of power systems has become one of the major concerns of utilities. As far as reliability is concerned the stability of electric power systems is the most important criterion since a system cannot operate effectively under unstable conditions. In particular the behavior of the excitation control system can aid stability by regulating the generator terminal voltage as well as other parameters of the system. With the arrival of new technologies, excitation control systems have become faster and more reliable, thus improving the stability of the system. One type of excitation control system in current use employs an exciter-alternator with output rectifier . Modeling of the excitation control system is of vital importance for the understanding of the stability problem in a power system.

Stability in a power system is determined by its transient and dynamic characteristics. Dynamic characteristics describe the behavior of the power system during normal operation. In this mode of operation small changes in load change the operating conditions of the generating unit. Transient characteristics describe the behavior of a power system after a major change has occurred. Major changes

or disturbances occur because of faults in the lines and opening of breakers. These abrupt changes create new conditions in the power system to which it must adjust. Instability can be observed in a power system by observing the phase angles of the generators. Oscillations of these angles or the loss of synchronism in an extreme case is the sign of instability. Also instability can be observed by observing the abnormal behavior of other parameters such as voltages, currents or output power.

The generating unit serves to transform the fuel into useful electric energy. The three fundamental parts of a generating system are the boiler, the turbine and the generator with their respective control mechanisms (see Figure 1.1). The excitation control system is designed to control the terminal voltage of the main generator. This is achieved because the excitation control system provides power to the field winding of the main generator.

A simplified picture of an excitation control system is given in Figure 1.2. The regulator is designed to regulate terminal voltage. Regulation of terminal voltage is not sufficient to guarantee stability. In fact, for very high values of regulator gain the regulator might actually result in instability. This instability could occur in the dynamic range of operation when only small disturbances are involved and also as a result of a transient disturbance following which growing oscillation might occur as the result of the regulator effect. In order to avoid this problem, lower regulator gain might be

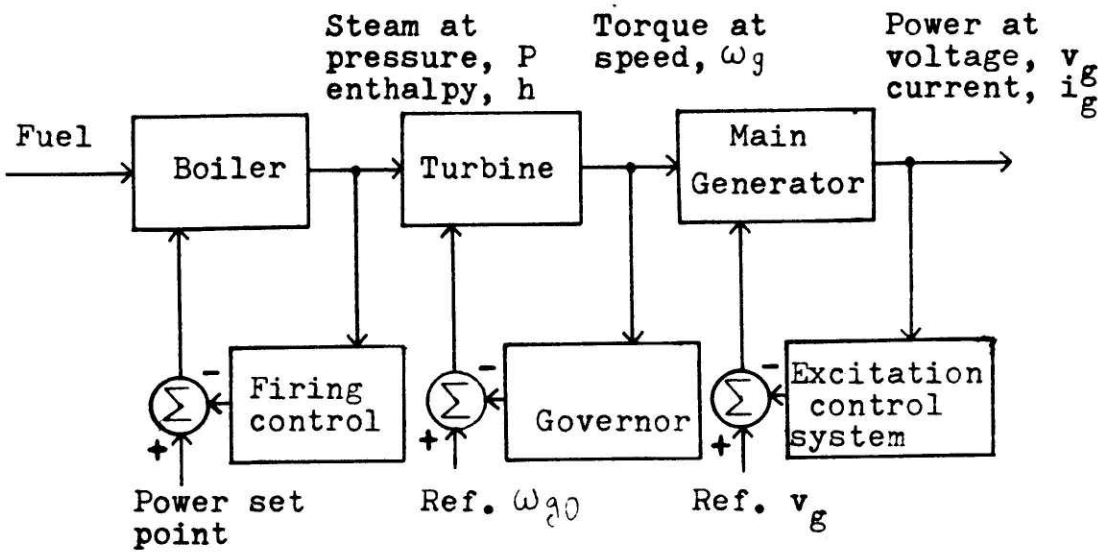

Figure 1.1 Block diagram of generating unit

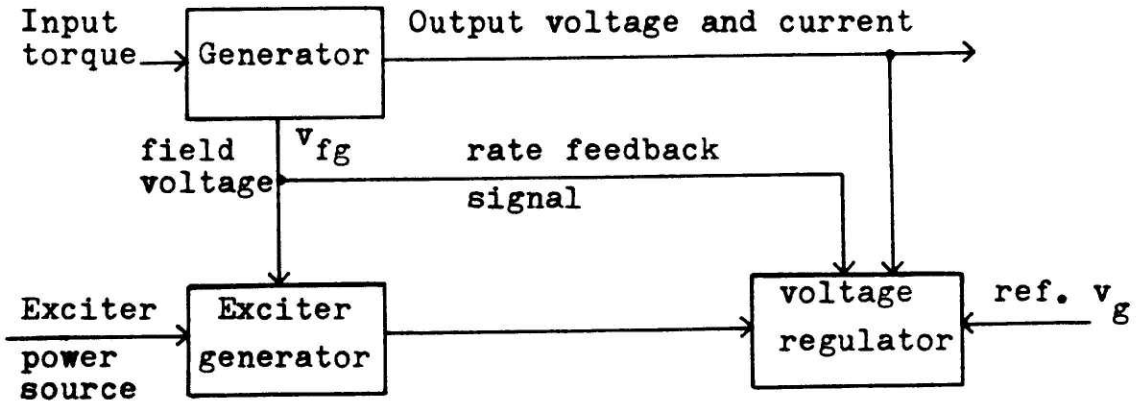

Figure 1.2 Block diagram of excitation control system

used but also the use of additional regulating signals is a good measure. A signal often used is the exciter generator output voltage in order to introduce a rate feedback signal in the system. This signal is indicated as "rate feedback signal" on Figure 1.2. In general, we want a fast response for the regulator system since this is useful when large disturbances are involved and it becomes necessary to react against the decay of flux linkage by increasing the field current in the main generator.

In order to find out how a power system will respond in steady-state or transient conditions, computer simulations are done. Since the behavior of the generating unit against the power system and against other generating units is the principal factor that determines stable operation, modeling of this piece of the power system is of great interest for stability study purposes. More detailed information on this subject can be found in Reference [1] and [2].

1.1.2 I.E.E.E. Models for Excitation Systems

Present day models [3] of excitation control systems were developed assuming very simple structures for the systems. Hence, when applied to complex modern excitation control systems they may become a black-box type of representation with little correlation between the parameters of the model and the actual physical device. This lack of similarity manifests itself in the difficulty of finding

parameters for the model appropriate for representing the actual system. These models are given in Reference [3].

A typical model proposed by the I.E.E.E. committee in Reference [3] is given in Figure 1.3. This is the Type I model which is used to model excitation control systems such as the Alterrex excitation control system. The block diagram with time constant T_r represents the regulator's input filter. The main regulator transfer function is represented as a gain K_a and a time constant T_a. Following this, the maximum and minimum limits of the regulator are imposed so that large input error signals cannot produce a regulator output which exceeds practical limits. The exciter-alternator is modeled by the time constant T_e, the constant K_e and the feedback loop S_e which represents the exciter's magnetic saturation. The major loop damping is provided by the feedback transfer function with scale factor K_f and time constant T_f from exciter output E_{fd} to the first summing point. The signal coming from the power system stabilizer into the regulator would be considered under the heading of "other signals" which are added to one of the summing points. A power stabilizing signal is usually derived from rotor speed. One problem with this model is that there is no clear correlation between the parameters of the model and the parameters of the real system. This is particularly true for the exciter-alternator. There are also other effects that this model doesn't represent.

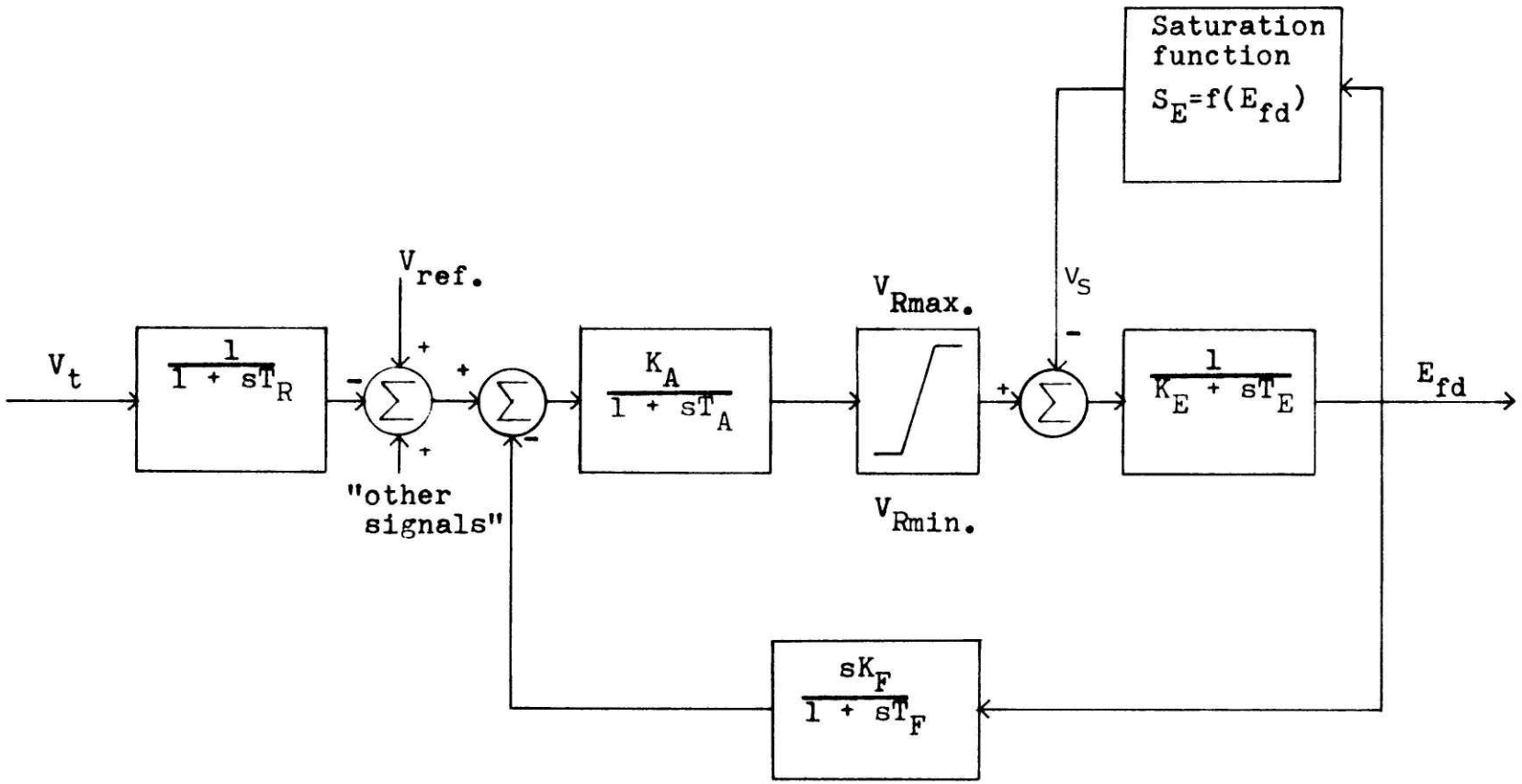

Figure 1.3 Block diagram of IEEE type I model

1.2 Purpose of this Thesis

1.2.1 The New Approach

The purpose of this work was to develop new modeling techniques for modern excitation control systems. In developing these models extremely simplified functional black-box types of relationships were avoided in favor of a representation based on the internal physical properties of the devices in question. Thus, the end result was a model in which a correspondence can be estabished between the important parameters of the real system and those of the model.

Creating a generalized technique for every possible excitation control system would had meant a monumental if not impossible job. The approach chosen in this thesis is to concentrate on the modeling of a specific system: The Alterrex* excitation control system. The Alterrex excitation control system possesses the characteristic typical to most modern excitation control systems. Therefore the techniques developed here could be utilized with modifications for other modern excitation control systems.

Modern excitation control system is understood in this thesis to mean systems that provide power to the field winding of the main generator by means of an ac power source with output

---

* Registered trademark of the General Electric Co.

rectifier. Sometimes the ac power source is obtained from the same output voltage of the main generator as in the case of the Generrex* system.

The model developed in this thesis is complex and represents the properties of the Alterrex excitation control system in considerable detail. The degree of complexity is greater than that which would normally be considered necessary for a transient or dynamic stability study. However, the object of this thesis is to develop an accurate model directly from the physical device. This model can then be used to study Alterrex performance in detail or as a basis for exploring simpler, lower order models.

1.2.2 The Alterrex Excitation Control System

The Alterrex excitation control system is shown schematically in Figure 1.4. Notice that the output of the exciter-alternator is rectified by the output rectifier feeding the field winding of the main generator. The exciter-alternator itself is self-excited by using a potential transformer connected from its output voltage to an SCR controlled 3 phase rectifier. There is also another excitation loop consisting of the current transformers with the current boost bridge. During normal conditions the power input to the field winding comes from the SCR bridge and the diode bridge is forward biased

---

* Registered trademark of the General Electric Co.

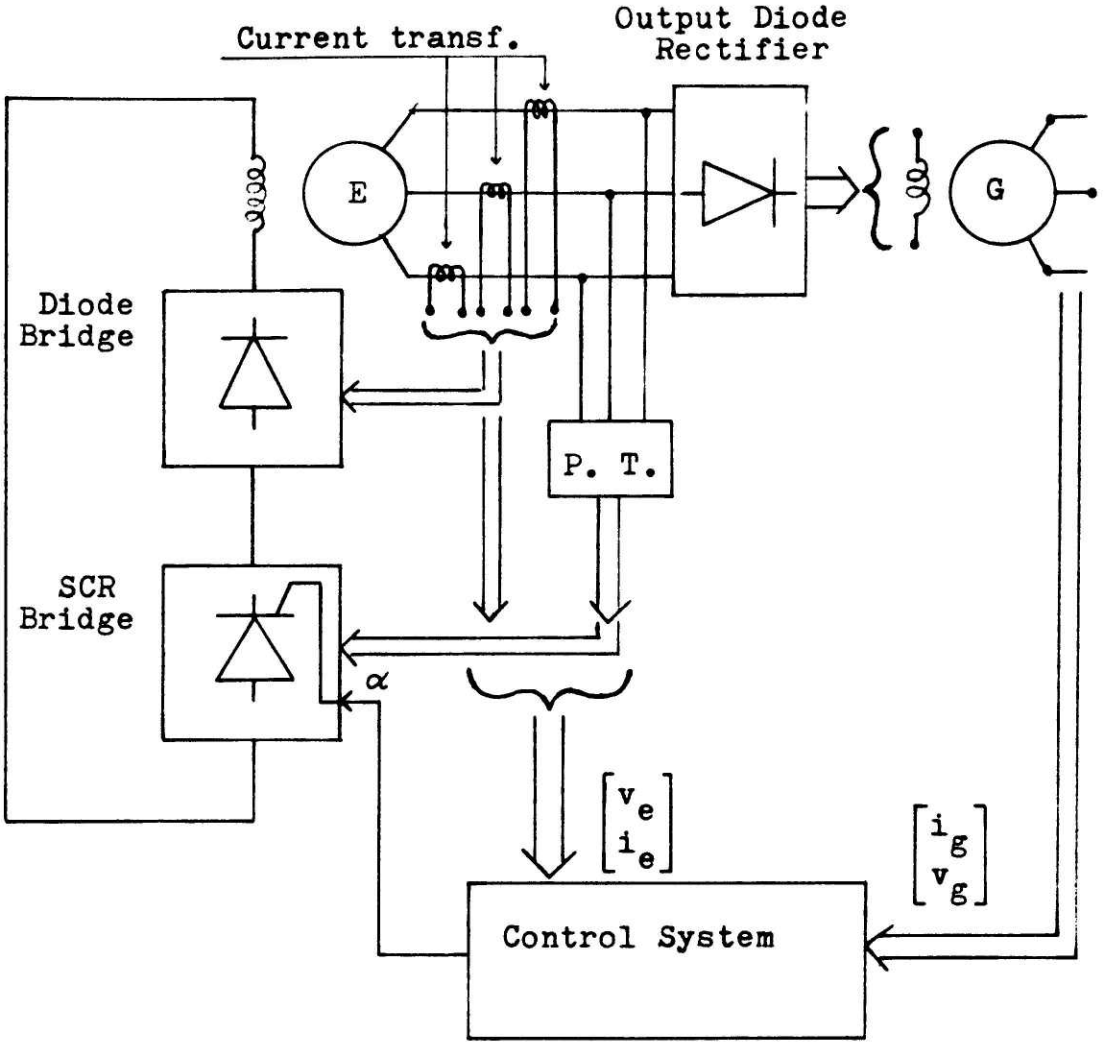

Figure 1.4 Schematic of Alterrex system. The letter E stands for exciter-alternator and G for main generator. The letters P. T. stand for potential transformers.

without contributing any current to the exciter-alternator. In case the voltage of the exciter-alternator goes low the diode bridge then supplies power to the exciter-alternator's field winding.

In order to obtain this type of behavior the turns ratios of the potential and current transformers are properly adjusted. The saturation characteristics of the current transformers are also important.

The control system is shown in Figure 1.4 as a single block. Figure 1.5 shows a more detailed version of the different parts of the control system in block diagram form. The control system is divided in several subsystems identified in Figure 1.5. These are the firing angle system, the automatic regulator, the active-reactive current compensator (A.R.C.C.), the current limit system (C.L.S.), the exciter minimum voltage limit system (E.M.V.L.S.), the phase limit system (P.L.S.), the underexcited reactive ampere limit system (U.R.A.L.S.) and the manual regulator. Switch s is either in position 1 or 2 depending on whether the system is controlled from the manual regulator or the automatic regulator. The control system inputs are the exciter and generator currents (i_1'',i_g) and voltages (v_e,v_g). The output from the regulator is a continuous signal v_R. This continuous signal is the input to the firing angle system which generates the gate signals that are used to fire the SCR's of the self-

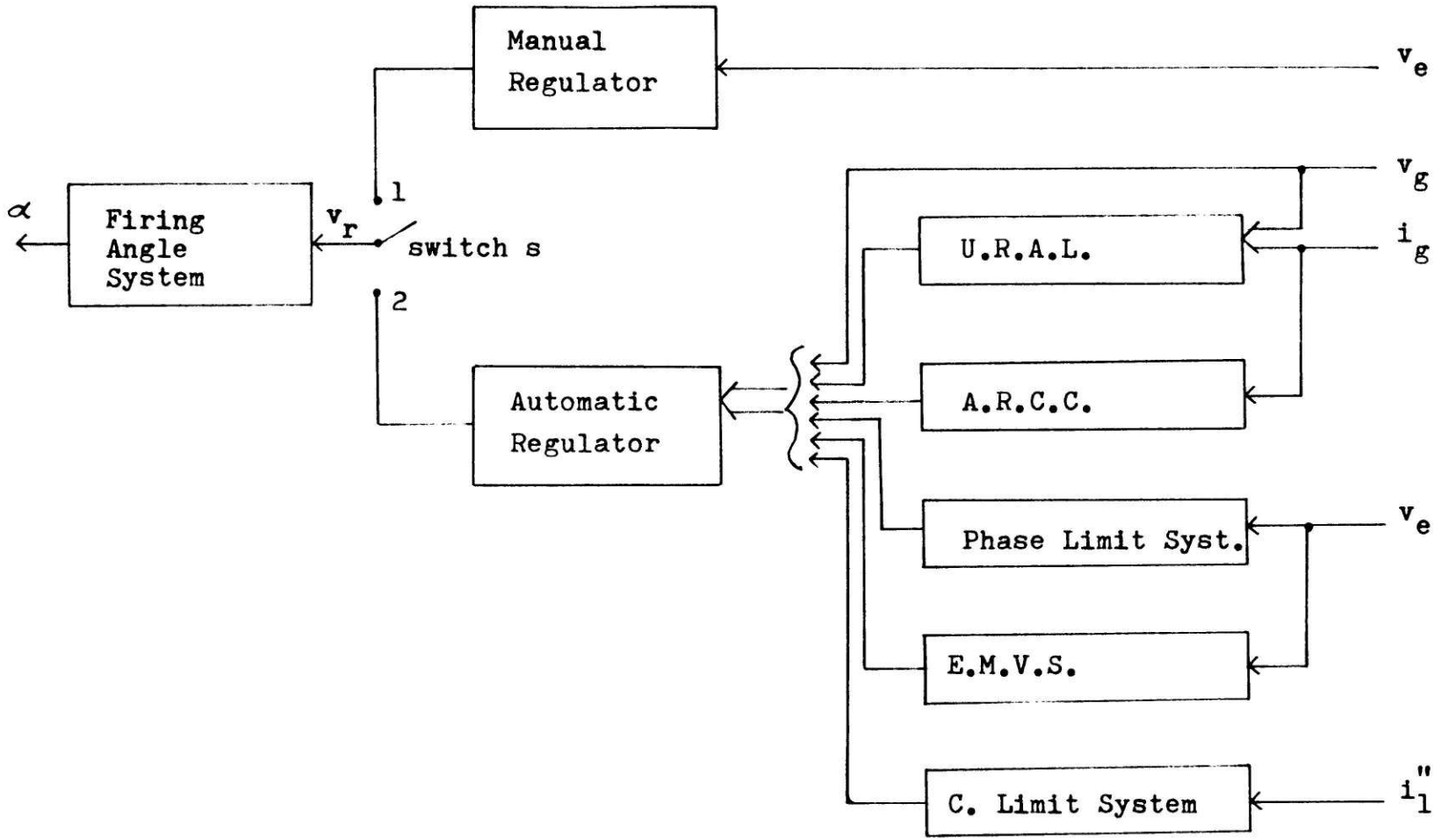

Figure 1.5 Block diagram of control system

excited exciter-alternator. For more detailed information about this system the reader is referred to the Alterrex manual distributed by the General Electric Co. [4].

1.2.3 Organization and Scope of the Thesis

The thesis has been organized into 6 Chapters. Chapter II through V can be considered the main body of the thesis. Chapter VI consists of the conclusions and suggestions for further work. In Chapter II a basic problem consisting of an exciter-alternator with output rectifier and powered by a dc source is treated. This problem allow us to introduce the model for the exciter-alternator with output rectifier without having to deal with the saturation and self-excitation effects of the exciter-alternator. Chapter III then extends the techniques developed in Chapter II to include the effects of magnetic saturation and self-excitation thus obtaining a model more directly related to the Alterrex excitation control system. The current boost system is also modeled in Chapter III.

In Chapter IV the control system is modeled. Chapter V puts together the information in the 3 previous chapters and adds the main generator equations in order to obtain the complete final model of the Alterrex excitation control system. The model is simulated without the current boost system and the limiting systems. The results are in

agreement with expected behavior for this system. The results are also compared with results obtained using the I.E.E.E. Type I model.

Methods are developed to obtained the solution for the equations of the model. Because the model is nonlinear the method is based on iterative numerical techniques which could be implemented in a digital computer. The results obtained using this method in Chapters II and III are compared to results using a linearized perturbation analysis for the case where the system is disturbed with small perturbations about the steady state equilibrium points. This is done as an approximate way of determining whether the numerical method used is giving meaningful answers.

As a final comment it must be pointed out that this model has been developed having in mind the effect of excitation control systems on the dynamic behavior of the main generator. In doing this certain effects of little significance for dynamic analysis such as harmonic components in the system variables have been neglected. Therefore the user of this model should understand its limitations before using it for purposes other than those specified in this thesis.

Chapter II: MODEL OF SEPARATELY-EXCITED EXCITER-ALTERNATOR WITH OUTPUT RECTIFIER

2.1 Introduction

In this chapter the case of a single synchronous generator with output rectifier and with a highly inductive load is analyzed. This system is analyzed because understanding of this particular problem helps to understand the exciter-alternator problem. The analogy between the ac synchronous generator with rectifier and inductive load and the exciter-alternator with rectifier and feeding the field winding of the main generator is based on the fact that the field winding of the main generator is also highly inductive. However the exciter-alternator with rectifier will also be affected by the back emf produced by the changes in the main synchronous generator armature flux. This effect is equivalent to having a voltage source in series with an inductor at the load of the exciter-alternator. In this chapter the back emf effect at the load of the exciter-alternator is ignored. This effect will be included in the complete model presented in Chapter V. Except for this, both systems are equivalent and they will be referred to commonly as the exciter-alternator with output rectifier. The problem of the exciter-alternator with output rectifier can be subdivided into two basic problems; The problem where the exciter-alternator is

separately-excited and the problem where it is self-excited. In this chapter the former problem will be treated. The latter problem will be treated in Chapter III.

2.2 Derivation of the Model Equations

The schematic of the separately-excited exciter-alternator with output rectifier is shown in Figure 2.1. The field winding of the exciter-alternator is separately-excited with a dc voltage source v_{fe}. This problem is not as trivial as it might seem since the use of a rectifier at the output gives rise to complications not encountered in the classical problem involving a synchronous machine with an ac load. For example in the present problem harmonics are present in the line currents i_a, i_b, i_c due to the phase controlled rectifier.

The phase controlled rectifier is an important part of this system, therefore it seems convenient to summarize briefly the behavior of the rectifier before continuing to solve the problem. Figure 2.2 shows a sketch of the waveforms of the output voltage across the bridge, the current through the load and the current through phase a, $v_L(t)$, $i_L(t)$ and $i_a(t)$ respectively. It also shows the average components of $i_L(t)$ and $v_L(t)$, i.e. $i_L(t)_{(dc)}$ respectively. The other phase currents i_b and i_c will be similar to $i_a(t)$ but shifted by 120 degrees and 240 degrees respectively. Two sets of figures are shown, one showing the waveforms obtained with the

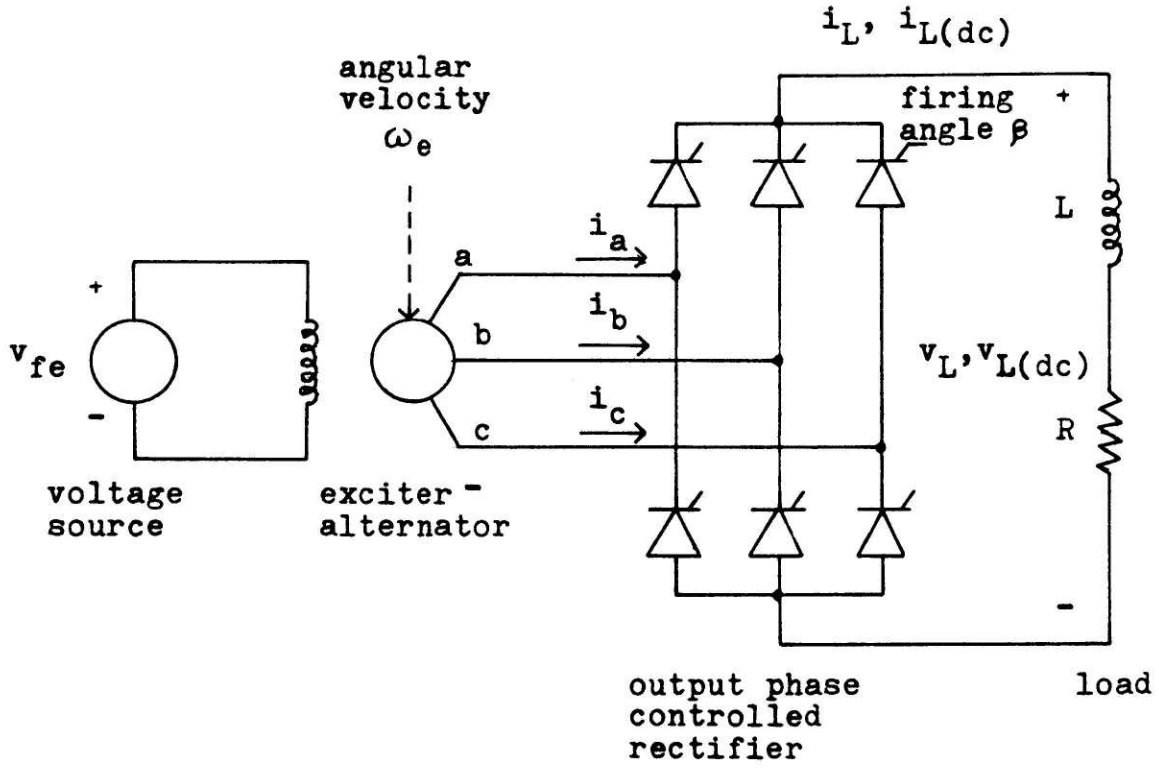

Figure 2.1 Schematic of separately-excited exciter-alternator

firing angle $\beta=0$ degrees and the other at some $\beta=\beta_0$. The waveforms for $\beta=0$ are identical to those which one would obtain using a 3 phase diode bridge. Notice that the phase current $i_a(t)$ goes from zero to I_{LC}, the magnitude of $i_{L(dc)}(t)$, instantaneously, i.e. the current commutates instantly from one leg of the bridge to another. This is a consequence of the assumption that the terminal voltages behave as sinusoidal voltage sources with no impedance. In the real case, the reactance of the alternator will not allow the phase currents to jump instantaneously in time and instead the current will go from zero to I_{LC} in a finite interval of time called the commutation interval. This effect has been neglected in the model presented in this thesis.

Notice also that the current $i_L(t)$ appears as having very little ripple. This is consistent with the assumption that the inductive nature of the load will filter the harmonics of the current significantly. In practice there exists a ripple, therefore $i_{L(dc)}(t)$ represents the average of dc component of the instantaneous current $i_L(t)$. While $i_{L(dc)}(t)$ and $v_{L(dc)}(t)$ represent average values their magnitudes may change with time and therefore they are considered functions of time. Figure 2.2 represents the variables in question for the particular case where the system has reached steady-state or equilibrium and $i_{L(dc)}(t)$ and $v_{L(dc)}(t)$ are constants.

In order to understand the behavior of the separately-excited exciter-alternator it is convenient to approach the

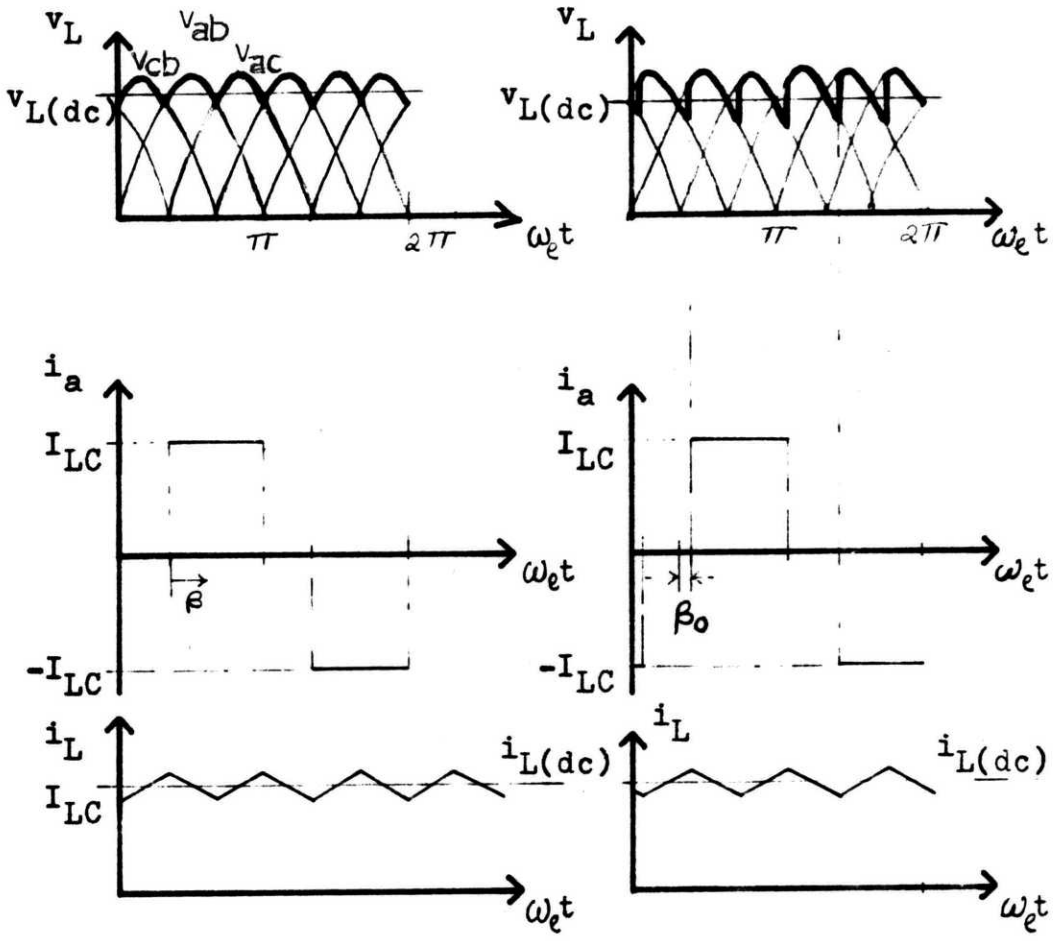

Figure 2.2 Schematic showing the 3-phase rectifier waveforms for $\beta = 0$ and $\beta = \beta_o$.

problem heuristically. This approach will suggest the mathematical model to be used for this system. First consider the assumption that the terminal voltages form a balanced sinusoidal set. This assumption neglects the effect of armature current harmonics and dc currents on the armature fluxes and voltages. Similarly, the effects of harmonics and ripple in the field current will be ignored. These approximations will be applied to the exciter-alternator throughout this analysis, permitting the exciter-alternator to be represented in standard d-q transformation representation. Since the harmonic components do not play a significant role in the transfer of energy from the exciter-alternator to the main generator field winding, these approximations are felt to be justified. In a consistent fashion, the load ripple will be ignored; the load will be modeled in terms of $i_{L(dc)}(t)$ and $v_{L(dc)}(t)$. From this point on these two variables will be referred to as $i_L(t)$ and $v_L(t)$.

The d-q transformations transform armature quantities into a reference frame rotating with the rotor. This frame of reference consists of two orthogonal axes: the direct (d) and the quadrature (q) axes. For more detailed information on d-q transformations consult Reference [1].

In conclusion it is possible to construct a mathematical model that represents the effect of the dc components of the variables in the rotor circuits and the fundamental components of the ac variables on the armature circuits. This then ignores all the harmonics of the system variables, or more

precisely all the harmonics due to the rectifier at the output of the machine. During transient conditions the ac variables are amplitude modulated due to changes in magnitude of the rotor and armature currents and frequency modulated due to changes in rotor speed. The frequency components arising due to these effects are independent of rectifier action and are accounted for in this model.

The following equations in terms of the direct and quadrature axis variables will be used as the model for the synchronous machine of the separately-excited exciter-alternator. Adkins [1] is given as a reference for these equations. The d-axis variables are indicated by the subscript d, q-axis variables by the subscript q and the subscript e stands for exciter-alternator quantities. The subscript k is used to indicate damper winding variables and f is used to indicate field winding variables.

$$v_{de} = v_e \sin \delta_e \qquad (2.1)$$

$$v_{qe} = v_e \cos \delta_e \qquad (2.2)$$

Variable v_e represents the amplitude of the exciter-alternator terminal voltage in per unit. Variable δ_e represents the phase angle between the terminal voltage of the exciter-alternator and the quadrature axis. This variable so

familiar in standard two - reaction theory has here an interesting meaning. In standard two - reaction theory this variable is often measured with respect the infinite bus which is the absolute electrical frame of reference, i.e. it is oscillating at constant nominal frequency. In the present case however there is no easily identifiable infinite bus, rather the reference frame of the fundamental component of exciter-alternator terminal voltage is used. Equations (2.1) and (2.2) are used to transform the terminal voltage into two fictitious components of voltage on the direct and quadrature axes. These voltages are v_{de} and v_{qe} repsectively.

$$i_{de} = i_1 \sin(\delta_e + \Theta_1) \qquad (2.3)$$

$$i_{qe} = i_1 \cos(\delta_e + \Theta_1) \qquad (2.4)$$

Variable i_1 is used to represent the amplitude of the fundamental component of exciter-alternator current in per unit. Variable Θ_1 is used to represent the phase angle between the fundamental exciter-alternator terminal current and exciter-alternator terminal voltage. Equations (2.3) and (2.4) are used to transform the terminal current into two fictitious components of current along the direct and quadrature axes, i_{de} and i_{qe} respectively.

The different components of flux linkages on the direct and quadrature axes can be represented as follows:

$$\lambda_{de} = - X_{de}\, i_{de} + X_{mde}\, i_{fe} + X_{mde}\, i_{kde} \tag{2.5}$$

$$\lambda_{kde} = - X_{mde}\, i_{de} + X_{mde}\, i_{fe} + X_{kde}\, i_{kde} \tag{2.6}$$

$$\lambda_{fe} = X_{ffe}\, i_{fe} - X_{mde}\, i_{de} + X_{mde}\, i_{kde} \tag{2.7}$$

$$\lambda_{qe} = - X_{qe}\, i_{qe} + X_{mqe}\, i_{kqe} \tag{2.8}$$

$$\lambda_{kqe} = - X_{mqe}\, i_{qe} + X_{kqe}\, i_{kqe} \tag{2.9}$$

Notice that the model employed here represents the exciter-alternator by one damper winding on each rotor axis. The symbol λ is used to represent linkage flux and X is used to represent inductances or reactances in per unit. The subscript m used on the inductances, is used to indicate mutual inductances. Equations (2.5) through (2.9) are used to define per unit flux linkages on the d-q axis in terms of the various per unit rotor currents. Notice that the generator convention has been chosen for armature currents i_{de} and i_{qe}; positive armature currents are defined as flowing out of the armature terminals, producing a demagnitizing effect on the exciter-alternator fluxes.

Fluxes λ_{de} and λ_{qe} linking the transformed armature are fixed with respect the rotor d-q axes but are in motion

with respect the physical armature winding. As a result, the per unit voltages v_{de} and v_{qe} include speed voltage terms as follows:

$$v_{de} = - (\omega_e/\omega_{eO}) \lambda_{qe} - R_{ae} i_{de} \quad (2.10)$$

$$v_{qe} = (\omega_e/\omega_{eO}) \lambda_{de} - R_{ae} i_{qe} \quad (2.11)$$

The variable R_{ae} represents armature winding resistance. The voltages are diminished due to the ohmic drop across the armature winding resistance. Variable ω_e is the angular speed of the rotor. Variable ω_{eo} is the nominal angular speed of the rotor. Both variables are measured in electrical radians per seconds. Strictly speaking there should be a third term in Equations (2.1) and (2.2) according to Faraday's law. This third term is due to the fact that fluxes λ_{qe} and λ_{de} are not just rotating in space with respect the armature winding but at the same time they are changing in magnitude. In this model these terms will be neglected. This is consistent with the assumptions neglecting dc and harmonic armature currents.

The per unit voltage equations for the remaining rotor windings can be written as:

$$\frac{d\lambda_{fe}}{dt} = - \omega_{eO} R_{fe} i_{fe} + \omega_{eO} v_{fe} \quad (2.12)$$

$$\frac{d\lambda_{kde}}{dt} = - \omega_{eO} R_{kde} i_{kde} \quad (2.13)$$

$$\frac{d\lambda_{kqe}}{dt} = - \omega_{e0} R_{kqe} i_{kqe} \qquad (2.14)$$

These equations are in per unit, therefore, the dimensions of the equations must be balanced by multiplying the right side by ω_{e0}.

The following equations represent the effect of the rectifier and the R-L load:

$$\frac{di_L}{dt} = - \frac{\omega_{Lo}}{L} R\, i_L + \frac{\omega_{Lo}}{L} v_L \qquad (2.15)$$

$$(2.33)\ T_1\, v_e \cos \beta = v_L \qquad (2.16)$$

$$i_L = (T_2/0.78)\, i_1 \qquad (2.17)$$

$$\theta_1 = \beta \qquad (2.18)$$

Variables v_L and i_L are the average voltage across and average current through the R-L load in per unit. Equation (2.15) is the state equation due to the inductive nature of the load. Equations (2.16) through (2.18) represent the rectifier bridge. These equations are standard in the rectifier literature [5]. The multiplying function $(2.33)\cos\beta$ in Equation (2.16) comes about after integrating the waveform shown in Figure 2.2 over the interval $[\beta, \beta + \pi/3]$. Since the function to be integrated on this interval is sinusoidal the multiplying function is a cosine function. Equation (2.17) and (2.18) come from the fourier series of the instantaneous

exciter-alternator terminal current in terms of i_L. T_1 and T_2 are normalizing constants. Since these equations were originally derived for actual dimensions it becomes necessary to balance the equations if per unit values are used. For example, if (2.16) was in actual dimensions it could be per unitized by dividing the left side by the base value of v_e and the right side by the base value of v_L. Because equality must be maintained it is then necessary to multiply the left hand side by the base value of v_e and the right side by the base value of v_L. Bringing the last constant to the left side of the equations yields the value of T_1, i.e., $T_1 = v_{e(base)}/v_{L(base)}$. T_2 is obtained similarly. Equation (2.18) shows that the angle between the fundamental of exciter-alternator terminal current and voltage is equal to the rectifier's firing angle. This is an interesting effect due to the use of phase controlled rectifiers. A close comparison between the sketches given in Figure 2.2 illustrates more clearly this effect.

Equations (2.1) through (2.18) are sufficient to represent the separately-excited exciter-alternator with output rectifier. Table 2.2 given in the summary in Section 2.5 is included to help to distinguish between the variables and the known inputs and parameters values. Notice that the number of variables is 18, which is also the number of governing equations. The values of parameters can be obtained using the data provided by the manufacturer. The data provided by the manufacturer is based on tests made on the machine from the

armature side of the machine which yield the following constants well known in the synchronous machine theory literature: X_d, X_d', X_d'', X_q, X_q', X_q'', T_d', T_{dO}'', T_{qO}', T_q, and T_a. These constants are defined on Table 2.2. The transformations between these standard constants and the model parameters are also given in Table 2.2. References [1] and [6] are given for these constants and equations.

The mechanical input for the exciter-alternator is $\omega_e(t)$. The reason why ω_e rather than torque is considered to be the mechanical input is that the exciter-alternator is usually connected to a bigger machine (main generator) whose moment of inertia is much larger than the one for the smaller machine. The result is that the speed of the exciter-alternator is determined solely by the speed of the main generator.

With Table 2.2 plus the values of inputs and data information from the manufacturer it is possible to obtain the mathematical model for the separately-excited exciter-alternator using Equations (2.1) through (2.18). These equations are listed again in the summary.

2.3 Solution Techniques

2.3.1 Steady-State Solution

For constant inputs $\omega_e(t) = \omega_{eO}$, $\beta = \beta_O$ and $v_{fe} = v_{feO}$ it is possible to determine the equilibrium points or steady-state solution of this system by setting the derivative

terms of (2.1) through (2.18) equal to zero and solving the resulting equations algebraically. The resulting expressions are given below. These equations are derived in Appendix A. The equations determining the steady-state are:

$$\Theta_{10} = \beta_0 \tag{2.19}$$

$$\delta_{e0} = \text{Tan}^{-1}\left[\frac{X_{qe}\cos\Theta_{10} - R_{ae}\sin\Theta_{10}}{R_e + R_{ae}\cos\Theta_{10} + X_{qe}\sin\Theta_{10}}\right] \tag{2.20}$$

$$R_e = RT_2/(0.78(2.33)\cos(\beta_0 T_1)) \tag{2.21}$$

$$i_{feo} = v_{feo}/R_{fe} \tag{2.22}$$

$$i_{10} = \frac{X_{mde}\, i_{fe0}}{R_e\cos\delta_{e0} + R_{ae}\cos(\delta_{e0} + \Theta_{10}) + X_{de}\sin(\delta_{e0} + \Theta_{10})} \tag{2.23}$$

$$v_{eo} = R_e\, i_{10} \tag{2.24}$$

For given values of inputs v_{fe0} and β_0, and given the values of the parameters of Table 2.2, it is possible to obtained the equilibrium conditions for v_{e0}, i_{10}, δ_{e0}, i_{fe0} and Θ_{10} as follows. Θ_{10} is determined using (2.19). The parameter R_e is calculated using (2.21). This parameter represents the resistive impedance that the terminal of the exciter-alternator sees through the SCR bridge into the load. Notice that this parameter is a function of the firing angle β_0. With Θ_{10} and R_e then δ_{e0} can be calculated using (2.20). The value for i_{fe0} follows easily from (2.22). The value for i_{10} can then be calculated using

(2.23). The terminal voltage v_{e0} is then obtained using (2.24). With these values other variables such as fluxes can be calculated using the governing Equations (2.1) through (2.18).

2.3.2 Transient Solution

We shall now proceed to solve the equations for the transient response of the system. This presents some nontrivial problems because these equations are nonlinear and there is no clear direct method to put the equations in state-space form. In this section a numerical method to analyze the system will be developed. In developing this method the main issue dealt with will be to obtain the global behavior of the exciter system, i.e. to obtain the solution of the governing equations for general transient conditions. For example this could be finding the time trajectory describing how the system moves from rest to a particular equilibrium condition for a given input or from one steady-state to another steady-state in the case when the input changes from one value to another.

The mathematical expressions (2.1) through (2.18) along with the initial conditions $i_L(t_0)=i_{L0}$, $\lambda_{fe}(t_0)=\lambda_{fe0}$, $\lambda_{kde}(t_0)=\lambda_{kde0}$ and $\lambda_{kqe}(t_0)=\lambda_{kqe0}$ and the unknowns of Table 2.2 are sufficient information to determine the response of the separately-excited exciter-alternator given that we know the parameters. The governing Equations (2.1) through (2.18) however must be manipulated algebraically in

order to obtain equations suited to the following numerical procedure. The necessary manipulations to derive the following equations are given in Appendix A. It must only be remembered that these equations are not an addition to the governing equations but a derivation from them. The iterative numerical procedure is described below step by step.

Step 1 Equations (2.12), (2.13), (2.14), and (2.15) given in Section 2.2 and repeated here describe the energy storage elements of the system. These are the state equations.

$$\frac{d\lambda_{fe}}{dt} = - \omega_{e0} R_{fe} i_{fe} + \omega_{e0} v_{fe} \tag{2.12}$$

$$\frac{d\lambda_{kde}}{dt} = - \omega_{e0} R_{kde} i_{kde} \tag{2.13}$$

$$\frac{d\lambda_{kqe}}{dt} = - \omega_{e0} R_{Kqe} i_{kqe} \tag{2.14}$$

$$\frac{di_L}{dt} = - \frac{\omega_{L0}}{L} R\, i_L + \frac{\omega_{L0}}{L} v_L \tag{2.15}$$

Step 1 consists of integrating these state equations for a conveniently small interval of time, ΔT, thus that the system variables that are not states on the right hand side of the state equations can be considered constants, evaluated using $i_{fe}(t_0)$, $v_{fe}(t_0)$, $i_L(t_0)$ and $v_L(t_0)$. In this way it is possible to obtain the values for $\lambda_{fe}(t_0 + \Delta T)$, $i_L(t_0 + \Delta T)$, $\lambda_{kde}(t_0 + \Delta T)$ and $\lambda_{kqe}(t_0 + \Delta T)$ approximately.

With these values it is possible to solve for the rest of the other unknown variables at time $t_0 + \Delta T$. This is done in the following steps.

Step 2 Obtain $\delta_e(t_0 + \Delta T)$ iteratively using equation (2.25) as indicated below.

$$\delta_{e\,(K+1)} = \text{Tan}^{-1}\left[\frac{v_{de}(\delta_{e(K)})}{v_{qe}(\delta_{e(K)})}\right] =$$

$$= \text{Tan}^{-1}\left[\left((\omega_e/\omega_{e0})(X_{qe} - \frac{X^2_{mqe}}{X_{kqe}})(\frac{0.78\ i_L(t_0 + \Delta T)}{T_2}\cos(\delta_{e(K)} + \Theta_1) + \right.\right.$$

$$- R_{ae}\ \frac{(0.78\ i_L\ (t_0 + \Delta T))}{T_2}\ \sin\ (\delta_{e(K)} + \Theta_1)$$

$$\left.-(\omega_{e0}/\omega_{e0})\frac{X_{mqe}}{X_{kqe}}\lambda_{kqe}(t_0 + \Delta T)\right) /$$

$$\left((\omega_e/\omega_{e0})(K_3 + \frac{K_5^2}{K_7})(\frac{0.78\ i_L}{T_2})\ \sin\ (\delta_{e(K)} + \Theta_1) + (\omega_e/\omega_{e0})\cdot\right.$$

$$\left.(K_4 + \frac{K_5K_8}{K_7} - R_{ae}\ \frac{(i_L 0.78)}{T_2}\cos\ (\delta_{e(K)} + \Theta_1))\right] \qquad (2.25)$$

Subscript (K) is used to indicate the current value of the variable in question and (K+1) is used to represent the new value of the variable. Using (2.25) the value for $\delta_{e(K+1)}$ is estimated using $\delta_{e(K)}$.*

It is obvious that, $\delta_{e(1)} = \delta_e(t_0)$. The final value that $\delta_{e(K+1)}$ approaches is $\delta_e(t_0 + \Delta T)$. In order to determine the convergence of the procedure the following test is made after each iteration, let $E = \left|(\delta_{e(K+1)} - \delta_{e(K)}) / \delta_{e(K+1)}\right|$, then if $E \leq e$, where e is a conveniently small constant the value of $\delta_{e(K+1)}$ can be said to be approximately equal to $\delta_e(t_0 + \Delta T)$. The constant e is chosen so as to obtain the necessary precision. If after an iteration $E > e$ then it is necessary to go back and iterate again.

---

* Sometimes it is convenient or necessary to speed up convergence or to guarantee convergence by calculating the value of $\delta_{e(K+1)}$ as a linear combination of the new value calculated from (2.25) and the current value, that is,

$$Y = \text{Tan}^{-1}\left[\frac{v_{de}(\delta_{e(K)})}{v_{qe}(\delta_{e(K)})}\right]$$

$$\delta_{e(K+1)} = G\ Y + \delta_{e(K)}(1 - G)$$

where G is a constant that is chosen to speed up or slow down the iterative procedure. $G > 1.0$ speeds up the iterative procedure and $G < 1.0$ slows it down. In the particular problem solved here a value of $G = 0.5$ was used to assure convergence.

Step 3 Step 3 consists of finding $i_1(t_0 + \Delta T)$, $v_e(t_0 + \Delta T)$, θ_1, $i_{fe}(t_0 + \Delta T)$, $v_L(t_0 + \Delta T)$, $i_{kde}(t_0 + \Delta T)$ and $i_{kqe}(t_0 + \Delta T)$ using the results obtained in Step 1 and Step 2 and equations derived in Appendix A.

$$i_1(t_0 + \Delta T) = \frac{(0.78)}{T_2} i_L \tag{2.26}$$

$$\theta_1 = \beta(t_0) \tag{2.27}$$

$$i_{fe}(t_0 + \Delta T) = (\lambda_{fe} + -X_{mde} i_{kde} + X_{mde} i_1(t_0 + \Delta T)\sin (\delta_e + \theta_1))/X_{ffe} \tag{2.28}$$

$$v_e(t_0 + \Delta T) = \Big[((\omega_e/\omega_{e0})(X_{qe} - \frac{X^2_{mqe}}{X_{kqe}})(\frac{0.78 i_L}{T_2} \cos(\delta_e + \theta_1) +$$

$$- R_{ae}(\frac{0.78 i_L}{T_2} \sin(\delta_e + \theta_1) - (\omega_e/\omega_{e0})\frac{X_{mqe}}{X_{kqe}} \lambda_{kqe})^2 +$$

$$+ \Big((\omega_e/\omega_{e0})(K_3 + \frac{K_5^2}{K_7})(\frac{0.78 i_L}{T_2})\sin(\delta_e + \theta_1) + (\omega_e/\omega_{e0})(K_4 + \frac{K_5 K_8}{K_7}) +$$

$$- R_{ae} (\frac{0.78 i_L}{T_2}) \cos (\delta_e + \theta_1)\Big)^2 \Big]^{1/2} \tag{2.29}$$

$$i_{kde}(t_0 + \Delta T) = \Big(\lambda_{kde} + X_{mde} (\frac{0.78 i_L}{T_2}) \sin (\delta_e + \theta_1) +$$

$$- X_{mde} i_{fe} \Big) / X_{kde} \tag{2.30}$$

$$i_{kqe}(t_0 + \Delta T) = \Big(- \lambda_{kqe} + X_{mqe} \frac{i_L(0.78)}{T_2} \cos(\delta_e + \theta_1) \Big) / X_{kqe} \tag{2.31}$$

$$v_L(t_0 + \Delta T) = (2.33\ T_1)\ v_e \cos \beta \tag{2.32}$$

With these results it is possible to go back to Step 1 and integrate the state equations again to obtain $i_L(t_0+2\Delta T)$, $\lambda_{fe}(t_0+2\Delta T)$, $\lambda_{kde}(t_0+2\Delta T)$ and $\lambda_{kqe}(t_0+2\Delta T)$ for the next time interval and repeat the whole procedure. Therefore, using this method it is possible to obtain the time response of the system for any length of time knowing the initial conditions, the inputs and parameters. This method can be implemented via a digital computer.

2.3 Solution Example

In order to illustrate the utility of this method the following problem is solved. For simplicity the damper windings and leakage inductances of the exciter-alternator are neglected. Consider the problem with parameters given directly in model notation by Table 2.1, with initial conditions $i_1 = \lambda_{fe} = \lambda_{kde} = \lambda_{kqe} = 0$ and inputs $\beta = 0$, $\omega_e = 377$ rad/sec and $v_{fe} = 6.0\times10^{-4}$ p.u. The steady-state values can be obtained using the method given in Section 2.3.1 and are given in Table 2.1. Now it is of interest to find out how the system approaches this steady-state condition from rest. The numerical method of Section 2.3.2 was implemented on a digital computer.

The results obtained for $i_L(t)$ using the method proposed above are plotted versus time in Figure 2.3. As can be seen from this plot the current rises and overshoots before converging to the steady-state value.

The response obtained using the technique of Section 2.2 holds for any value of inputs and for any possible system conditions; as a result this method should also yield the response of the system for the case of small perturbations about an equilibrium point. Therefore, it is possible to test how meaningful the answers given by the numerical procedure are by solving the problem for small disturbances using the numerical method, and comparing the results with the results obtained analytically using a system of equations obtained by linearizing the governing equations about an equilibrium point. The linearized equations are given in Appendix A.

Considered the system at rest at an equilibrium condition. The equilibrium is disturbed with an impulse which causes small changes of the variables about the steady-state values. According to the numerical method of Section 2.3.2, the result for $i_L(t)$ is as shown in Figure 2.4 plotted versus time. From this plot it can be observed that the response is a decaying sinusoid with time period of about 56 seconds and an excursion from the steady-state with a maximum value of 0.0026 p.u. The problem can be solved analytically using the roots of

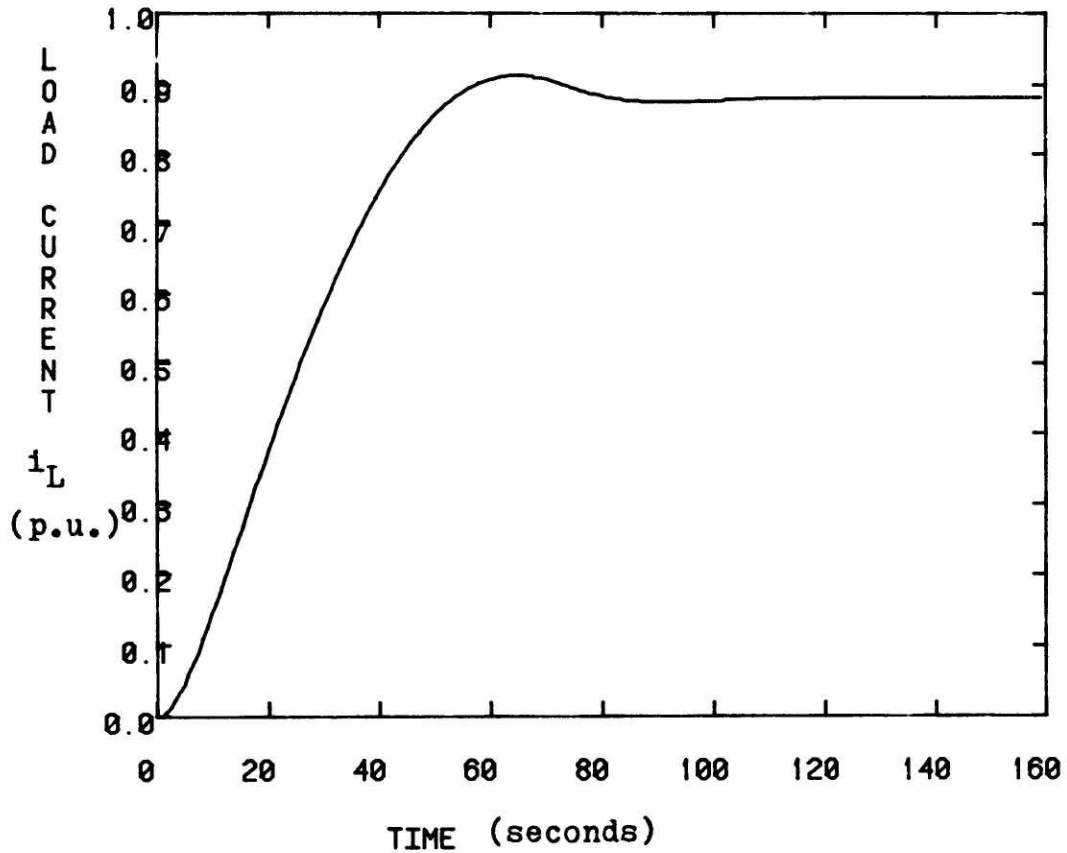

Figure 2.3 Computer plot of the load current i_L.

the characteristic Equation of (A.41) given in Appendix A. The solution for the impulse input, $v_{fe} = 1q(t)$ [volts]* is

$$\Delta i_L = \frac{e^{-(\zeta\omega_n t)}}{M} \sin(\omega_n h t) \quad [p.u.] \tag{2.33}$$

where, $h = \sqrt{1 - \zeta^2}$

$$M = \omega_n h \, v_{fe}^b \, (4.573 \times 10^{-2}) \tag{2.34}$$

Parameters $\omega_n, \zeta, v_{fe}^b$ are given in Table 2.1. It follows from (2.33) that the time period of oscillation is 59 seconds and the maximum value for the excursion from the steady-state value, Δi_L is equal to:

$$\Delta i_L = \frac{e^{\left(-\zeta\pi/2 \,/\, \sqrt{1 - \zeta^2}\right)}}{M} = 0.0026 \quad [p.u.] \tag{2.35}$$

which are very close to the values obtained with the numerical method as they should be.

---

*q(t) is used to represent the impulse function.

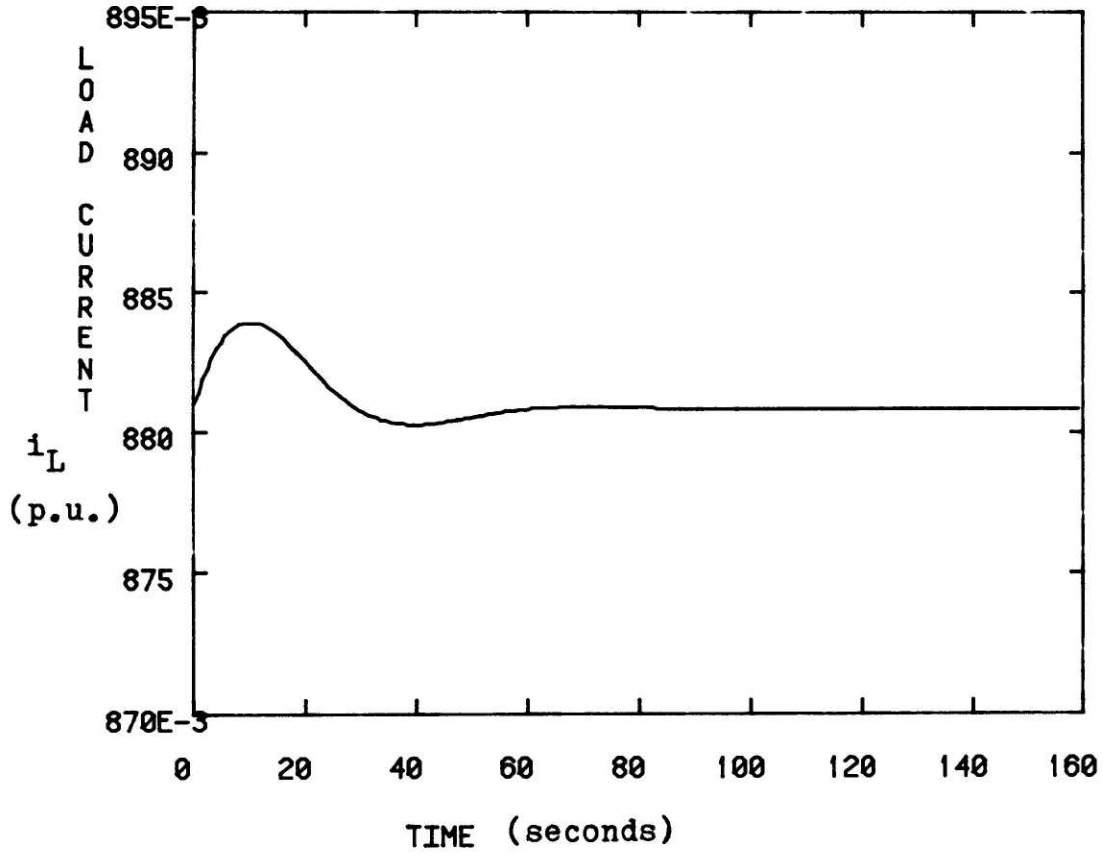

Figure 2.4 Computer plot of the load current i_L.

Table 2.1

Parameters for solution example of Section (2.4)

X_{de}	1.4 p.u.
X_{qe}	1.4 p.u.
X_{mde}	1.4 p.u.
X_{mqe}	1.4 p.u.
X_{ffe}	1.4 p.u.
ω_{e0}	377. rad/sec.
ω_{L0}	377. rad/sec.
L	3.388×10^{4} p.u.
R	0.6 p.u.
v_{fe}	6.0×10^{-4} p.u.
β_0	0.0 rad
R_{fe}	8.5×10^{-4} p.u.
i_{l0}	0.687 p.u.
i_{fe0}	0.706 p.u.
v_{e0}	0.227 p.u.
δ_{e0}	76.7312 degrees
ω_n	0.122 rad/sec.
ζ	0.496 p.u.
v_e^b	1000V (line-to-line)
i_l^b	1.732×10^{3} Amps
i_{fe}^b	46.05 Amps
v_{fe}^b	3.257×10^{4} volts
v_L^b	1000 volts (line-to-line)
i_L^b	1.732×10^{3} Amps
T_1	1.0
T_2	1.0

2.5 Summary

Equations for the model of the separately-excited exciter-alternator are derived in Section 2.2 based on heuristic reasoning. These are Equations (2.1) through (2.18). A steady-state solution method is given in Section 2.3.1. A numerical procedure to obtain the transient response is developed in Section 2.3.2. The solution technique requires solving some of the basic equations simultaneously to obtain a more suitable version of some of the equations. The resulting equations are given in Section 2.3.2 and derived in Appendix A. The numerical procedure is summarized in this section using a flowchart given below. Finally, Table 2.2 is given here to help differentiate between known parameters and variables. The parameters of the model are not usually given by the manufacturer directly. Instead a set of parameters based on tests are given in the data sheets typically provided by the manufacturers. The equations necessary to go from the manufacturer's parameter data to the model parameters are given in Table 2.2. The purpose of this summary is to stress the following points.

(i) Equations (2.1) through (2.18), repeated below, and only these equations, cons titute the mathematical model for the separately-excited exciter-alternator. All other equations given here are derivations from these basic equations.

(ii) The mathematical model can be solved using the numerical method described in 2.3.2 and given here in flowchart form.

(iii) The model parameters can be derived directly from the manufacturer supplied machine parameters using the formulas of Table 2.2.

The equations for the separately-excited exciter-alternator machine equations:

$$v_{de} = v_e \sin \delta_e \tag{2.1}$$

$$v_{qe} = v_e \cos \delta_e \tag{2.2}$$

$$i_{de} = i_1 \sin (\delta_e + \Theta_1) \tag{2.3}$$

$$i_{qe} = i_1 \cos (\delta_e + \Theta_1) \tag{2.4}$$

$$\lambda_{de} = -X_{de}\, i_{de} + X_{mde}\, i_{fe} + X_{mde}\, i_{kde} \tag{2.5}$$

$$\lambda_{kde} = - X_{mde}\, i_{de} + X_{mde}\, i_{fe} + X_{kde}\, i_{kde} \tag{2.6}$$

$$\lambda_{fe} = X_{ffe}\, i_{fe} - X_{mde}\, i_{de} + X_{mde}\, i_{kde} \tag{2.7}$$

$$\lambda_{qe} = -X_{qe}\, i_{qe} + X_{mqe}\, i_{kqe} \tag{2.8}$$

$$\lambda_{kqe} = -X_{mqe}\, i_{qe} + X_{Kqe}\, i_{kqe} \tag{2.9}$$

$$v_{de} = - (\omega_e/\omega_{eO})\, \lambda_{qe} - R_{ae}\, i_{de} \tag{2.10}$$

$$v_{qe} = (\omega_e/\omega_{eO})\ \ de - R_{ae}\, i_{qe} \tag{2.11}$$

$$\frac{d\lambda_{fe}}{dt} = - \omega_{eO}\, R_{fe}\, i_{fe} + \omega_{eO}\, v_{fe} \tag{2.12}$$

$$\frac{d\lambda_{kde}}{dt} = - \omega_{eO}\, R_{kde}\, i_{kde} \tag{2.13}$$

$$\frac{d\lambda_{kqe}}{dt} = - \omega_{eO}\, R_{kqe}\, i_{kqe} \tag{2.14}$$

load equation:

$$\frac{di_L}{dt} = - \frac{\omega_{LO} R}{L}\, i_L + \frac{\omega_{LO}}{L}\, v_L \tag{2.15}$$

output rectifier equations:

(2.33) $$T_1\, v_e \cos\beta = v_L \tag{2.16}$$

$$i_L = (T_2/0.78)\, i_1 \tag{2.17}$$

$$\Theta_1 = \beta \tag{2.18}$$

Table 2.2

System Variables	Input Variables	Parameters
	Known Quantities	
v_{de}	β	X_{de}
v_{qe}	ω_e	X_{mde}
v_e	v_{fe}	X_{kde}
δ_e		X_{ffe}
i_{de}		X_{mqe}
i_{qe}		X_{qe}
i_l		X_{kqe}
Θ_l		ω_{e0}
		R
λ_{de}		v_e^b
λ_{kde} (state)		i_l^b
λ_{fe} (state)		i_L^b
λ_{qe}		v_L^b
λ_{kqe} (state)		R_{ae}
i_L (state)		v_{fe}^b (not used in
i_{fe}		i_{fe}^b this chapter)

Table 2.2 continued

System Variables	Input Variables	Parameters
	Known Quantities	
i_{kde}		$T_1 = v_e^b / v_L^b$
i_{kqe}		$T_2 = i_1^b / i_L^b$
v_L		L
		v_e^b (L-L)
		$KVA^b = \frac{3 v_e^b i_1^b}{\sqrt{3}}$
		R_{ae}
		R_{fe} [ohms]
		X_{ae}
		$T_{do}' = \frac{1}{\omega_{eo} R_{fe}} (X_{fe} + X_{mde})$
		$T_d' = \frac{1}{\omega_{eo} R_{fe}} (X_{fe} + \frac{X_{mde} X_{ae}}{X_{mde} + X_{ae}})$
		$T_{do}'' = \frac{1}{\omega_{eo} R_{kde}} (X_{kde} + \frac{X_{mde} X_{fe}}{X_{mde} + X_{ae}})$
		$T_d'' = \frac{1}{\omega_{eo} R_{kde}} (X_{kde} + \frac{X_{mde} X_{ae} X_{fe}}{X_{mde} X_{ae} + X_{mde} X_{fe} + X_{ae} X_{fe}})$

Table 2.2 continued

System Variables	Input Variables	Parameters
	Known Quantities	
		$T_{qO}' = \frac{1}{\omega_{eO} R_{kqe}} (X_{kqe} + X_{mqe})$
		$T_q' = \frac{1}{\omega_{eO} R_{kqe}} \left(X_{kqe} + \frac{X_{mqe} X_{ae}}{X_{mqe} + X_{ae}}\right)$
		$X_{de} = X_{ae} + X_{mde}$
		$X_{de}' = X_{ae} + \frac{X_{mde} X_{fe}}{X_{mde} + X_{fe}}$
		$X_{de}'' = X_{ae} + \frac{X_{mde} X_{fe} X_{kde}}{(X_{mde} X_{fe} + X_{mde} X_{kde} + X_{fe} X_{kde})}$
		$X_q = X_{ae} + X_{mqe}$
		$X_q' = X_{ae} + \frac{X_{mqe} X_{kqe}}{X_{mqe} + X_{kqe}}$
		R_{fe} (in ohms) not used in this chapter
		$T_a = \frac{1}{\omega_{eO} R_{ae}} \frac{(X_d'' + X_q'')}{2}$

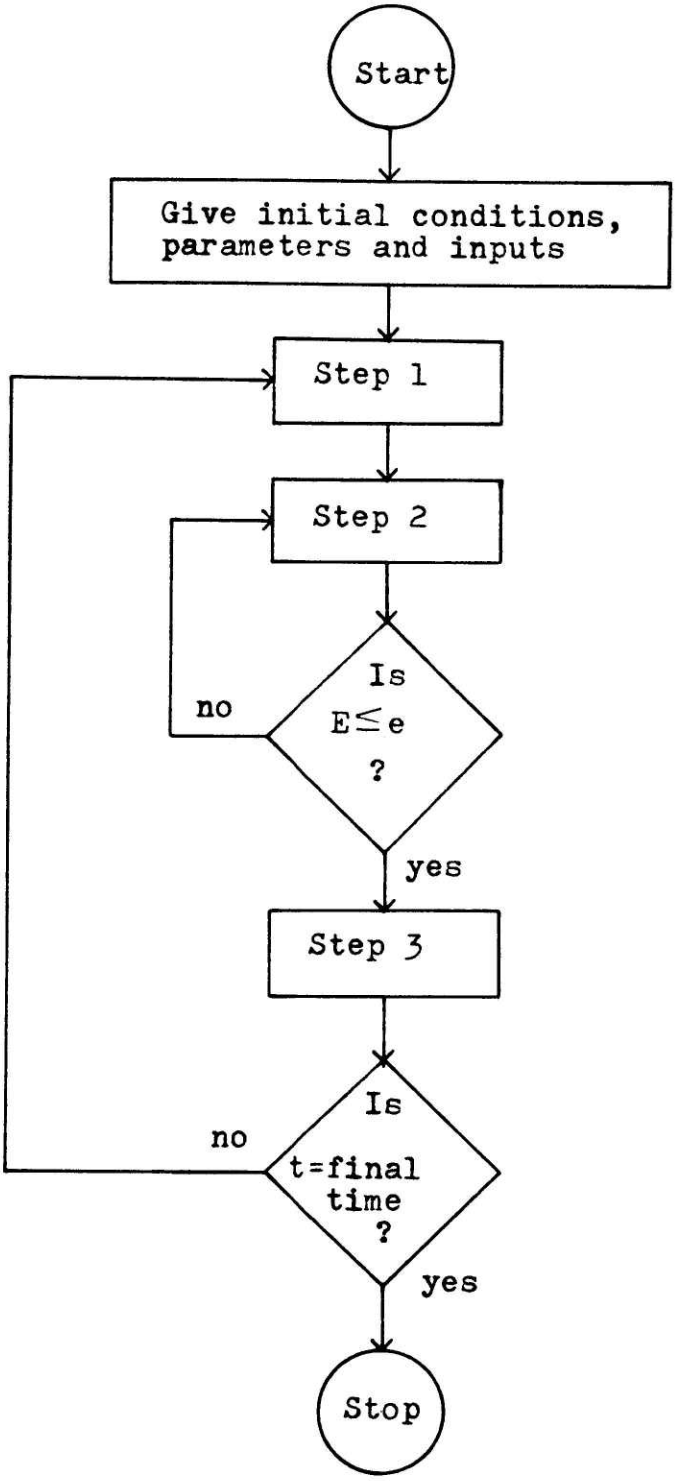

Figure 2.5 Flowchart for the method described in section 2.3.2

Chapter III: MODEL OF SELF-EXCITED EXCITER-ALTERNATOR WITH OUTPUT RECTIFIER

3.1 Introduction

The previous chapter considered the case of an exciter-alternator excited with a dc field voltage source. In the Alterrex system the exciter-alternator is excited by its own output, i.e., it is self-excited. Furthermore, the voltage across the exciter-alternator field winding can be changed. By changing this voltage one is able to control the exciter-alternator terminal voltage. Figure 3.1 shows the schematic of a system that resembles more closely the Alterrex system. The exciter-alternator output is connected to a diode bridge feeding an inductive load just as in the case treated before except that here rectification is via a diode bridge. However, the exciter-alternator field voltage is obtained by rectifying the exciter ac voltage output using an SCR bridge. The firing angle α of the SCR bridge can be changed, thus changing the exciter-alternator field voltage which in turn will change the exciter-alternator ac output voltage and therefore the dc voltage across the load. This system will be called the self-excited exciter-alternator with output rectifier. In this chapter magnetic saturation of the exciter-alternator is modeled.

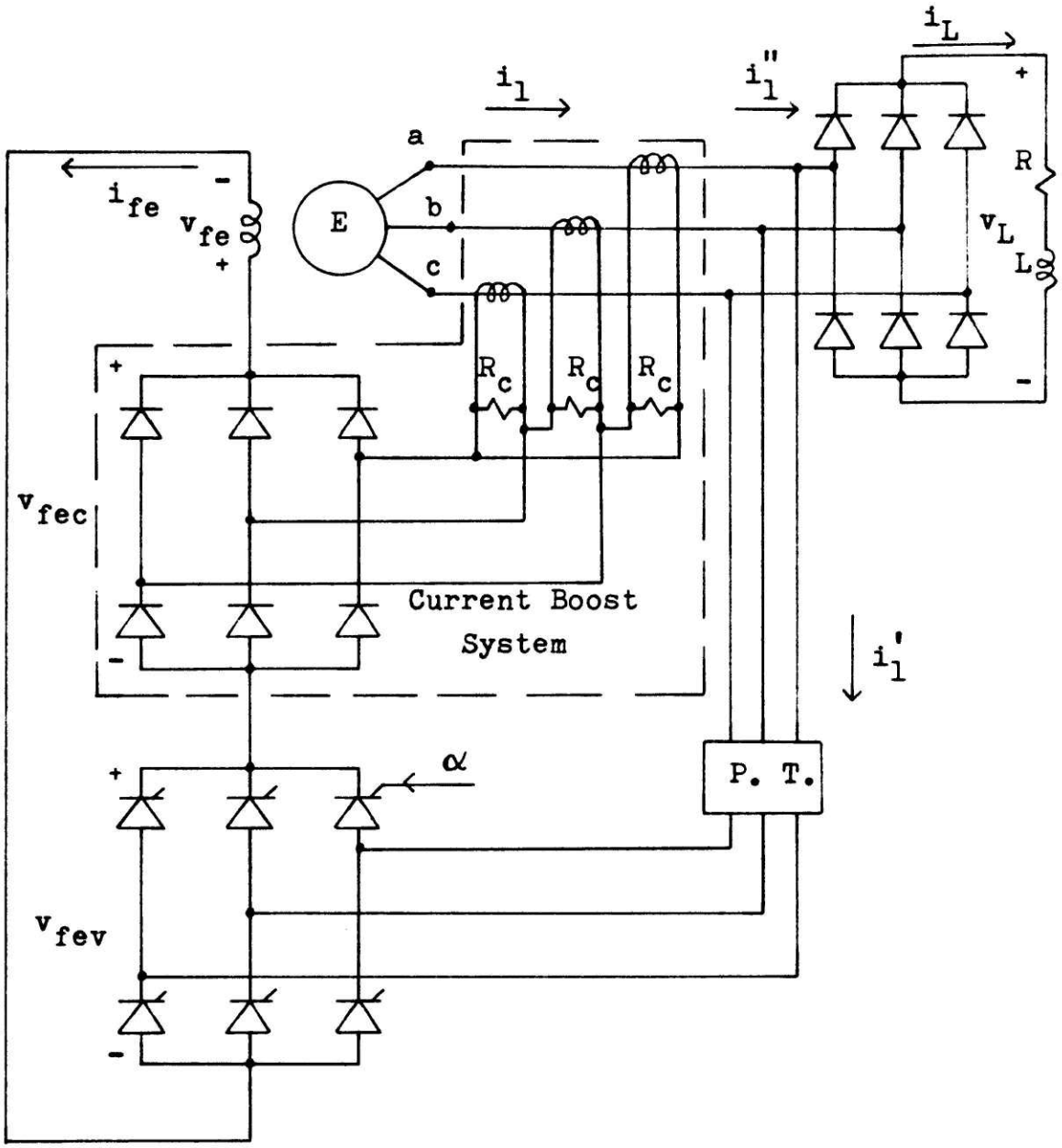

Figure 3.1 Schematic of self-excited exciter-alternator with the current boost system. The letter E stands for exciter-alternator and P. T. for potential transformer.

3.2 Modifications to Exciter-Alternator Model of Chapter II to Include Effects of Self-Excitation, Saturation and the Current Boost System in the Model Equations

The governing equations for this system differ from the separately-excited exciter-alternator because of the self-excitation introduced via the SCR bridge. However, both systems are similar in many respects and the new governing equations can be obtained from the equations given for the separately-excited exciter-alternator in Chapter II. The exciter-alternator can still be described by Equations (2.1) through (2.14). These equations are found in Section 2.5. In order to model self-excitation, the effects of magnetic saturation must be included. The following assumptions are proposed to handle the magnetic saturation of the exciter-alternator:

(1) Assume all leakages inductances and the quadrature-axis mutual inductance (X_{mqe}) to be constants.

(2) The only saturable element is the direct-axis mutual inductance (X_{mde}).

(3) The non-linear inductance X_{mde} is only a function of the mutual direct axis flux or equivalently of the currents i_{de}, i_{fe}, i_{kde} which produce fluxes on the direct axis, i.e., $X_{mde} = X_{mde}(i_{de}, i_{fe}, i_{kde})$.

(4) The function $X_{mde} = X_{mde}(i_{fe}, i_{de}, i_{kde})$ must be obtained empirically. This can be done using data from the open-circuit saturation curve (open-circuit voltage vs. field current). The form of the function $X_{mde}(i_{fe}, i_{de}, i_{kde})$ may be chosen in any fashion which will yield a good fit to the data. In general, then a polynomial of the form, $X_{mde} =$

$$= \sum_{n=0}^{m} C_n (i_{fe} + i_{kde} - i_{de})$$

with an arbitrary number of terms m will fit the data as accurately as needed. For the purposes of this thesis, Equation (3.1) (with m = 3) will be used to model saturation in the exciter-alternator.*

$$X_{mde} = C_0 + C_1 (i_{fe} + i_{kde} - i_{de}) + C_2 (i_{fe} + i_{kde} - i_{de})^2 + \\ + C_3 (i_{fe} + i_{kde} - i_{de})^3 \qquad (3.1)$$

It must be observed that this is only an approximate way of handling this non-linear effect. In order to simplify the calculations leakage inductances and X_{mde} were assumed constant, although in reality this may not be necessarily so.

---

* This expression only holds for a given range of values.

For the purposes of this chapter as in Chapter II, an R-L load is assumed at the output of the exciter-alternator. Thus, this load is represented by Equation (2.15).

The equations for the output rectifier of the self-excited exciter-alternator can be obtained from the rectifier equations of the separately-excited exciter-alternator with minor modifications. In the self-excited exciter-alternator case a diode bridge is used instead of an SCR. Equations (2.16) can be modified simply by setting $\beta = 0$. Equation (2.17) applies directly to the problem after changing i_1 to i_1''. Equation (2.18) is not applicable to the present problem. The two equations for the output diode rectifier are then (3.2) and (3.3) given below.

$$v_L = (2.33)\ T_3\ v_e \tag{3.2}$$

$$i_L = (T_4/0.78)\ i_1'' \tag{3.3}$$

T_3 and T_4 are normalizing constants which come into the equations because of the normalization of the equations as is described in Chapter II. The variable i_1'' represents the fundamental component of current going into the output rectifier. It is obvious that because of the rectifier effect these equations only hold for positive currents i_L and i_1''. For modeling purposes as soon as these currents go negative they are set to zero and the voltage v_L is also set to zero.

The field winding of the exciter-alternator is fed via a potential transformer and the SCR rectifier. It is important to find a model for the potential transformer that predicts the voltage drop across it. This voltage drop is primarily due to the leakage inductance of the transformer. On the other hand it is not really important to model the magnetic energy storage capacity of this inductance. Therefore a very simple model is chosen for the transformer based on the voltage drop due to the fundamental component of current flowing through it. In the present case however the phasor magnitudes are considered functions of time. As shown in Figure (3.2) the resulting equations in terms of d-q quantities are:

$$v'_{de} = v'_e \sin(\gamma + \delta_e) \tag{3.4}$$

$$v'_{qe} = v'_e \cos(\gamma + \delta_e) \tag{3.5}$$

Variable v'_e represents the fundamental component of voltage at the secondary side of the potential transformer.
The variable γ is the phase angle between v_e and v'_e.
The variables v'_{de} and v'_{qe} are the projection on the direct and quadrature axes of the voltage v'_e. Therefore, Equations (3.4) and (3.5) are used to project v'_e on the direct and quadrature axes.

$$i'_{de} = i'_1 \sin(\gamma + \delta_e + \Theta'_1) \tag{3.6}$$

$$i'_{qe} = i'_1 \cos(\gamma + \delta_e + \Theta'_1) \tag{3.7}$$

Variable i_1' is used to represent the fundamental component of current flowing through the potential transformer. The variable Θ_1' is the phase angle between i_1' and v_e'. Then i_{de}' are the projections of i_1' on the direct and quadrature axes.

$$v_{de}' = v_{de} + (\omega_e/\omega_{e0})\, X_p\, i_{qe}' \tag{3.8}$$

$$v_{qe}' = v_{qe} - (\omega_e/\omega_{e0})\, X_p\, i_{de}' \tag{3.9}$$

X_p is the leakage reactance (at frequency ω_{e0}) of the transformer. In actual dimensions the voltage v_e will be stepped down by N_p, the turns ratio of the transformer. Therefore the base value for v_e' is chosen to be v_e^b/N_p. The effect of an increase of magnitude of i_{qe}' and i_{de}' is to increase the imaginary part v_{de}' and decrease the real part v_{qe}' and therefore to increase γ.*

---

* Equations (3.8) and (3.9) are obtained by equating the real (q) and imaginary (d) variables of the phasor equation for the transformer in terms of fundamental components of transformer variables, i.e., $v_e \angle -\delta_e = v_e' \angle -\delta_e - \gamma +$ $+ j(\omega_e/\omega_{e0})\, Xp\, i_1' \angle -\delta_e - \gamma - \Theta_1'$

The SCR bridge equation can be obtained from equation (2.16) through (2.18) by using a change of variables. The following equations are obtained.

$$v_{fev} = (2.33)\ T_5\ v_e'\ \cos\ \alpha \tag{3.10}$$

$$i_{fe} = (T_6\ (0.78))\ i_1' \tag{3.11}$$

$$\theta_1' = \alpha \tag{3.12}$$

T_5 and T_6 are normalizing constants dependent on the base values of v_e', v_{fev}, i_{fe} and i_1'. The variable α represents the firing angle of the SCR bridge. The variable v_{fev} is the average voltage across the SCR bridge. The phase angle between the fundamental component of current i_1' and the fundamental component of voltage v_e', θ_1', is set by the firing angle of the SCR bridge according to Equation (3.12). Notice that these equations only hold for positive currents. See similar comments for Equations (3.2) and (3.3).

Current i_1'' is obtained by using Kirchhoff's current law at the terminal of the exciter-alternator. This yields:

$$i_{de}'' = i_{de} - i_{de}' \tag{3.13}$$

$$i_{qe}'' = i_{qe} - i_{qe}' \tag{3.14}$$

where,

$$i''_{de} = i''_1 \sin(\delta_e) \tag{3.15}$$

$$i''_{qe} = i''_1 \cos(\delta_e) \tag{3.16}$$

Variables i''_{de} and i''_{qe} represent the projections on the direct and quadrature axes of i''_1. Using this equations it is possible to construct a phasor diagram for the exciter-alternator as shown in Figure 3.2.

With the model modified to include self-excitation and saturation it is possible now to make one more addition. This consists of adding equations to include the effects of the current boost system. This system is shown in Figure 3.1. The behavior of the current boost system is more complicated than might appear at first sight. What follows is an explanation of why the current boost system is used and how it works.

During normal operation, exciter-alternator field current control is obtained by phase control of the SCR bridge rectifier. For certain transient conditions the control system that changes the variable α might force this variable to be 90° which means that the average voltage across the field winding will be zero. If this condition is maintained for too long the exciter-alternator output voltage might decay close to zero. Then the control system won't be able to raise the output voltage again by changing the angle α, i.e., this system has "collapsed". The purpose of the current boost system is to save the system from collapsing. If the exciter-alternator

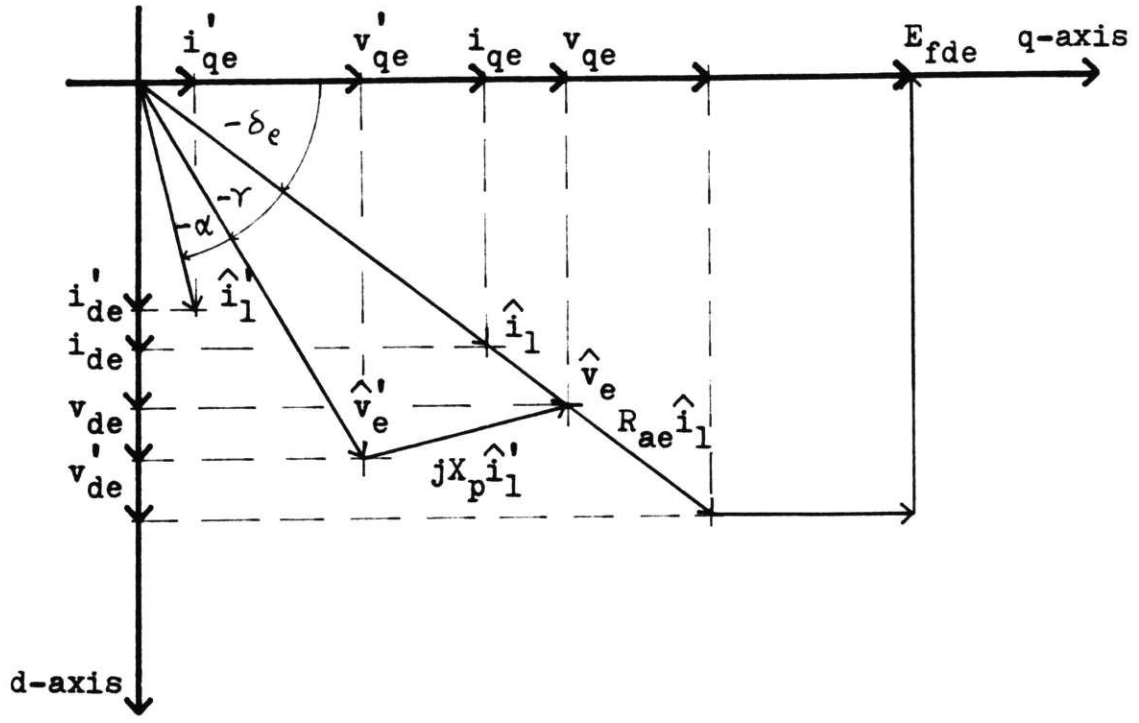

Figure 3.2 Phasor diagram for self-excited exciter-alternator

terminal voltage decreases and the exciter-alternator field current decreases beyond a certain limit, the current boost system takes control by providing current feedback to the field winding. This current feedback is regenerative, hence, the field current will build up until the current transformers feeding the diode bridge in the current boost system saturate. This occurs at rated full load field current. Once the system builds up terminal voltage to normal levels again the current boost system ceases to operate. It should be emphasized that the current boost system operates under transient conditions only.

During normal operation the current boost system has no effect on the rest of the exciter-alternator. The SCR bridge voltage is high enough to keep all the diodes in the current boost system forward biased. Current i_{fe} is divided between the three legs of the current diode bridge. The currents coming from the current transformers are also flowing through the diodes of the current boost system and the current in each individual diode is modulated by the currents from the current transformers. It is shown in Appendix B that for values of currents such that $\frac{2\ i_L}{N_C} < i_{fe}$, where N_C is the current transformer turns ratio, the current boost system is not in operation. This is defined as Mode I of operation of the current boost system.

As the output voltage collapses, the current i_{fe} decreases. The current boost system is designed in such a way

that the current modulation taking place in the current boost bridge "forces" certain diodes to reverse bias and others to remain forward biased when i_{fe} falls under certain level relative to i_L. At this point the current boost system commences to operate. It is shown in Appendix B that this mode of operation occurs for $i_{fe} \geq \frac{2}{N_c} i_L$. This mode of operation will be called Mode II of operation.

For Mode I then the system is governed by the equations given above alone. However, for Mode II we have to include the effect of the current boost system. For Mode II the current boost system has a topology as shown in Figure 3.3. In the following analysis the leakage inductances and winding resistances of the current transformers will be neglected. This is done to simplify the problem and because these elements are considered to have a second order effect on the system. The mutual inductance of the current transformers is non-linear, i.e., it saturates. The current transformers are designed so that at the point of saturation, the current boost system will be supplying rated full load field current.

The saturation curve for the current transformers will be modeled as shown in Figure 3.4. The variables shown in this schematic are defined in Figure 3.3. Variables λ_m and i_m are the values of flux and current at which the current transformers saturate. L_c is the value of mutual inductance in the linear region. R_c is a resistor connected across

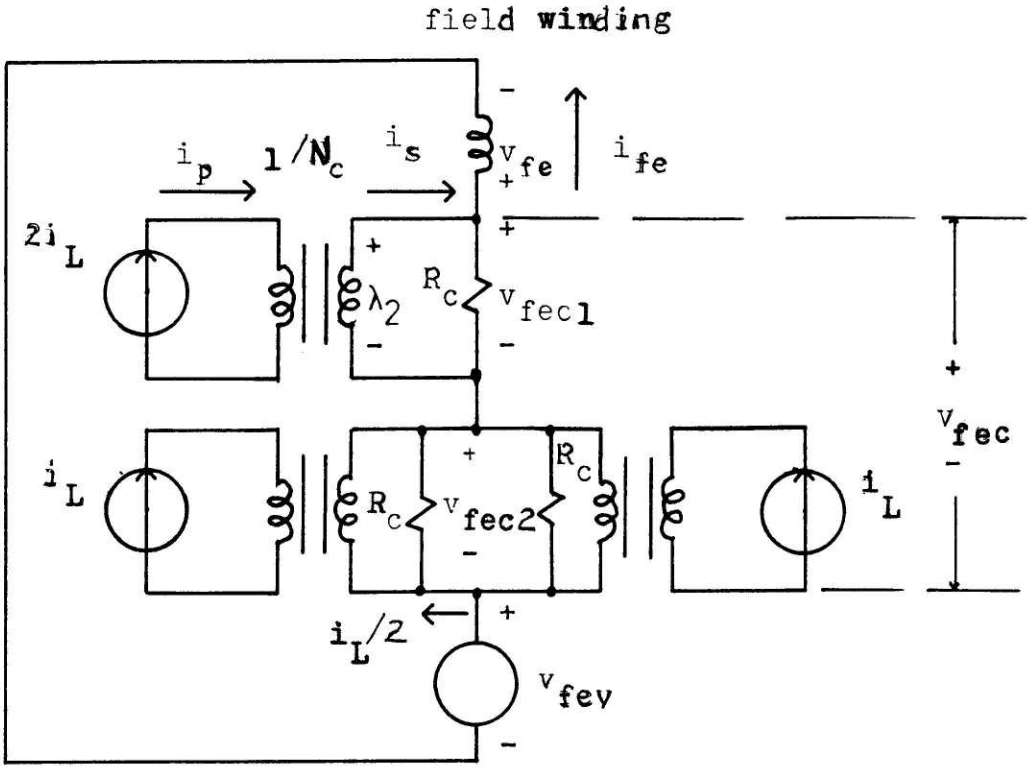

Figure 3.3 Schematic of equivalent circuit for the current boost system in Mode II of operation.

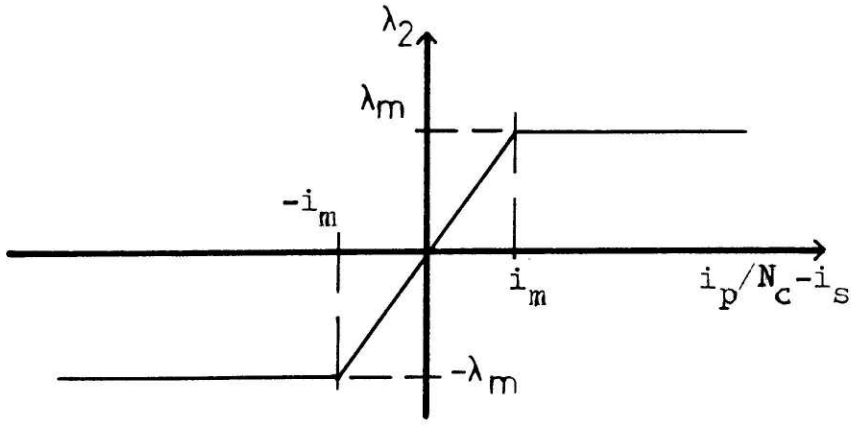

Figure 3.4 Sketch of saturation curve for current transformer.

the secondary of the current transformers. Parameters L_c and λ_m, i_m can be found from the saturation curve of the current transformers (Figure 3.4). Variables v_{fec1} and v_{fec2} are the average voltages across the upper and lower halves of the topology in Figure 3.3. The variables i_p and i_s are the primary and secondary currents of the upper transformer in Figure 3.3. The variable λ_2 is used to represent the total flux in the core of the upper transformer. Notice that the exciter-alternator terminal currents are shown as current sources with values dependent on i_L. This topology is explained in Appendix B. The saturation model shown in Figure 3.4 is expressed in terms of the variables of the upper transformer, however, this model is also used for the other current transformers. Based on this information the governing equations for the current boost system are derived in Appendix B and given below.

$$\frac{dv_{fec}}{dt} = \begin{cases} -\frac{(\omega_{e0}R_c)}{L_c} v_{fec} + \frac{(3R_c)}{2} D; \; i - \frac{2v_{fec}}{3R_c} < i_m \text{ and } \frac{2i_L}{N_c} \geq i_{fe} \\ -\frac{(\omega_{e0}R_c)}{L_c} v_{fec} + \frac{(R_c)}{2} D; \; i \geq i_m > \frac{i}{2} - \frac{v_{fec}}{R_c} \text{ and } \frac{2i_L}{N_c} \geq i_{fe} \\ v_{fec} = 0; \; i \geq 2i_m \text{ or } \frac{2i_L}{N_c} < i_{fe} \end{cases} \tag{3.17}$$

$$D = \frac{di}{dt} = Y_1 \frac{d\lambda_{fe}}{dt} + Y_2 \frac{d\lambda_{kde}}{dt} + Y_3 \frac{d\lambda_{kqe}}{dt} + Y_4 \frac{di_L}{dt} \tag{3.18}$$

$$i = \frac{2i_L}{N_c} - i_{fe} \tag{3.19}$$

Noticed that the input to the state Equation (3.20), D, is only available during transient conditons because D is a function of therate of change of the states. It follows that the current boost bridge has no effect on the steady-state conditions.

Each of the three expressions given for Equation (3.17) hold exclusive of all the others when the given inequalities are satisfied. Notice from Figure 3.3 that the current flowing through each of the lower transformers is half of the current going through the upper one. Therefore, as the current increases, the upper transformer saturates before the lower transformers. If the current increases further even the lower transformers will saturate in which case all the transformers are saturated. Equation (3.17) describes the three possible saturation states. The first expression at the top represents the behavior of the current boost bridge in Mode II when all the transformers are unsaturated. The middle expression is used to model the behavior of the current boost system when the upper transformer of Figure 3.3 saturates but the lower ones remain unsaturated. The third expression holds for the case when all the transformers are saturated and, therefore, the voltage across the current boost bridge, v_{fec}, is zero. During Mode I the bridge is forward biased and v_{fec} is also zero, therefore, the bottom expression also holds for Mode I.

The variable v_{fec} represents the average voltage across the current boost bridge. Constants Y_1 through Y_2 are given in Appendix B. The voltage across the field winding is then the sum of the SCR bridge voltage and the current boost bridge voltage and is given by

$$v_{fe} = v_{fec} + v_{fev} \tag{3.20}$$

In this section the equations for the self-excited exciter-alternator model were derived. Obtaining the equations involved modifying certain equations from the separately-excited exciter-alternator and adding new ones. The complete model is described by Equations (2.1) through (2.15) and (3.1) through (3.20). All other equations are derived from these 35 basic equations. These equations are listed in the summary in Section 3.5. A table is also given in the summary to help differentiate between variables, parameters, and inputs. As explained in Chapter II, the parameters for the exciter-alternator model given by the manufacturer differ from the parameters used in the model and transformations given in Table 2.2 are needed to obtain the model parameters. Notice that there are 35 unknown variables and 35 equations. Equations (2.1) through (2.15) and (3.1) through (3.20) are then the 35 basic equations the parameters of which can be obtained using Tables 2.2 and 3.2.

3.3 Solution Techniques

3.3.1 Steady-State Solution

It is interesting to notice that the self-excited exciter-alternator works using a positive feedback loop, i.e., the self-excitation loop. This is interesting because normally this would drive a system into instability and it would never reach steady-state. In the present case, however, the problem is stable and it achieves steady-state. The reason behind this is that as the exciter-alternator terminal voltage goes up the non-linear direct axis mutual inductance modeled by Equation (3.1) saturates, thus, creating a unique point where the machine remains stable. This is a well known fact in self-excited dc machines and it happens to be true for this case too. The reader should see Section (5-6) of Reference [6] and Chapter 5 of Reference [7].

Conceptually, the problem can be illustrated graphically as shown in Figure 3.5. It shows the voltage-current characteristics of the exciter-alternator and of the load seen by the exciter-alternator. These two curves meet at only one point creating a unique steady-state condition. Notice that the exciter-alternator characteristics are non-linear because the direct axis mutual inductance saturates. Otherwise the exciter-alternator characteristics would look like the airgap line.

In order to solve for the steady-state condition or equilibrium points of the system the derivative terms of the governing equations are set to zero and the resulting equations are solved simultaneously. All the equations necessary to solve the steady-state condition are derived in Appendix B from the governing equations. Appendix B also explains how to use these equations to get the equilibrium points. In this section we will limit ourselves to giving a brief explanation of the procedure outlining at the same time some of the most important equations used to solve the steady-state conditions. The derivation of these equations can be found in the Appendix B.

Basically, the problem can be thought of obtaining the values corresponding to the intersection between the load and exciter-alternator characteristics (see Figure 3.5). The load characteristic is obtained by determining the driving point impedance at the exciter-alternator terminal; let us call its magnitude Z_e.

The exciter-alternator during steady-state is loaded by the output rectifier. The exciter-alternator is also loaded by the self-excitation loop to its own field winding modified by the SCR bridge and the potential transformer. Therefore, the load characteristics will depend on the equations describing the characteristics of these devices.

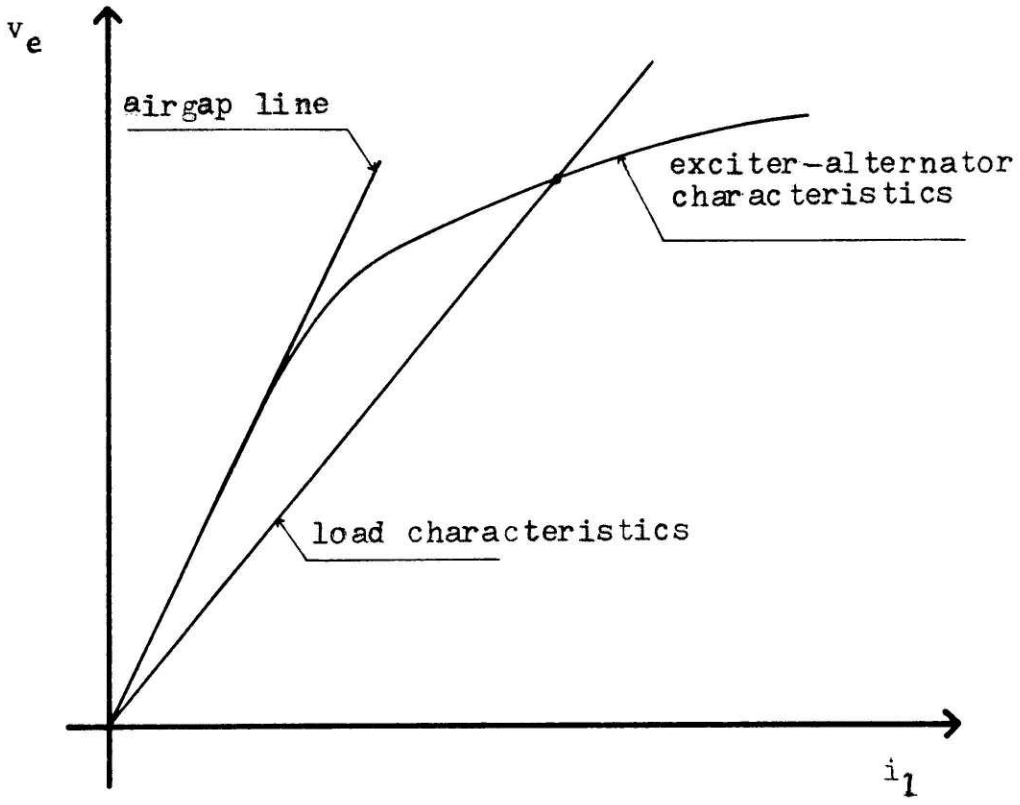

Figure 3.5 Sketch of exciter-alternator load characteristics.

Once Z_e is found, this is equivalent to having found the load characteristics, i.e., the slope of the load line of Figure 3.5. It was explained before that the steady-state is reached due to the fact that for a given load the non-linear inductance X_{mde} changes as to oppose further changes in voltage. For different loads X_{mde} will settle at different steady-state values. Therefore, the value at which the non-linear inductance X_{mde} settles, let us call it X_{mde0}, is a function of the load, i.e., Z_e. Equation (3.21) below gives the value of X_{mde0} as a function of Z_e.

$$X_{mde0} = \left[\sqrt{Z_e^2 - (-R_{ae} \sin(\delta_e+\Theta_1)+X_{qe}\cos(\delta_e+\Theta_1))^2} + \right.$$
$$\left. + X_{ae} \sin(\delta_e+\Theta_1)+R_{ae} \cos(\delta_e+\Theta_1) \right] \Bigg/ \left[\frac{Z_e(T_6/0.78)}{Z_p} - \sin(\delta_e+\Theta_1) \right] \qquad (3.21)$$

Quantities Z_e, δ_e, Θ_1 and Z_p depend on the parameters and loading conditions of the machine and can be found as described in Appendix B. Then the non-linear characteristics of the exciter, Equation (3.1) is used to solve for $(i_{fe} - i_{de})$ setting $X_{mde} = X_{mde0}$. Then using,

$$i_1 = (i_{fe} - i_{de}) \Bigg/ \left[\frac{Z_e\ (T_6/0.78)}{Z_p} - \sin(\delta_e+\Theta_1) \right] \qquad (3.22)$$

and v_e then follows,

$$v_e = Z_e\ i_L \qquad (3.23)$$

Equations (3.21), (3.22) and (3.23) are derived in Appendix B. With i_1 and v_e the steady-state values of other variables can be found using the governing equations.

3.3.2 Transient Solution

In this section a solution technique to obtain the transient response of the governing equations is developed. The method is a numerical technique to obtain the global solution of the mathematical model presented in Section 3.2. The method here is more involved than for the case of the separately-excited exciter-alternator but it is also based on the same basic idea. In this section certain auxiliary equations derived from the basic equations are used. These equations are given without much explanations. The reader is expected to look at Appendix B under auxiliary equations for their derivation. The numerical global solution is obtained as indicated below.

Step 1. Step 1 consists of integrating the state equations of the self-excited exciter-alternator (2.12) through (2.15) and (3.17) given below for a small time step ΔT so that variables other than the states can be considered to be constants calculated at t_0 the initial time.

$$\frac{d\ \lambda_{fe}}{dt} = -\ \omega_{e0}\ R_{fe}\ i_{fe}\ (t_0) + \omega_{e0}\ v_{fe}\ (t_0) \tag{3.24}$$

$$\frac{d\ \lambda_{kde}}{dt} = -\ \omega_{e0}\ R_{kde}\ i_{kde}\ (t_0) \tag{3.25}$$

$$\frac{d\ \lambda_{kqe}}{dt} = -\ \omega_{e0}\ R_{kqe}\ i_{kqe}\ (t_0) \tag{3.26}$$

$$\frac{di_L}{dt} = -\ \frac{\omega_{L0}}{L} R\ i_L + \frac{\omega_{L0}}{L}\ v_L\ (t_0) \tag{3.27}$$

$$\frac{dv_{fec}}{dt} = \begin{cases} -\ \dfrac{(\omega_{e0} R_c)}{L_c}\ v_{fec} + \dfrac{(3R_c)}{2}\ D\ (t_0), & i - \dfrac{2v_{fec}}{3R_c} < i_m \text{ and} \\ \dfrac{2i_L}{N_c} \geq i_{fe} \\ -\ \dfrac{(\omega_{e0} R_c)}{L_c}\ v_{fec} + \dfrac{(R_c)}{2}\ D\ (t_0), & i \geq i_m > \dfrac{i}{2} - \dfrac{v_{fec}}{R_c} \text{ and} \\ \dfrac{2i_L}{N_c} \geq i_{fe} \\ v_{fec} = 0; & i \geq 2i_m \text{ or } \dfrac{2i_L}{N_c} < i_{fe} \end{cases} \tag{3.28}$$

In the case of Equation (3.28) the inequalities must be established just before integration so as to decide what expression to integrate of the three possible expressions given for (3.28). The term D is given by (3.18) and (3.19).

Step 2. Knowing $i_L\ (t_0 + \Delta T)$ from the step before $i_L''\ (t_0 + \Delta T)$ can be found using Equation (3.3). It is necessary to find $i_1\ (t_0 + \Delta T)$ to obtain the solution of

the problem. This can be done using Equation (3.29). However, this requires knowing $i_1'(t_0+\Delta T)$ and $\gamma(t_0+\Delta T)$. The variable $\gamma(t_0+\Delta T)$ at this time is unknown. What is done here is to find these values iteratively. At the start it is assumed that $\gamma(t_0+\Delta T)$ and $i_1'(t_0+\Delta T)$ are equal to $\gamma(t_0)$ and $i_1'(t_0)$. Once new values for γ and i_1' are found in later steps they are used again to estimate a new value for i_1. The variable θ_1 is also calculated in the same way. This is repeated until the procedure converges. Then it follows that,

$$i_{1(K)} = \left(\left(i_1''(t_0+\Delta T) + i_{1(K-1)}' \cos\left(\gamma_{(K-1)}+\alpha\right)\right)^2 + \left(i_{1(K-1)}' \sin\left(\gamma_{(K-1)}+\alpha\right)\right)^2\right)^{1/2} \qquad (3.29)$$

$$\theta_{1(K)} = \mathrm{Tan}^{-1}\left[\frac{i_{1(K-1)}' \sin\left(\gamma_{(K-1)}+\alpha\right)}{i_1''(t_0+\Delta T) + i_{1(K-1)}' \cos\left(\gamma_{(K-1)}+\alpha\right)}\right] \qquad (3.30)$$

Here the subscript (K) indicates the iteration at which the estimate is obtained. Therefore, in the first iteration the first estimate of i_1 is obtained, $i_{1(1)}$. The quantities $i_{1(0)}'$ and $\gamma_{(0)}$ are taken to be $i_1'(t_0)$ and $\gamma(t_0)$ respectively.

Step 3. With these estimates the value of $\delta_{e(K)}$ is calculated iteratively just as it was done for the case of the separately-excited exciter-alternator in Chapter II.

Step 4. Now it is possible to find the rest of the system variables as follows.

$$i_{fe(K)} = \left(\lambda_{fe}(t_0 + \Delta T) + X_{mde}\, i_{1(K)} \sin\left(\delta_{e(K)} + \Theta_{1(K)} \right) \right) \Big/ X_{ffe} \tag{3.31}$$

$$i_{kde(K)} = \left(\lambda_{kde}(t_0 + \Delta T) + X_{mde} \frac{(0.78 i_L)}{T_2} \sin\left(\delta_e + \Theta_1 \right) + \right.$$

$$\left. - X_{mde}\, i_{fe} \right) \Big/ X_{kde} \tag{3.32}$$

$$i_{kqe(K)} = \left(- \lambda_{kqe} + X_{mqe} \left(\frac{i_L(0.78)}{T_2} \right) \cos\left(\delta_e + \Theta_1 \right) \right) \Big/ X_{kqe} \tag{3.33}$$

$$v_{e(K)} = \left[\left((\omega_e/\omega_{e0})(X_{qe} - \frac{X^2_{mqe}}{X_{kqe}}) \frac{(0.78 i_L)}{T_2} \cos\left(\delta_e + \Theta_1 \right) + \right. \right.$$

$$- R_{ae} \frac{(0.78 i_L)}{T_2} \sin\left(\delta_e + \Theta_1 \right) - (\omega_e/\omega_{e0}) \frac{X_{mqe}}{X_{kqe}} \lambda_{kqe} \Big)^2 +$$

$$+ \left((\omega_e/\omega_{e0}) \left(K_3 + \frac{K_5^2}{K_7} \right) \frac{(0.78 i_L)}{T_2} \sin\left(\delta_e + \Theta_1 \right) + (\omega_e/\omega_{e0}) \left(K_4 + \right. \right.$$

$$\left. \left. \frac{K_5 K_8}{K_7} - R_{ae} \frac{(0.78 i_L)}{T_2} \cos\left(\delta_e + \Theta_1 \right) \right)^2 \right]^{1/2} \tag{3.34}$$

$$i'_{1(K)} = i_{fe} \Big/ (T_6/0.78) \tag{3.35}$$

$$v'_{e(K)} = \sqrt{v^2_{e(K)} - \left((\omega_e/\omega_{e0})\, X_p\, i'_{1(K)} \cos\alpha \right)^2} +$$

$$- (\omega_e/\omega_{e0})\, X_p\, i'_{1(K)} \sin\alpha \tag{3.36}$$

$$\gamma_{(K)} = \text{Tan}^{-1} \left[\frac{(\omega_e/\omega_{e0})\, X_p\, i'_{1(K)} \cos\alpha}{v'_{e(K)} + (\omega_e/\omega_{e0})\, X_p\, i'_{1(K)} \sin\alpha} \right] \tag{3.37}$$

Variables $i_{fe(K)}$, $i_{kde(K)}$, $i_{kqe(K)}$, $v_{e(K)}$, $i'_{l(K)}$, $v'_{e(K)}$ and $\gamma_{(K)}$ can be obtained using (3.31), (3.32), (3.33), (3.34), (3.35), (3.36), and (3.37) respectively. Constants K_1 through K_8 are given in Appendix A. Notice that in the steps above the variables found are not the actual variables at $t_0+\Delta T$ but the K^{th} estimate because calculating these values involved using $i_{l(K)}$ and $\Theta_{l(K)}$.

Step 5. At this point we are in a position to test whether the K^{th} estimates of the variables found do really approach the values of the variables at $t_0+\Delta T$. Therefore, Step 5 consists in testing the convergence of the K^{th} estimate found in the previous steps. If the estimates have converged within acceptable limits, then it is possible to integrate the state equations again and repeat the procedure for the next time step. If convergence has not been achieved then it is necessary to find new estimates in terms of the old ones. This is done by using Equations (3.29) and (3.30) for the next iteration, that is

$$i_{l(K+1)} = ((i''_l\,(t_0 + \Delta T) + i'_{l(K)} \cos\,(\gamma_{(K)}+\alpha\,))^2 + + (i'_{l(K)} \sin\,(\gamma_{(K)} + \alpha))^2)^{1/2} \qquad (3.38)$$

$$\Theta_{l(K+1)} = \mathrm{Tan}^{-1}\left[\frac{i'_{l(K)} \sin\,(\gamma_{(K)} + \alpha)}{i''_l\,(t_0 + \Delta T) + i'_{l(K)} \cos\,(\gamma_{(K)}+\alpha)}\right] \qquad (3.39)$$

Convergence is tested as follows:

$$E_1 = \left| (i_{1(K+1)} - i_{1(K)}) / i_{1(K+1)} \right| \qquad (3.40)$$

$$E_2 = \left| (i_{1(K+1)} - i_{1(K)}) / i_{1(K+1)} \right| \qquad (3.41)$$

(a) If $E_1 \leq e_1$ and $E_2 \leq e_2$, where e_1 and e_2 are conveniently small constants, then $i_{1(K)}$ and $\theta_{1(K)}$ have converged according to the error criterions e_1 and e_2; therefore the values obtained in the K^{th} iteration are approximately equal to the values of the variables at $t_0+\Delta T$. In this case it is possible to go to Step 6.

(b) If $E_1 > e_1$ or $E_2 > e_2$ then this means that the K^{th} estimates have not converged in which case it is necessary to obtain the $(K+1)^{th}$ estimate, that is go back to Step 3 using the values of $i_{1(K+1)}$ and $\theta_{1(K+1)}$ obtained in Step 5 and repeat Steps 3, 4 and 5.

Step 6. In Step 6 a new value of X_{mde} is calculated using Equation (3.42) and (3.43). Also the value for v_L is calculated using (3.44). The value of v_{fe} is calculated using (3.45) and (3.46).

$$i_{de}(t_0+\Delta T) = i_1 \sin(\delta_e+\Theta_1) \tag{3.42}$$

$$X_{mde}(t_0+\Delta T) = C_0 + C_1(i_{fe}+i_{kde}-i_{de}) +$$

$$+ C_2(i_{fe}+i_{kde}-i_{de})^2 + C_3(i_{fe}+i_{kde}-i_{de})^3 \tag{3.43}$$

$$v_L(t_0+\Delta T) = (2.33)\, T_3\, v_e \tag{3.44}$$

$$v_{fev}(t_0+\Delta T) = (2.33)\, T_5\, v_e' \cos\alpha \tag{3.45}$$

$$v_{fe}(t_0+\Delta T) = v_{fec} + v_{fev} \tag{3.46}$$

Notice that a new value of X_{de} and X_{ffe} must also be calculated using X_{mde}. Now it is possible to go back to Step 1 and integrate for the next time step repeating the whole procedure to obtain the values for $t_0+ 2\ \Delta T$.

Notice that there are three iterative loops nested in this method. The outer one is due to the fact that the state equations must be integrated for each time step. The next iterative loop is caused because of the need to find i_1 and Θ_1 for every time step in Step 2. The innermost iterative loop is described in Step 3 and is due to the fact that δ_e must be found iteratively for every value of $i_{1(K)}$ and $\Theta_{1(K)}$ found. The solution procedure is summarized in the flowchart (Figure 3.8) given in the summary in Section 3.5. The flowchart should help visualize this method. The different blocks in the flowchart refer to the different steps in the method just described.

3.4 Solution Example

In order to illustrate the utility of this method the numerical procedure is implemented in a digital computer and some problems are solved using it. In solving these problems the effects of damper windings and current boost system are ignored for simplicity; also X_p is set to zero. The steady-state values are also calculated as described in Section 3.3.1 and Appendix B. The values for the parameters used in this problem and for steady-state values are given in Table 3.1. These parameters belong to the Alterrex exciter-alternator. The steady-state symbols are denoted by the subscript "0".

Using the numerical method the equations for the self-excited exciter-alternator system without damper windings and without the current boost system is solved using the parameters given in Table 3.1. The response obtained for i_L is given in Figure 3.6. The initial conditions for this response are $i_L = \lambda_{fe} = 0$, i.e., the system starts at rest. At time t_0 an impulse is applied to the field winding of the machine in order to start the "build up process"* that takes the machine from rest to a given steady-state. Notice from Figure 3.6 that the current builds up very slowly. This happens

---

* The reader should make in his mind an analogy between the build up process in dc machines and the build up process here. If necessary References [6] and [7] should be reviewed.

Table 3.1

Parameters, Steady-State Values

and

Input for the Solution Example of Section 3.4

X_{ae}	0.135 p.u.
X_{de}	0.69 p.u. (unsaturated)
X_{qe}	0.64 p.u. (saturated)
X_{mde}	0.555 p.u. (unsaturated)
X_{mqe}	0.505 p.u. (saturated)
X_{ffe}	0.725 p.u.
X_{fe}	0.170 p.u.
R_{fe}	8.199×10^{-4} p.u.
R_{ae}	3.781×10^{-3} p.u.
N_p	2 turns
v_e^b	420 volts (line-to-line)
$v_e'^b$	v_e^b / N_p
ω_{eO}	754.0 rad/sec
v_{fe}^b	3.451×10^4 volts
i_{fe}^b	45.78 amps
KVA^b	3160 KVA

Table 3.1 (continuation)

R	0.94×10^{-3} p.u.
L	0.5 p.u.
ω_{LO}	377.0 rad/sec
R_{fe}(in ohms)*	0.931 Ω at 125°C
T_3	7.884×10^{-4} ____
T_4	1.447 ____
T_5	2.33×10^{-3} ____
T_6	189.77 ____
C_0	0.555 ____
C_1	-o.253/68.165 ____
C_2	0.6312/68.165 ____
C_3	-0.4071/68.165 ____
α	70° = 1.2217 rad.
X_p	0 p.u.
i_{lO}	0.9897 p.u.
i_{feO}	2.1235 p.u.
v_{eO}	0.93661 p.u.
δ_{eO}	0.5883 rad.

* R_{fe} (in ohms) is used to find the base values of the field winding.

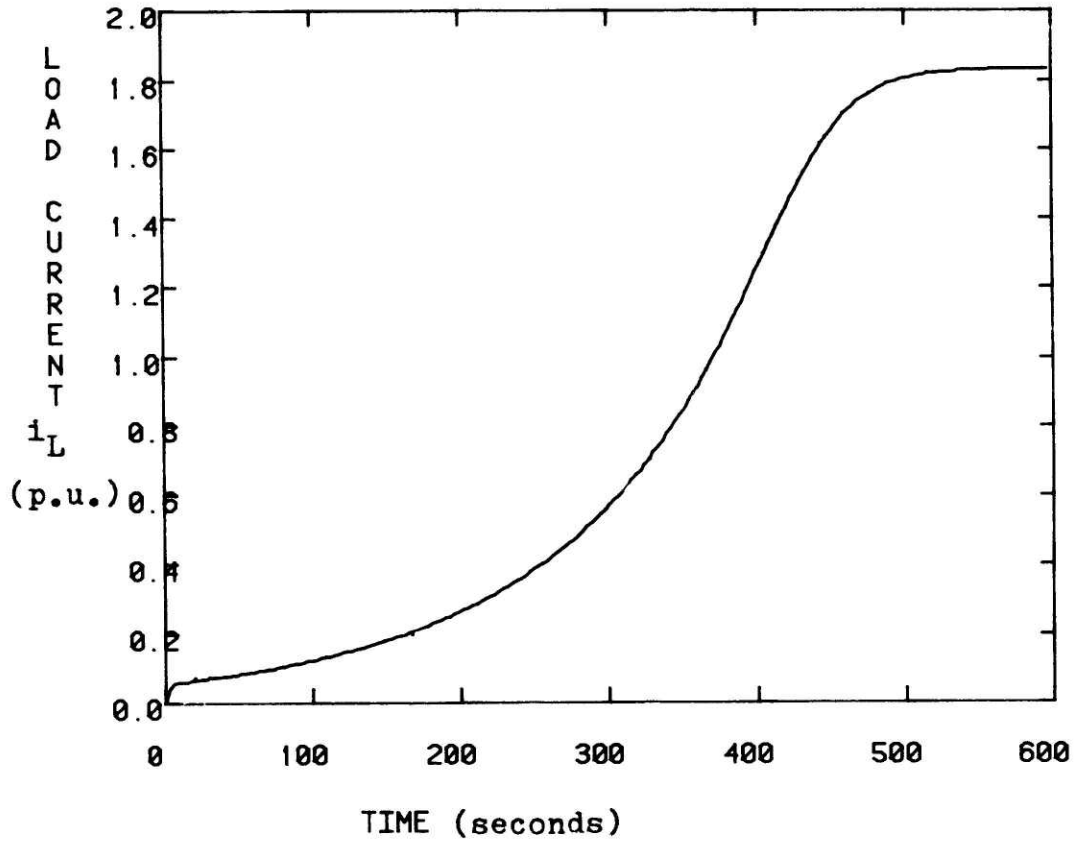

Figure 3.6 Computer plot of the load current i_L.

because the time constants of the exciter-alternator are rather large. However, the system could be made to build up faster by using a time varying input for α so that at the start α is such that forces the system to build up very fast but as the system builds up the firing angle is returned to its nominal value for steady-state operation.

It is of interest now to test how meaningful the answers given by the numerical method are by solving the problem for small disturbances using the numerical method, and comparing the results with the results obtained analytically using a linearized system of equations obtained by linearizing the governing equations about an equilibrium point. The linearized equations and coefficients can be found in Appendix B. From the linearized equations the response to the impulse $\Delta\alpha = 0.0135\ q(t)^*$ is described by

$$\Delta i_L = 0.294\ (e^{-0.111t} - e^{-0.286t}) \qquad (3.47)$$

The symbol Δ in front of the system variables is used to represent the perturbed variables from the equilibrium position, i.e., $\Delta\alpha = \alpha - \alpha_0$ and $\Delta i_L = i_L - i_{LO}$. According to (3.47) the response has a fast growing part and a slowly decaying part, from which it can deduce that the response first

---

* $q(t)$ is used as the impulse function.

rises fast, peaks and then decays slowly. The peak occurs at about 5 seconds and the excursion from the steady-state is of about 0.1 p.u.

The response was also obtained using the numerical method. The result for i_L is plotted in Figure 3.7. As can be seen, it behaves approximately as predicted by the linearization.

3.5 Summary

Equations for the model of the self-excited exciter-alternator were derived in Section 3.2. The derivation of these equations involved modifying some equations from Chapter II and adding new ones to account for the effect of self-excitation and saturation of the exciter-alternator. The governing equations are (2.1) through (2.15) and (3.1) through (3.20). These equations are summarized below. These equations and only these equations constitute the mathematical model for the self-excited exciter-alternator system. Any other equation used is derived from these 35 basic equations. The derivations of the other equations used in this chapter can be found in Appendix B. A solution technique to solve for the steady-state condition is given in Section 3.3.1. A numerical method to obtain the transient solution is given in Section 3.3.2. The numerical procedure is summarized in the flowchart given in Figure 3.8. A table is given here to help differentiate between knowns and variables. The parameters of the exciter-alternator are obtained from the data provided by the

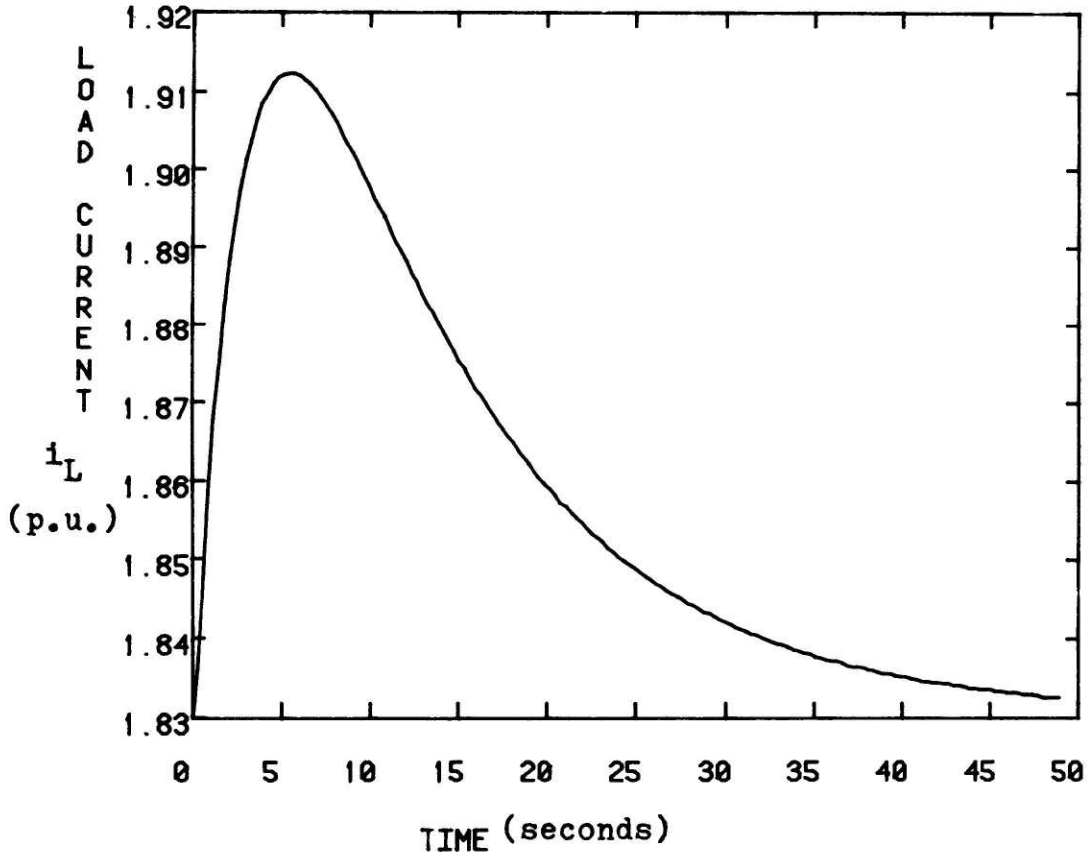

Figure 3.7 Computer plot of the load current i_L.

manufacturer as described in Chapter II in Table 2.2. With the information given in this chapter the user could model a self-excited exciter-alternator with R-L load given a data sheet from the manufacturer is provided.

The equations for the self-excited exciter-alternator.

Exciter-Alternator equations:

$$v_{de} = v_e \sin \delta_e \tag{2.1}$$

$$v_{qe} = v_e \cos \delta_e \tag{2.2}$$

$$i_{de} = i_l \sin (\delta_e + \theta_l) \tag{2.3}$$

$$i_{qe} = i_l \cos (\delta_e + \theta_l) \tag{2.4}$$

$$\lambda_{de} = -X_{de}\, i_{de} + X_{mde}\, i_{fe} + X_{mde}\, i_{kde} \tag{2.5}$$

$$\lambda_{kde} = -X_{mde}\, i_{de} + X_{mde}\, i_{fe} + X_{kde}\, i_{kde} \tag{2.6}$$

$$\lambda_{fe} = X_{ffe}\, i_{fe} - X_{mde}\, i_{de} + X_{mde}\, i_{kde} \tag{2.7}$$

$$\lambda_{qe} = -X_{qe}\, i_{qe} + X_{mqe}\, i_{kqe} \tag{2.8}$$

$$\lambda_{kqe} = -X_{mqe}\, i_{qe} + X_{kqe}\, i_{kqe} \tag{2.9}$$

$$v_{de} = -(\omega_e/\omega_{e0})\, \lambda_{qe} - R_{ae}\, i_{de} \tag{2.10}$$

$$v_{qe} = (\omega_e/\omega_{e0})\, \lambda_{de} - R_{ae}\, i_{qe} \tag{2.11}$$

$$\frac{d\lambda_{fe}}{dt} = -\omega_{e0}\, R_{fe}\, i_{fe} + \omega_{e0}\, v_{fe} \tag{2.12}$$

$$\frac{d\lambda_{kde}}{dt} = -\omega_{e0}\, R_{kde}\, i_{kde} \tag{2.13}$$

$$\frac{d\lambda_{kqe}}{dt} = -\omega_{e0}\, R_{kqe}\, i_{kqe} \tag{2.14}$$

$$X_{mde} = C_0 + C_1 (i_{fe} + i_{kde} - i_{de}) + C_2 (i_{fe} + i_{kde} - i_{de})^2 +$$

$$+ C_3 (i_{fe} + i_{kde} - i_{de})^3 + C_4 (i_{fe} + i_{kde} - i_{de})^4 \qquad (3.1)$$

Load equation:

$$\frac{di_L}{dt} = -\frac{\omega_{LO} R}{L} i_L + \frac{\omega_{LO}}{L} v_L \qquad (2.15)$$

Output Rectifier equations:

$$(2.33)\ T_3 v_e = v_L \qquad (3.2)$$

$$i_L = (T_4/0.78)\ i_1'' \qquad (3.3)$$

Potential Transformer equations:

$$v_{de}' = v_e' \sin(\gamma + \delta_e) \qquad (3.4)$$

$$v_{qe}' = v_e' \cos(\gamma + \delta_e) \qquad (3.5)$$

$$i_{de}' = i_1' \sin(\gamma + \theta_1') \qquad (3.6)$$

$$i_{qe}' = i_1' \cos(\gamma + \theta_1') \qquad (3.7)$$

$$v_{de}' = v_{de} + (\omega_e/\omega_{eO})\ X_p\ i_{qe}' \qquad (3.8)$$

$$v_{qe}' = v_{qe} - (\omega_e/\omega_{eO})\ X_p\ i_{de}' \qquad (3.9)$$

SCR Rectifier equations:

$$(2.33)\ T_5 \cos(\alpha) v_e' = v_{fev} \qquad (3.10)$$

$$i_{fe} = (T_6/0.78)\ i_1' \qquad (3.11)$$

$$\theta_1' = \alpha \qquad (3.12)$$

Terminal Current equations:

$$i''_{de} = i_{de} - i'_{de} \tag{3.13}$$

$$i''_{qe} = i_{qe} - i'_{qe} \tag{3.14}$$

$$i''_{de} = i''_{1} \sin(\delta_e) \tag{3.15}$$

$$i''_{qe} = i''_{1} \cos(\delta_e) \tag{3.16}$$

Current Boost System equations:

$$\frac{dv_{fec}}{dt} = \begin{cases} -\left(\frac{\omega_{e0} R_c}{L_c}\right) v_{fec} + \left(\frac{3 R_c}{2}\right) D; & i - \frac{2 v_{fec}}{3 R_c} < i_m \text{ and } \frac{2i_L}{N_c} \geq i_{fe} \\ -\left(\frac{\omega_{e0}}{L_c} R_c\right) v_{fec} + \frac{R_c}{2} D; & i \geq i_m > \frac{i}{2} - \frac{v_{fec}}{2} \text{ and } \frac{2i_L}{N_c} \geq i_{fe} \\ v_{fec} = 0; & i \geq 2 i_m \text{ or } \frac{2i_L}{N_c} < i_{fe} \end{cases} \tag{3.17}$$

$$D = \frac{di}{dt} = Y_1 \frac{d\lambda_{fe}}{dt} + Y_2 \frac{d\lambda_{kde}}{dt} + Y_3 \frac{d\lambda_{kqe}}{dt} + Y_4 \frac{di_L}{dt} \tag{3.18}$$

$$i = \frac{2i_L}{N_c} - i_{fe} \tag{3.19}$$

$$v_{fe} = v_{fec} + v_{fev} \tag{3.20}$$

Table 3.2

Unknown Quantities System Variables	Known Quantities Input Variables	Known Quantities Parameters
v_{de}	α	X_{de}
v_{qe}		C_0, C_1, C_2 C_3
v_e		X_{kde}
δ_e		X_{ffe}
i_{de}		X_{mqe}
i_1		X_{qe}
i_{qe}		X_{kqe}
Θ_1		ω_{e0}
λ_{de}		R_{ae}
λ_{kde}		X_{ae}
λ_{fe}		R_{fe}
λ_{qe}		R_{kde}
λ_{kqe}		R_{kqe}
i_L		X_{fe}
i_{fe}		X_{ffe}
		N_p
		N_c
i_{kde}		T_3
v_L		T_4
i_{kqe}		T_5
X_{mde}		T_6
i_1''		R
v_{de}'		L
v_e'		X_p

Table 3.2 - Continued

Unknown Quantities System Variables	Known Quantities Input Variables	Known Quantities Parameters
v'_{qe}		λ_m
γ		i_m
θ'_1		L_c
i'_1		R_c
i'_{de}		Y_1
i'_{qe}		Y_2
v_{fev}		Y_3
i''_{de}		Y_4
i''_{qe}		R_{fe} (in ohms)
v_{fec}		v_{fe}^b
i		i_{fe}^b
v_{fe}		v_e^b
D		KVA^b
		$v_e'^b$

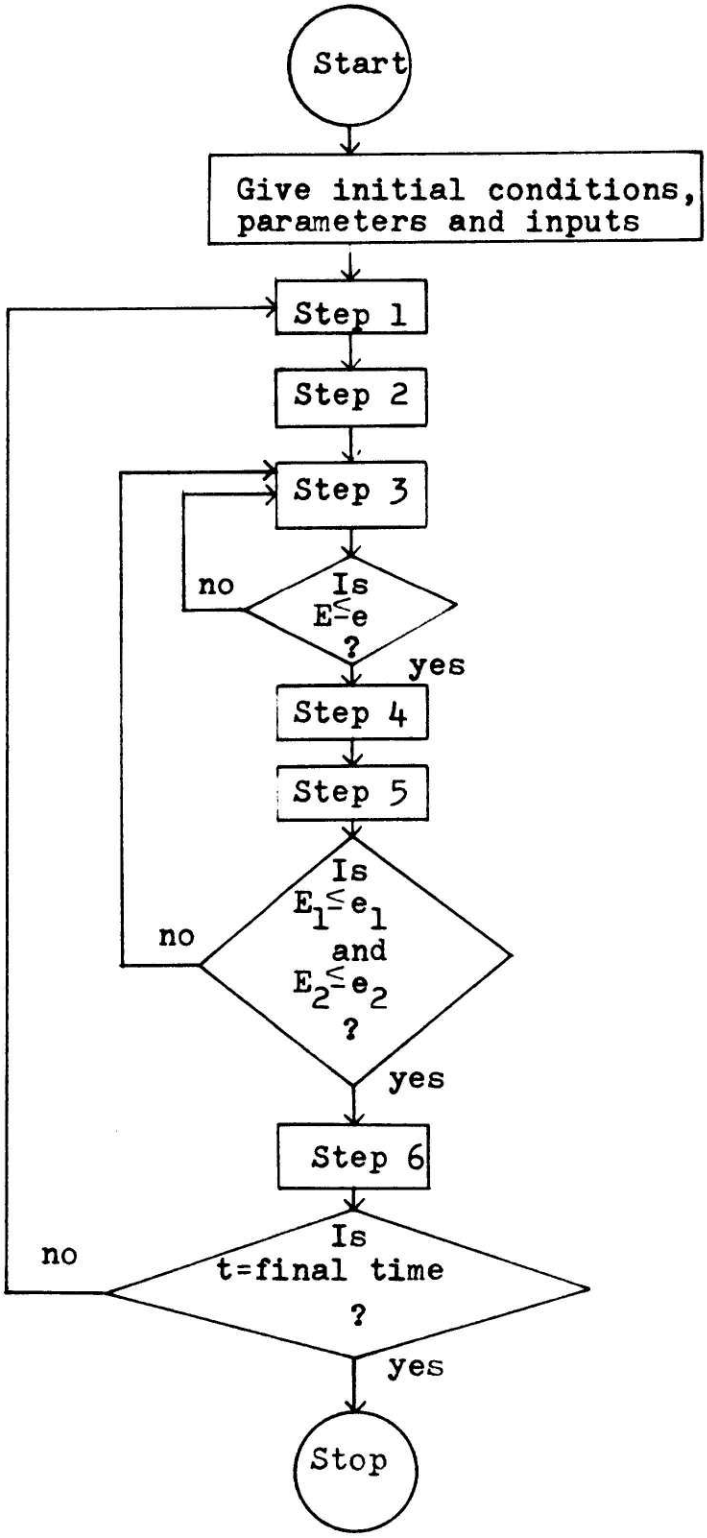

Figure 3.8 Flowchart for the method described in section 3.3.2

Chapter IV: MODEL FOR THE CONTROL SYSTEM

4.1 INTRODUCTION

In this chapter the model for the control system of the Alterrex excitation control system is given. It is important to have the equations describing the behavior of the control system because the control system has a strong effect on the dynamic behavior of the Alterrex system. On the other hand it is desirable to obtain a model which exhibits the essential features of the control function yet is not overly detailed for practical use. Therefore certain simplifying assumptions have been made.

Some of the states of this model are introduced by certain lead-lag compensators consisting of R-C networks. The states introduced by some filters consisting of R-C networks have also been considered. All the other elements of the control system have been assumed not to possess any energy storage capacity, and thus not to introduce additional states. The voltage drop across solid-state junctions have been ignored. The model of the control system is nonlinear. The nonlinearities come about because of saturation of the amplifiers and other effects such as the effect introduced by the limiting systems that will be treated in Section 4.5.

The control system can be divided in several subsystems as can be seen in Figure 4.1. Figure 4.1 shows eight basic blocks: the firing angle system, the automatic regulator, the active reactive current compensator (A.R.C.C), the current

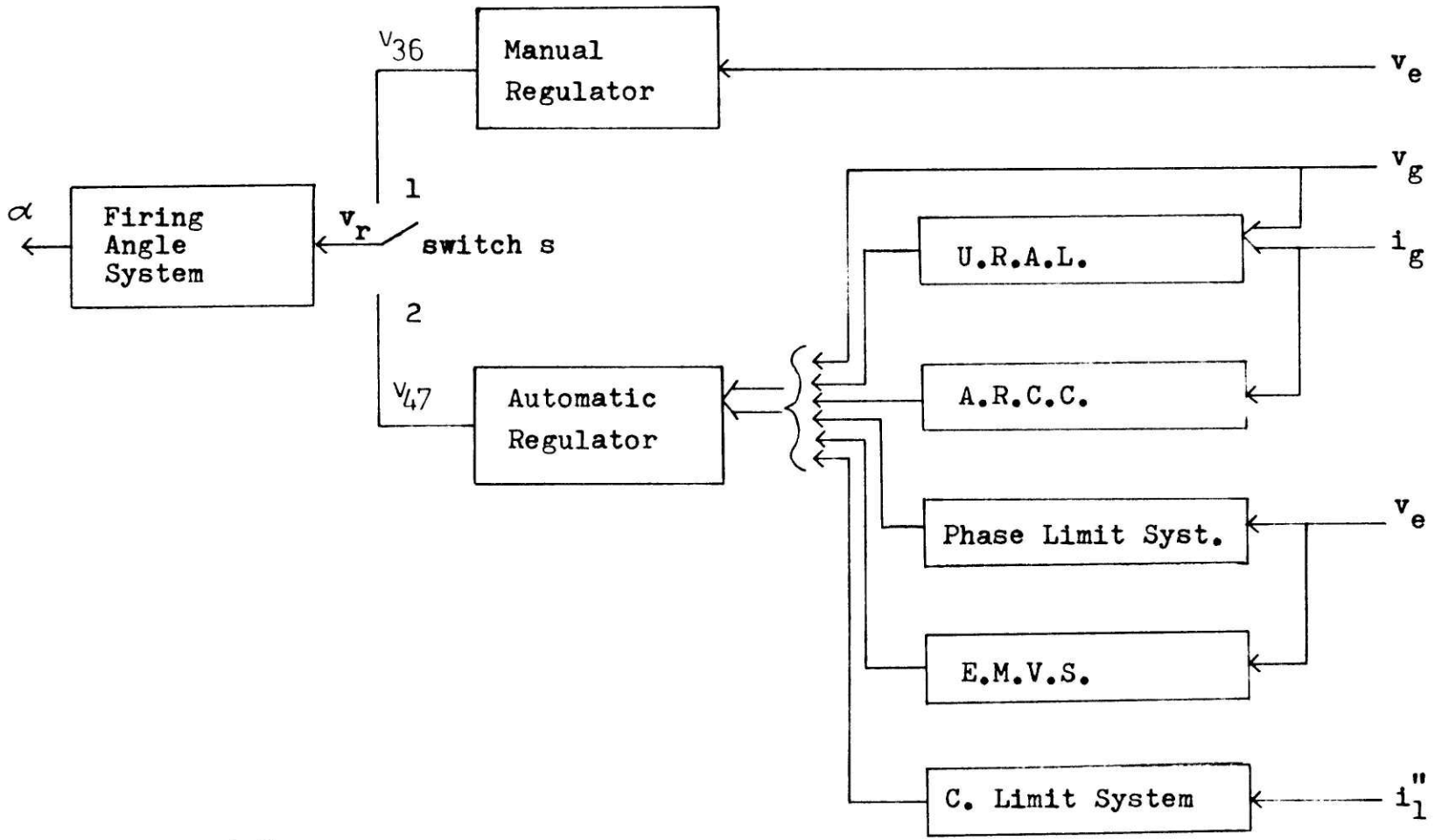

Figure 4.1 Block diagram of control system

limit system, the exciter minimum voltage limit system (E.M.V.S.), the phase limit system, the underexcited reactive ampere limit system (U.R.A.L.) and the manual regulator. Switch s is either in position 1 or 2 depending on whether the system is controlled from the manual regulator or the automatic regulator.

The control system inputs are the exciter-alternator and the main generator currents and voltages. Also the power factor angle θ_g between the main generator terminal voltage and current is an input. The output from the regulator is a continuous signal v_R. This continuous signal is the input to the firing angle system which generates the gate signals that are used to fire the SCR bridge supplying voltage to the Alterrex exciter-alternator field winding.

The purpose of this chapter is to present the model of the control system. The philosophy followed in this chapter is to give the expressions for the control system rather than derive them. Explanations are given for the expressions in terms of the actual physical devices of the system. These explanations are somewhat limited by the fact that it is not possible to show the actual schematics of the Alterrex control system. However, the reader who has access to an Alterrex Manual [4] may find it useful in understanding the control system as described in this chapter. The model is given in block diagram form and the necessary expressions to obtain the governing equations of the system from the block diagram are given in Section 4.7. Section 4.7 includes a table listing the values

for the model parameters of the Alterrex control system. The parameters values are given in Table 4.1 in Section 4.7.

Because the governing equations are not given explicitly but in terms of the block diagram two examples are given, one in Section 4.2 and another in Section 4.7, to demonstrate how to obtain the governing equations using the block diagrams. This should help to clarify how to use the information given here to obtain the necessary governing equations for the control system.

4.2 Firing Angle System

The firing angle system is used to generate the gate signals that are used to fire the SCRs of the Alterrex exciter-alternator. The input to the firing angle system can be either taken from v_{36} or v_{47}, that is from the automatic regulator, exciter minimum voltage limit system and phase limit system output or from the manual regulator output depending on the position of the switch s as can be seen in Figure 4.1.

The model for the firing angle system is given by the block diagram of Figure 4.2. This is a good place to explain how to use the block diagrams presented in this chapter. First notice that the block diagram is read from right to left as indicated by the arrows. This makes it easier to relate back to the actual schematics. Every block of the diagram is represented by a symbol that stands for a functional relationship between the input variables indicated by the arrows coming into the block and the output indicated by the

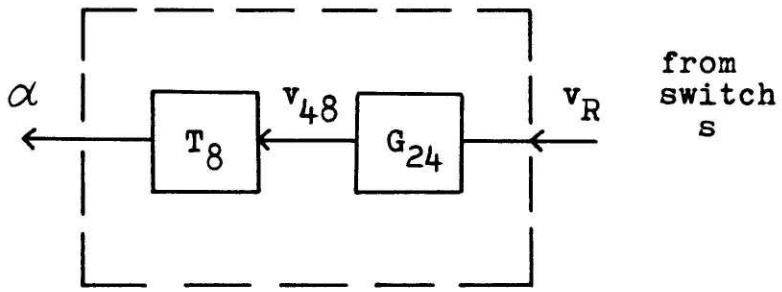

Figure 4.2 Block diagram of firing angle system

arrow pointing away from the block. These functions are indicated by the letter G with a subscript. These functions can be linear or nonlinear.

In the case of the firing angle system we have the function G_{24} relating the input v_R and the output v_{48}. The expression G_{24} is given in Section 4.7 as Equation (4.8). It is simply a multiplicative constant $-g_0$ times v_R. Therefore we have:

$$v_{48} = G_{24}\ (v_R) \tag{4.1}$$

$$= -g_0\ v_R \tag{4.2}$$

In this chapter the parameters of the system will be denoted with positive constants g_0 through g_{61}, p_0 through p_{10} and a_1 and a_2. The symbol v with a subscript is used to represent the input and output signals (voltage signals except where noted) for the different blocks of the diagram. The signal v_{48} (in radians) is the input to the block T_8. The letter T with a subscript is used in this chapter to represent a special type of relationship. The relationship is a nonlinear one and comes about because of saturation in the solid-state and magnetic elements of the system. This nonlinearity can be represented by a linear region in which the block can be represented by a unity gain. However if the given input goes above or below a given limit value, the output of the block is clipped to that limiting

value. From this discussion it follows that in order to specify a function T all that is needed is to specify the limiting values at which the input gets clipped. The limits of the function T_8 are specified in Section 4.7 as given by (4.9). Therefore it follows that:

$$\alpha = \begin{cases} v_{48} \; ; & 0 \text{ rad} \leq v_{48} \leq \text{rad}. \\ 0 \; ; & v_{48} < 0 \text{ rad}. \\ \pi \; ; & v_{48} > \pi \text{rad}. \end{cases} \tag{4.3}$$

Therefore Equations (4.2) and (4.3) constitute the governing equations for the firing angle system.

The control system model has been developed in such a way that the signal v_R is always a negative quantity. Since the angle α is positive and the constant g_0 in (4.2) is also positive a negative sign must be used in expression (4.3) so that v_{48} comes out positive as it should. Therefore for v_R more negative (smaller) α gets bigger and for v_R less negative (bigger) α becomes smaller. Recall from Chapter III that if α ranges between 0 and π then an increase in α implies a smaller exciter-alternator field voltage and a decrease in α implied an increase in the exciter-alternator field voltage as indicated by Equation (3.10).

4.3 Automatic Regulator

The automatic regulator is designed primarily to hold constant voltage at the main generator terminals. The model for the automatic regulator is given in Figure 4.3. The regulator senses v_g by means of a potential transformer and the ac output voltage of this is rectified. This process is represented by block G_2 in Figure 4.3. The expression for G_2 is given by Equation (4.10), which shows that G_2 is a multiplicative negative constant. This negative constant will cause signal v_2 to be negative and in fact all the other signals throughout the automatic regulator will be negative. Signal v_2 is filtered by a low pass R-C filter in order to eliminate the ripple left after rectifying. This process is represented by G_3. This filter is very fast (very small time constant) compared to other dynamics of the feedback loop. In spite of this the dynamics of the filter have been considered in the present model. The expression for G_3 is given by (4.11) in Section 4.7.

Notice that v_3 has been added to a voltage v_{b1}*. This voltage is due to the dc bias voltage used for the transistors and other biasing voltages used in the circuitry. There are a number of these voltages added throughout the model

---

* The symbol Σ is used to represent addition. For example in the present case we have $v_4 = v_3 + v_{b1}$.

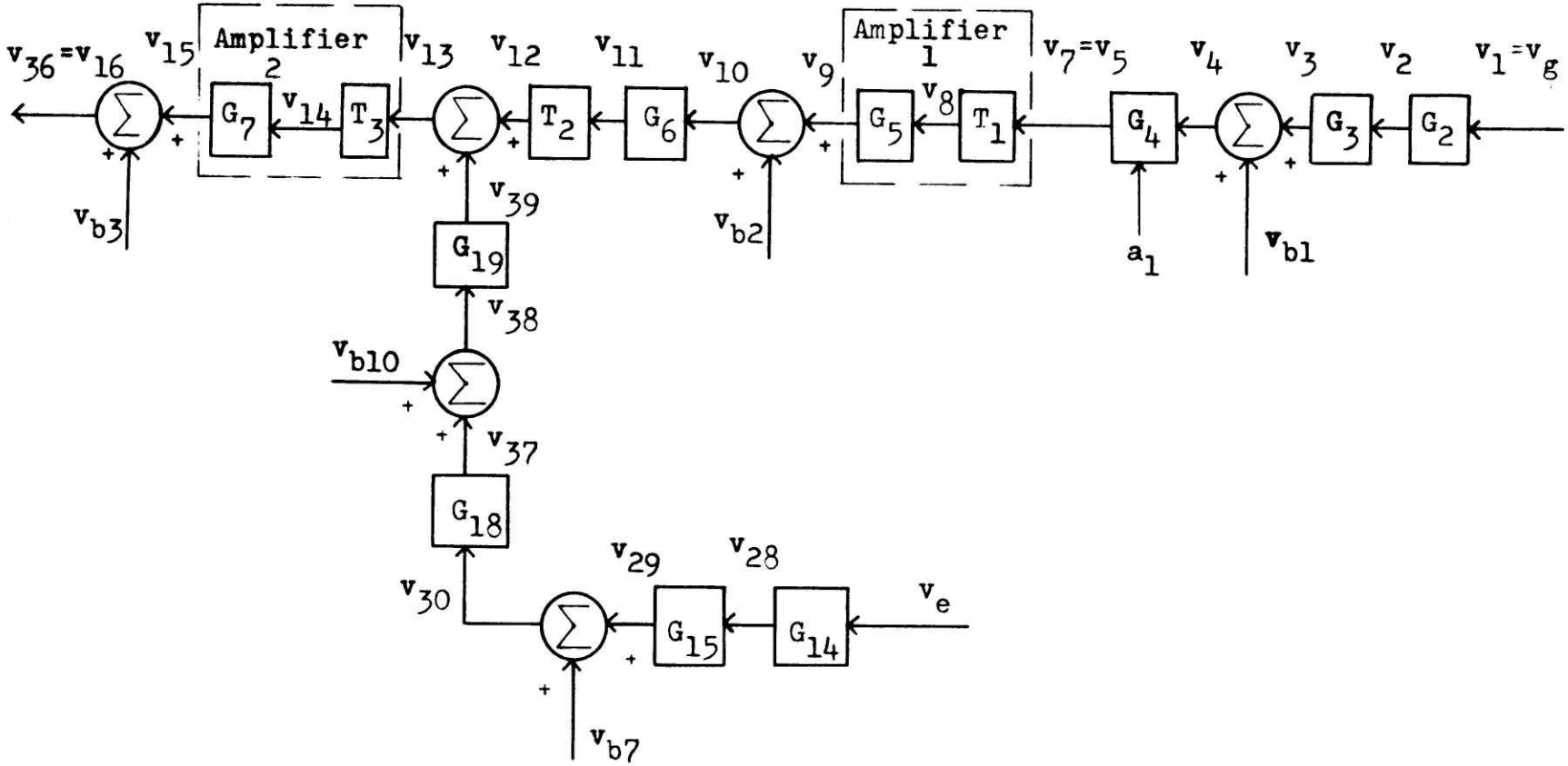

Figure 4.3 Block diagram of automatic regulator.

due to this effect. They have been indicated with the subscript b. These voltages must not be confused with inputs or reference signals. In fact these voltages have very little effect, if any, on the dynamic behavior of this system. The value for v_{b1} is given by (4.12) in Section 4.7.

The signal v_4 is now processed by block G_4. The function G_4 represents a resistive voltage divider. The expression for G_4 is given in Section 4.7 as Equation (4.13). Notice that the expression is given in terms of the adjustable parameter a_1. For given values of a_1, g_5 and g_6 G_4 is a multiplicative constant. By changing the adjustment a_1 then the value of G_4 can be changed.

The output from G_4 is v_5 which in this case it is also equal to v_7, the input to Amplifier 1. Amplifier 1 is a dc transistor amplifier and is modeled by T_1 and G_5. The function G_5 is the gain of the amplifier and is given by equation (4.14) in Section 4.7. T_1 is used to represent the cutoff and saturation effect of the amplifier and is given by (4.15).

The output of the amplifier is superimposed on a bias voltage v_{b2} given by (4.16). The resulting signal v_{10} is processed by block G_6. G_6 is used to represent an R-C lead-lag network whose transfer function is given in Section 4.7 as (4.17). This is a very important element because it adds one of the most dominant states in the system.

A nonlinear element following G_6 is modeled by T_2 given in Section 4.7 as (4.18). The output of T_2 is v_{12}.

The signal v_{12} is modified by adding the signal v_{39} to obtain v_{13}. The signal v_{39} comes from what is called the nonlinear rate feedback. The signal v_{39} is basically a signal proportional to the rate of change of exciter terminal voltage v_e and is obtained as follows. The terminal voltage of the exciter, v_e, is stepped down using a transformer and rectified with a three phase rectifier. This process is represented using the block G_{14}. Function G_{14} is given by (4.19) in Section 4.7. Notice from (4.19) that G_{14} is a negative gain. This comes about because of the way the reference used to measure the voltage signal was defined in the circuitry. This negative sign will cause signal v_{28}, among others, to be a negative dc quantity. The output of G_{14} is signal v_{28} that goes into G_{15}. G_{15} represents the effect of an R-C low pass filter. The output of G_{15} is signal v_{29} which is added to the bias voltage v_{b7} given by (4.20). G_{15} is given by (4.21) in Section 4.7. Adding v_{29} and v_{b7} yield v_{30}.

The voltage v_{30} is now processed by the nonlinear rate feedback section of the system. First the voltage v_{30} is processed by a nonlinear gain G_{18} given by (4.22) in Section 4.7 yielding the signal v_{37}. The signal v_{37} is now added to a bias voltage v_{b10} whose value changes depending on the value of the output v_{38}. This voltage is given by (4.23) in Section 4.7. The result of adding v_{b10} and v_{37} is signal v_{38}. So far signal v_{38} can be considered proportional to the voltage v_e. The proportion changes depending on v_{38} as

manifested by the relationship G_{18}. The signal v_{38} is now processed by G_{19}. G_{19} is basically a differentiator but it also introduces a small delay in the nonlinear rate feedback loop. G_{19} is given by (4.24). Hence v_{39} is proportional to the rate of change of v_e. The purpose of adding a signal proportional to the rate of change of v_e in the feedback loop is to add damping to the system to help stabilize the exciter-alternator. The effect of this signal and the nonlinear gain G_{18} will be illustrated in Chapter V.

Signals v_{12} and v_{39} are added to obtain v_{13} therefore v_{13} has a component proportional to the rate of change of v_e with some delay and a component proportional to v_g with some delay due to the filtering introduced by G_2 and the delay introduced by the lead-lag network G_6. Notice that because of the way the reference has been defined this voltage is negative. This signal, v_{13}, is now amplified by the dc amplifier 2. Amplifier 2 is modeled by the saturating function T_3 and the gain G_7 as given in Section 4.7 by (4.25) and (4.26). The output of amplifier 2, v_{15}, is superimposed on the bias voltage v_{b3}. The resulting voltage is v_{16} which is also shown equal to v_{36}. If switch s shown in Figure 4.1 is in position 2 then v_R is also equal to v_{36}.

Therefore in conclusion the automatic regulator introduces a negative feedback signal based upon generator terminal voltage. The automatic regulator also has an input from exciter terminal voltage in order to introduce a stabilizing

signal for the exciter. Let us illustrate the behavior of the automatic regulator with the following example. Assume that the output of the automatic regulator of Figure 4.3, v_{16}, is connected to the input of the firing angle system, Figure 4.2, i.e. the switch s is in position 2. The input to the automatic regulator is taken from v_g. Therefore we have the closed-loop system defined as in Figure 1.4 by a self-excited exciter-alternator feeding the field winding of the main generator. The control system in Figure 1.4 is here defined by the automatic regulator and the firing angle system. Assume that the system is in steady-state working at given values of v_g, α and regulator signal voltages.

If there is an increase in generator terminal voltage, this will cause a decrease in the signal v_2 (recall that this voltage is the output of G_2 which is a negative gain). Similarly, without dwelling on the delays of the feedback loop caused by filtering and compensation, all the signals of the feedback loop will be decreased including v_R. A decrease in v_R causes an increase in v_{48} (recall that G_{24} was a negative gain). An increase in v_{48}, assuming it is between the limits set by T_8 will cause an increase in α. From Equation (3.25) in Chapter III it follows that the voltage across the field winding of the exciter-alternator is decreased from which follows that after some delay the exciter terminal voltage decreases causing a decrease in the field current of the main generator. This, after some delay, will cause the

terminal voltage to be decreased, which will tend to return back to its initial value.

The effect of the nonlinear rate feedback comes into play as follows. Assume that the exciter-alternator voltage for the case above decreases so fast that it results in overcorrection of the voltage v_g and therefore in instability. What rate feedback does, without dwelling on the effect of the nonlinear gain is explained as follows. If v_e decreases too fast it means that v_{28} increases rapidly (recall that G_{14} is a negative gain). As a result the differentiator G_{19} will produce a positive dc voltage for v_{39} momentaneously. Since v_{12} is negative a positive increment of voltage from v_{39} will cause v_{13} to be less negative than it would have been without the rate feedback effect. The angle α increases to a lesser extent which results in the exciter voltage not decreasing as fast and therefore in the main generator terminal voltage not being overcorrected. It follows that the nonlinear rate feedback helps to stabilize the system.

4.4 Active-Reactive Current Compensator

The main function of the automatic regulator, described in Section 4.3, is to keep the main generator terminal voltage v_g unchanged. Sometimes however it is desired to regulate the voltage at some point in the power system other than at the generator terminal. In that case it is necessary to substitute for v_g the signal that needs to be regulated. Because the actual voltage that needs to be regulated is anywhere in the

system, possibly far away from the physical location of the regulator, it is not always practical to make a connection between that point and the regulator.

What is done instead is to estimate the voltage in question. This is fairly simple to do because all that needs to be known is the impedance between the main generator terminal voltage and the voltage that needs to be regulated, the current flowing through it (generator terminal current, i_g), the generator terminal voltage v_g and the phase angle, Θ_g, between v_g and i_g. With these then it is possible to calculate the voltage to be regulated, substituting that voltage for v_g.

Figure 4.4 shows the block G_1 representing the process used to estimate a given voltage in the power system. This block is placed between v_g and the input to the automatic regulator, v_1. The expression for G_1 is given in Section 4.7 by (4.27). The expression is nonlinear because the voltage v_g and the voltage between the main generator terminals and the point of interest must be substracted vectorially.

4.5 Limiting Systems

The automatic regulator is designed to control the behavior of the generator terminal voltage or of some voltage in the power system. In the process of regulating these variables the automatic regulator might try to force certain variables in the system to increase (or decrease) above (or below) a certain limit beyond which the safety of the equipment

could be endangered. For example if the load at the output of the main generator is increased (i.e. if more power is demanded by the power system) this would tend to decrease the terminal voltage. Therefore the regulator will change the angle α in order to increase the exciter terminal voltage to correct the voltage v_g. The loading conditions might be such however that the exciter terminal voltage called by the control system to correct the decrease in v_g is too high and consequently the exciter terminal current goes above its rated value. This would mean endangering the safety of the equipment in order to keep the main generator terminal voltage constant. In a case like that the survival of the system takes priority and the regulation of v_g is maintained within safe limits. In order to do this, Limiting Systems are used.

The purpose of the Limiting Systems is then to limit the extent to which certain system variables can change by taking over control from the main generator terminal voltage of the automatic regulator when the survival of the system is in danger. The limiting systems used in the control system that are of importance are the following: the current limit system, the exciter minimum voltage limit system, the phase limit system and the underexcited reactive ampere limit system.

Before continuing with a description of these systems it is convenient to define two auxiliary functions. These are the functions C^h and C^L and are given in block diagram form in Figure 4.5. These functions may have n inputs but only one output. The output v_o in the case of C^h will be equal to

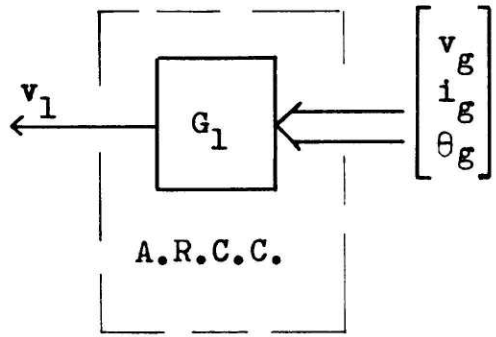

Figure 4.4 Block diagram of the Active Reactive Current Compensator

the highest input or inputs. For the block C^L the output will be equal to the lowest input or inputs. Let us call these functions "low signal comparator" and "high signal comparator." As will be seen shortly, these functions will help formulate in block diagram form the action of the limiting control systems.

4.5.1 The Current Limit System

Let us recall the example presented above. There it is shown that during certain conditions the automatic regulator might force the exciter terminal current and therefore the main generator field current to increase to levels which are undesirable for the safety of the system. A remedy for this is to use a current limit system which takes control of the regulator by cutting off the signal provided by the main generator terminal voltage and substituting in its place a signal proportional to i_1''.

This can be implemented by using a low signal comparator C_1^L placed in the automatic regulator between blocks G_4 and T_1. The resulting system is shown in Figure 4.6. The current i_1'' is obtained from the secondaries of the current boost transformers. The current is stepped down using current transformers connected from the secondary terminals of the current boost transformers which feed a resistive network. The resulting voltage signal from the resistive network is a

time varying voltage. This voltage is rectified resulting in a signal proportional to i_1''. The process just described is represented by G_8 which yields the output v_{17}. The expression for G_8 is given by (4.28) in Section 4.7. Notice that G_8 is a negative constant. This comes about because of the reference chosen to measure the voltages in the circuitry. The signal v_{17} is then passed through a low pass filter represented by G_9. The transfer function for G_9 is given by (4.29) in Section 4.7. The output of G_9 is signal v_{18} which is superimposed on the bias voltage v_{b4}, given by (4.30) in Section 4.7. This yields signal v_{19} proportional to i_1'' which is fed into C_1^L along with v_4. Therefore v_6 will be equal to the lowest of these two signals.

Let us now go through an example to show how a limiting system actually behaves. Assume that the system is at a given point operating in steady-state. The automatic regulator is regulating main generator terminal voltage very well so that any small deviation of this voltage from the nominal value is quickly corrected. Therefore it can be assumed that the voltage at the terminal of the main generator is always close to the nominal voltage and therefore the voltage signals throughout the automatic remain almost constant at some operating point.

Let us repeat now the experiment done in the previous section where the loading conditions are increased gradually so that the exciter terminal voltage and therefore exciter terminal current are increased to levels endangering the

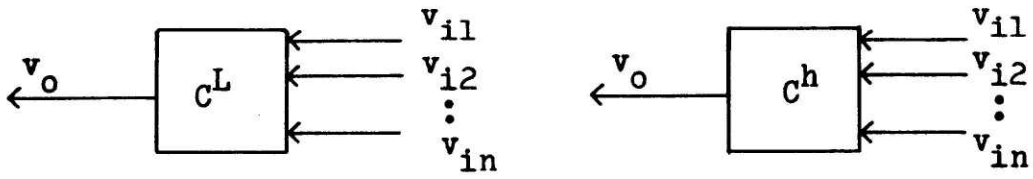

Figure 4.5 Block diagrams representing the functions C^h and C^L

survival of the system. As the exciter terminal current increases the input to the current limit system increases. Then this implies that signal v_{17} is decreasing (recall that G_8 is a negative gain). Signal v_{17} decreasing implies v_{18} and v_{19} decreasing. During normal operation the current limit system is designed so that v_{19} is less negative and therefore bigger than v_5 which usually remains fixed at some operating point. The current limit system is designed so that when the exciter terminal current is equal to the value of current which is considered to endanger the survival of the system v_{19} is equal to the value of v_5 which is always close to some operating point. Any further increase in i_1'' will cause v_{19} to fall below v_5 which means that v_6 would no longer be equal to v_5 but tends towards v_{19}. At this point the automatic regulator ceases to be a main generator terminal voltage regulator and becomes an exciter terminal current limiter. Therefore any further increase in i_1'' causes a decrease of v_{19} which after some delay causes a decrease in v_R, increasing α. Therefore exciter field voltage is decreased which decreases exciter-alternator terminal voltage which consequently decreases exciter terminal current. Therefore exciter terminal current is limited. Notice that now the exciter terminal current is well regulated which means that as long as the current limit system is in control the value of i_1'' remains almost constant which further implies that the

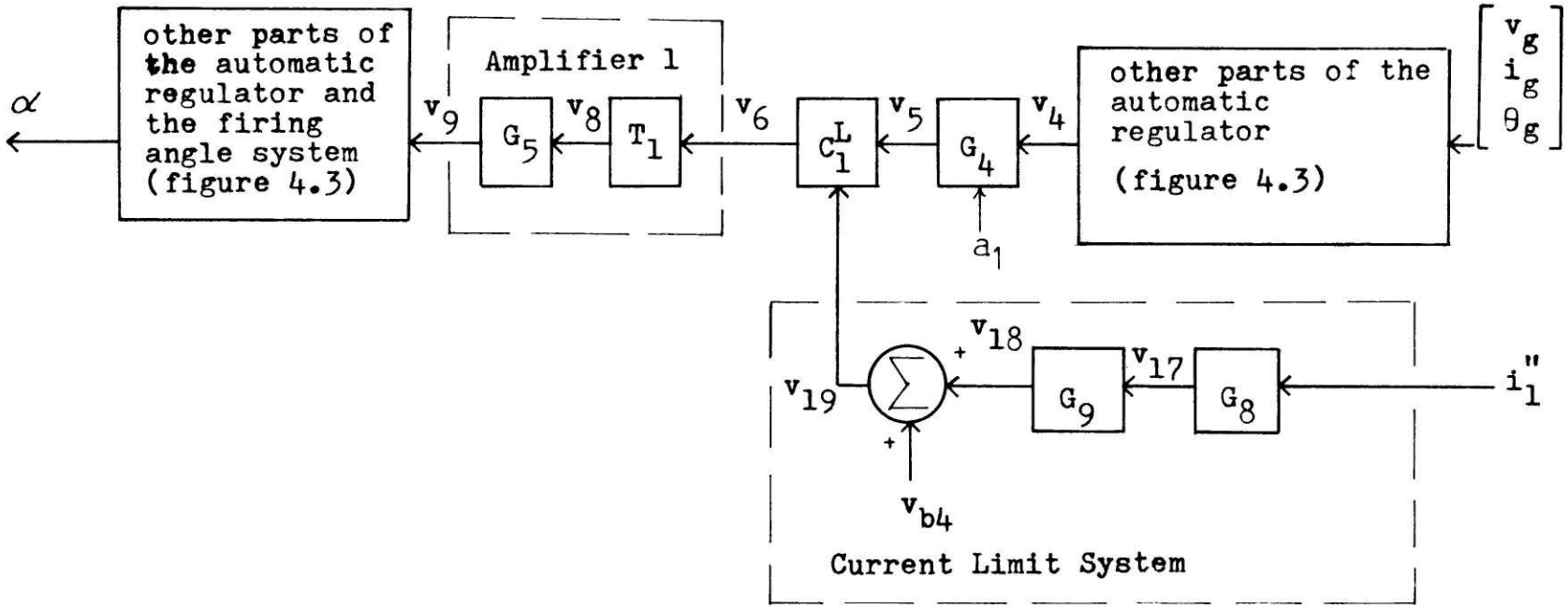

Figure 4.6 Block diagram of current limit system

signals throughout the regulator including v_{19} remain close to an operating point.

Say now that the loading conditions that caused the increase in exciter terminal current are changed so that the load demanded is decreased. Since the exciter terminal current is kept constant at the value required for the higher loading condition, the main generator voltage, which during the time the current limit system is in control is unregulated, will tend to increase to a value higher than nominal, but it also happens that this causes the signal v_5 to decrease to a value lower than the operating value of v_{19}, therefore at this moment the voltage v_6 will no longer be equal to v_{19} but it will become v_5 again. Therefore the automatic regulator goes back to regulate main generator terminal voltage.

4.5.2 The Underexcited Reactive Ampere Limit System

The underexcited reactive ampere limit system is designed to help maintain steady-state stability. This is achieved by imposing a limit on the magnitude of the generator underexcited reactive current. This limit is shown graphically in Figure 4.7. Figure 4.7 shows a portion of the capability curve for the underexcited region of the curve. In order to retain steady-state stability the main generator must operate inside the curve shown. Therefore what is needed is a system that takes over control of the automatic regulator by cutting off regulation of the terminal voltage, v_g, and introducing

instead a signal dependent on underexcited reactive current in order to regulate and limit the underexcited reactive current when it goes above levels that might endanger the stability of the system. Such a system is shown in Figure 4.8.

This system uses the function G_{10} given in Section 4.7 by expression (4.31). This expression comes about from the way the detecting circuitry was designed. The reader is referred to Reference [4]. Normally block G_{10} yields a negative output. Notice that block T_4 clips the signal v_{20} at 0 and 10 volts. Therefore normally the output at T_4 is zero. T_4 is given by (4.32). Under any other conditions voltage v_{21} is restricted to be between zero and ten volts. Because of the last statement and because v_{b5} is a constant biasing voltage equal to -24 volts, as given by (4.33) in Section 4.7, the resulting signal will always be a negative dc signal. Signal v_{27} is a dc signal proportional to the rate of change of exciter terminal voltage used to stabilize the underexcited reactive ampere limit system. This signal, v_{27}, is obtained by using the signal v_{38} from the nonlinear gain of the automatic regulator and processing it by the differentiator represented by G_{13}. The transfer function for G_{13} is given by (4.34) in Section 4.7. This signal has an effect on the underexcited reactive ampere limit system similar to the effect of v_{39} on the automatic regulator. The resulting signal v_{22} is fed now to amplifier 3 modeled by T_5 and gain G_{11}. T_5 and G_{11} are given by (4.35) and (4.36) respectively in Section 4.7. The resulting signal v_{24} is

then added to a bias signal v_{b6} given by (4.37). The resulting signal v_{25} is then processed by a lead-lag network, G_{12}. The expression for G_{12} is given by (4.38) in Section 4.7. The resulting signal v_{26} is the output from the U.R.A.L. Then using the high voltage comparator C_2^h between C_1^L and amplifier 1 the desired effect is obtained.

Assume that the underexcited reactive current goes below the limit set by the dashed lines in Figure 4.7. This would result in G_{10} producing a positive dc signal v_{20}. After this signal is processed by T_4 it results in a positive signal v_{21}. Due to the effect of the bias voltage v_{b6}, v_{22} comes out a negative signal. Without dwelling on the effect of the stabilizing signal v_{27} the signal v_{22} is approximately the result of v_{21} and v_{b5}. As the underexcited reactive current magnitude continues to increase the positive dc signal v_{21} increases which translates into the dc signal v_{22} being less negative, i.e. increasing. This will also translate in the other signals of the U.R.A.L. increasing. As this goes on there will be a point when v_{26} has increased so much that it is bigger (less negative) than the operating point v_6, therefore at this point v_7 ceases to be equal to v_6 and becomes equal to v_{26}, i.e. the underexcited reactive ampere limit system takes control of the automatic regulator. The underexcited reactive ampere limit system is designed to take control when the main generator operating point violates the underexcitation constraint on the capability curve.

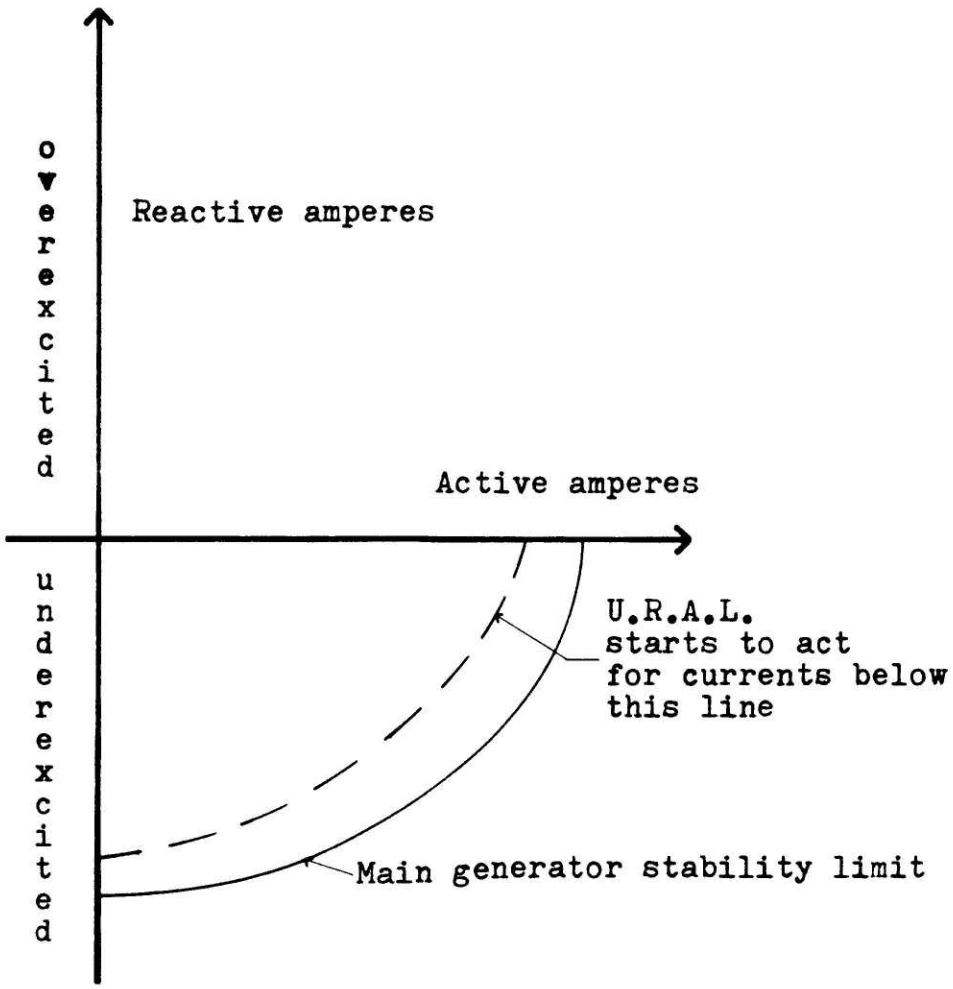

Figure 4.7 Graphical representation of U.R.A.L. limiting function

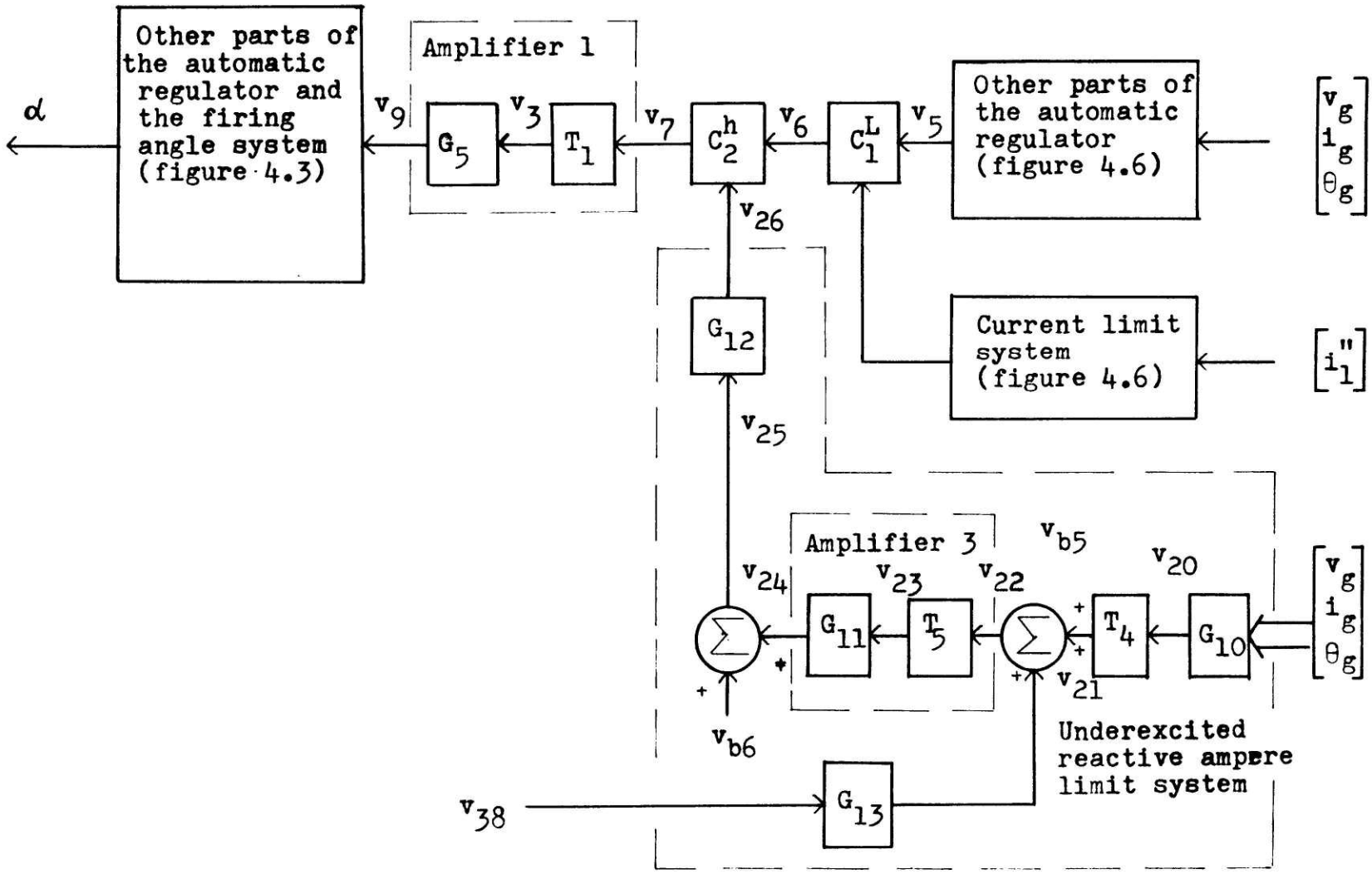

Figure 4.8 Block diagram of the Underexcited reactive ampere limit system

4.5.3 The Exciter Minimum Voltage Limit System

During certain transient conditions the regulator might force the angle α to be equal to 90° in which case the average voltage applied to the field winding of the exciter-alternator is zero. If this condition is maintained for too long the exciter-alternator output voltage may collapse as is indicated in the discussion of the current boost system in Chapter III. The purpose of the exciter minimum voltage limit system is to put a lower bound on the value of the exciter voltage such that it doesn't collapse. The exciter minimum voltage limit system is shown in Figure 4.9.

Notice that the first part of the system up to the point yielding signal v_{30} has been explained before when discussing the nonlinear rate feedback for the automatic regulator. Signal v_{30} is now processed by G_{16} which is a voltage divider which reduces the signal v_{30} to v_{31}. G_{16} is given by (4.39). The signal v_{31} is now added to the bias voltage v_{b8} yielding v_{32}. The bias voltage v_{b8} is given by (4.40). This signal is now amplified by Amplifier 4. Amplifier 4 is modeled by T_6 and G_{17} given by (4.41) and (4.42) respectively in Section 4.7. The output from Amplifier 4 is v_{34} which is added to bias voltage v_{b9}, given by (4.43), yielding v_{35} which goes into the signal comparator C_3^h along with v_{16}.

During normal condition v_{16} is bigger than v_{35} (less negative) which means the automatic regulator is in control of

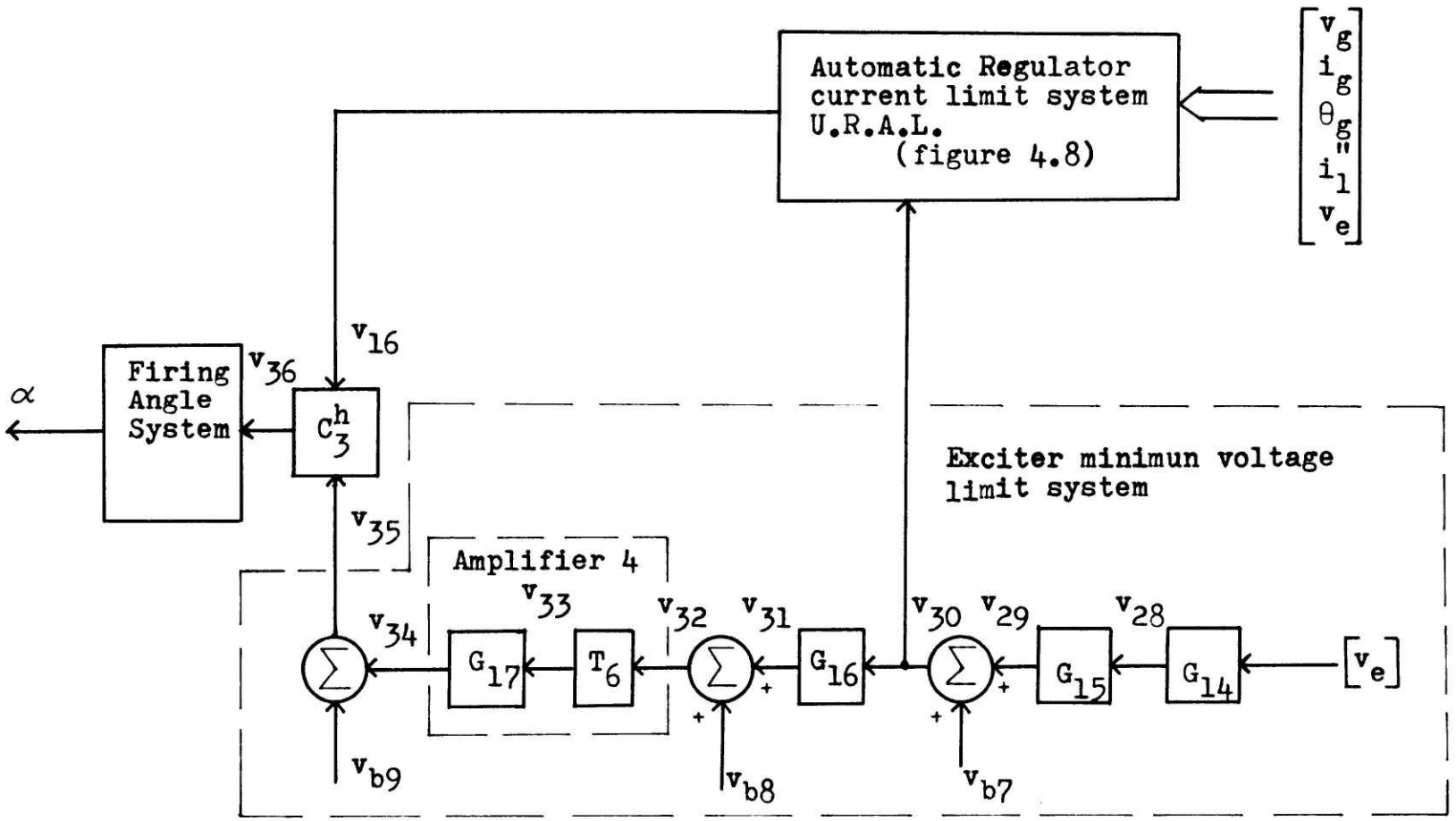

Figure 4.9 Exciter minimum voltage limit system

the firing angle system. Let us assume that the loading conditions are suddenly lowered to such an extent that the automatic regulator forces the exciter terminal voltage to go very low in order to keep the main generator terminal voltage constant. As the exciter terminal voltage goes low signal v_{30} increases (becomes less negative). Without dwelling on the delays of the system it can be seen that as v_{30} increases, v_{35} increases too. The system is designed so that v_{35} becomes higher than v_{16} for the value of exciter terminal voltage below which the system could be in danger of collapsing. The exciter minimum voltage limit system therefore takes control at this point and starts regulating V_e in order to keep it above the limit. When the conditions return to normal the automatic regulator takes control of the firing angle system again.

4.5.4 Phase Limit System

For some reason, the phase limit system is used to put a lower bound on the value of exciter field voltage in order to limit the degree of negative voltage which can be applied when attempting to quickly reduce exciter terminal voltage. This is accomplished by limiting the value of α. Therefore it is necessary to place a lower bound on voltage v_R as shown by Figure 4.10. A small component of v_{30}, v_{40}, is obtained from the voltage divider G_{20} and added to the bias voltage v_{b11} to obtain v_{41}. Expression for G_{20} and v_{b11} are given by (4.44) and (4.45) in Section 4.7. Signal v_{41} is

then processed by the divider G_{21} to yield v_{42}. G_{21} is given by (4.46).

The signal v_{42} is determined mostly by the fixed bias voltage v_{b11}. Therefore v_{42} is a fixed limit (it actually does change a little bit due to the small component from v_{30}). Therefore all that the phase limit system does is to take control of the firing angle system and set α to a fixed minimum value whenever it happens that v_{16} and v_{35} try to force the angle α to a value below which undesirable inversion of field voltage is obtained (recall that for angles between $\pi/2$ and π the SCR bridge actually gives negative average voltage to the field winding, according to Equation (3.25)).

4.6 Manual Regulator

The control system of the Alterrex system has also a manual regulator which may be used to control the level of excitation. This regulator is shown in Figure 4.11. Notice that the manual regulator is very similar to the minimum exciter voltage limit system.

As in the case of the exciter minimum voltage limit system the input v_e is rectified and filtered by a low pass filter. Both effects have been grouped using the same function G_{22}. The transfer function for G_{22} is given in Section 4.7 as Equation (4.47). Notice that G_{22} is a function of the adjustable parameter a_2. Notice also that the gain of transfer function is a negative constant. The output from G_{22} is superimposed on a bias voltage v_{b12} and the

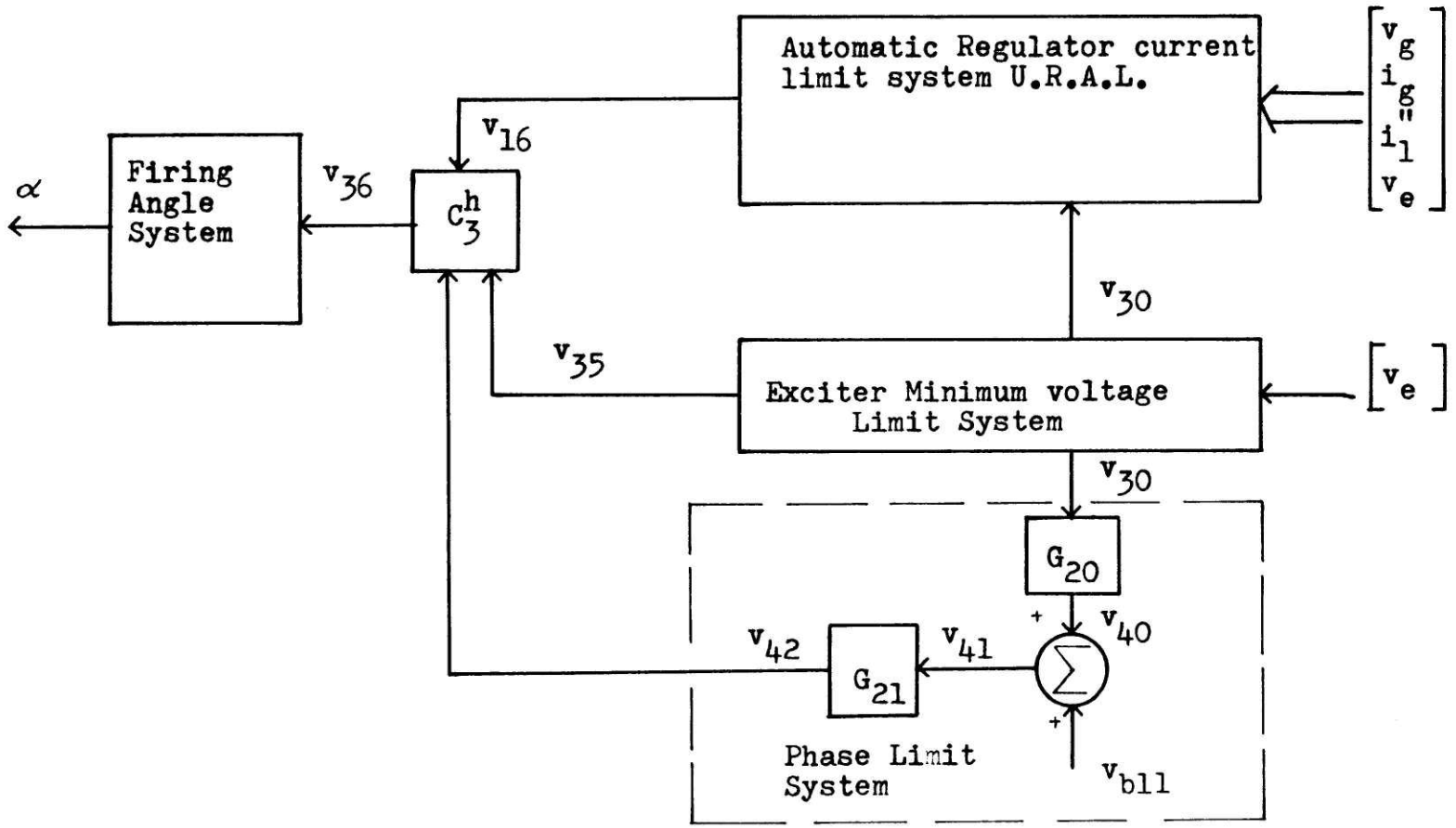

Figure 4.10 Block diagram for phase limit system

resulting signal, v_{44}, is amplified by Amplifier 5 modeled as G_{23} and T_7. The voltage v_{b12}, and functions T_7 and G_{23} are given by (4.48), (4.49) and (4.50) respectively in Section 4.7. The output from Amplifier 5, v_{46} is superimposed on v_{b13}, given by (4.51), resulting on v_{47} the output of the manual regulator.

When switch s is in position 1 the manual regulator is in total control of the system. Its main function is to regulate the level of excitation v_e. This is accomplished because as v_e tries to change the regulator reacts as to change α such that it corrects the change in v_e. By changing the adjustable parameter a_2 the overall closed-loop gain of the system can be changed and therefore the level of excitation can be controlled manually.

4.7 Mathematical Model For The Control System

In this section all the information given in this chapter is summarized. The complete block diagram for the control system is given in Figure 4.12. The expressions necessary to obtain the governing equations are listed below as (4.8) through (4.51). The expressions are written in terms of positive parameters g_0 through g_{61}, p_0 through p_{10} and adjustable parameters a_1 and a_2. The values for these parameters are given in Table 4.1. The control system is modeled in terms of actual units rather than in per unit. Since the inputs are in per unit, the blocks at the beginning of the model must account for this by multiplying the inputs by

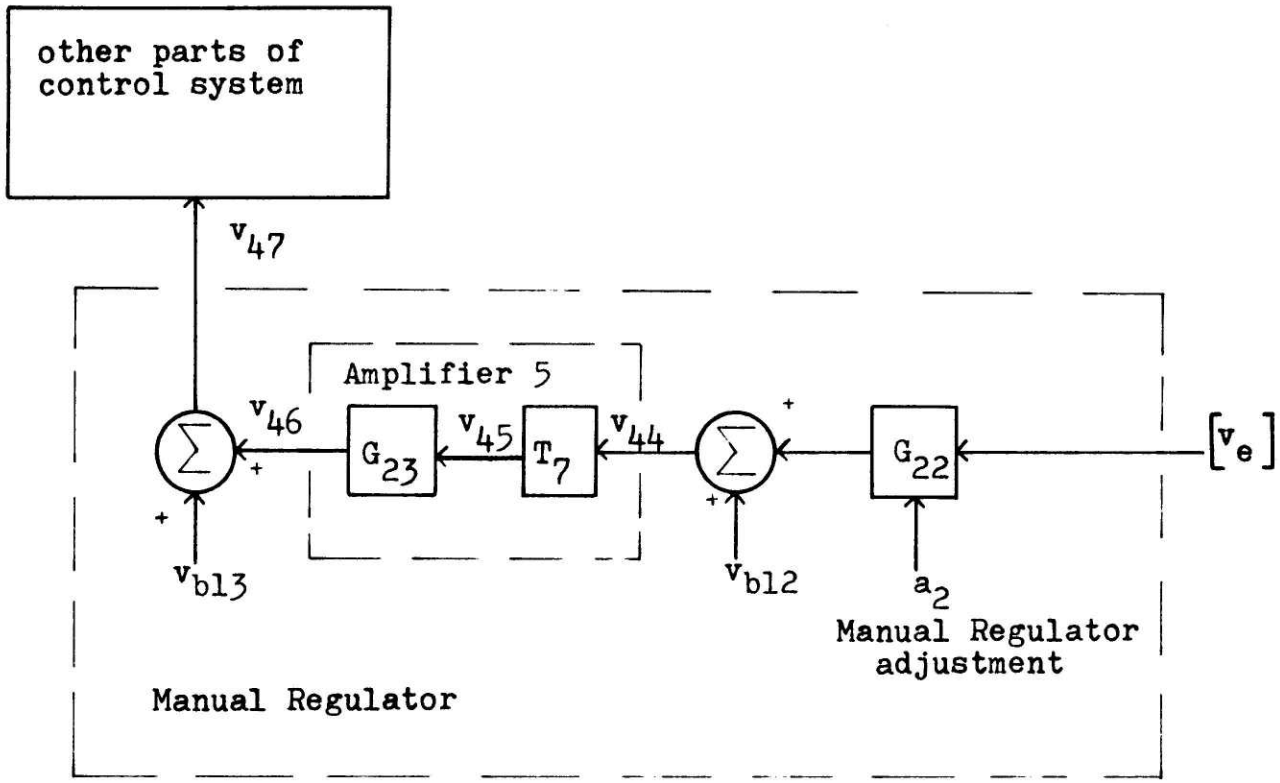

Figure 4.11 Block diagram of Manual Regulator.

the system base values. The letter s was used here to represent the derivative operator. So for example in the case of G_3 in the automatic regulator we have that the governing equations relating v_2 and v_3 is obtained using the transfer function for G_3 as follows:

$$v_3 = G_3(s)\ v_2 \tag{4.4}$$

$$= [g_4/(p_0 + s)]v_2 \tag{4.5}$$

then:

$$v_3(p_0 + s) = g_4\ v_2 \tag{4.6}$$

and:

$$\frac{dv_3}{dt} = -\ p_0\ v_3 + g_4\ v_2 \tag{4.7}$$

where (4.7) is the state equation relating v_3 and v_2.

Expressions (4.8) through (4.51) are:

Firing Angle System Equations

$$G_{24} = -g_0\ v_R \tag{4.8}$$

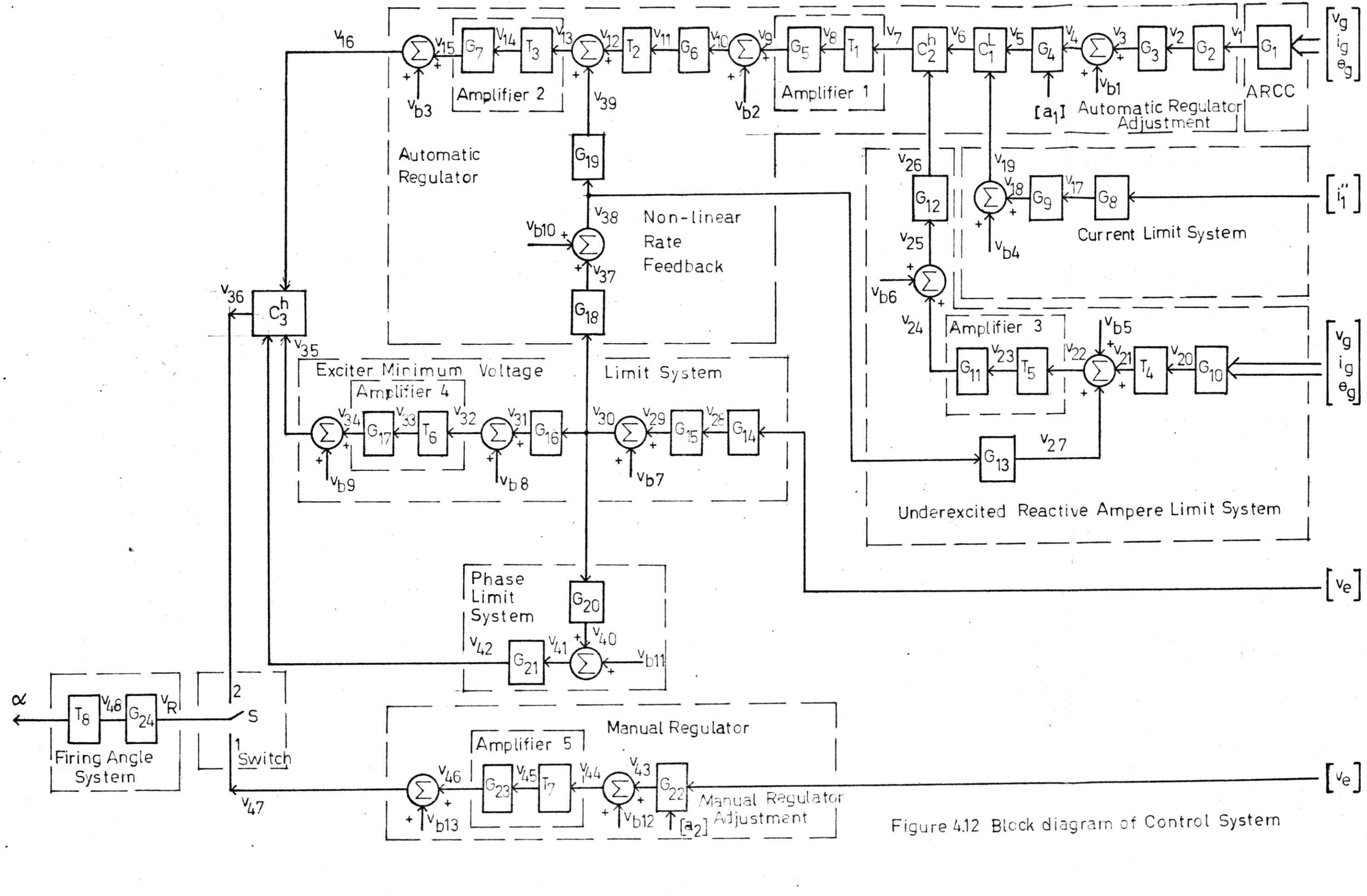

Figure 4.12 Block diagram of Control System

T_8: upper limit = g_1; lower limit = g_2 (4.9)

$$G_2 = -g_3 \tag{4.10}$$

$$G_3 = g_4/(p_0 + s) \tag{4.11}$$

$$v_{b1} = -g_5 \tag{4.12}$$

$$G_4 = a_1 g_6 + g_7 \tag{4.13}$$

$$G_5 = g_8 \tag{4.14}$$

T_1: upper limit = g_9; lower limit = $-g_{10}$ (4.15)

$$v_{b2} = 24 (-1 + g_8) = g_{57} \tag{4.16}$$

$$G_6 = \frac{g_{11} (s + p_1)}{(s + p_2)} \tag{4.17}$$

T_2: upper limit = g_{12}; lower limit = $-g_{13}$ (4.18)

$$G_{14} = -g_{14} \tag{4.19}$$

$$v_{b7} = -g_{15} \tag{4.20}$$

$$G_{15} = \frac{g_{16}}{s + p_3} \tag{4.21}$$

$$G_{18} = \begin{cases} g_{17} & v_{38} < -g_{18} \text{ volts} \\ g_{19} & v_{38} \geq -g_{18} \text{ volts} \end{cases} \tag{4.22}$$

$$v_{b10} = \begin{cases} -g_{20} \text{ volts} & v_{38} < -g_{18} \text{ volts} \\ -g_{21} \text{ volts} & v_{38} \geq -g_{18} \text{ volts} \end{cases} \tag{4.23}$$

$$G_{19} = \frac{g_{22}\, s}{s + p_4} \tag{4.24}$$

$$v_{b3} = 24\ (-1 + g_{23}) = g_{60} \tag{4.25}$$

$$G_7 = g_{23} \tag{4.26}$$

The Active-Reactive Current Compensator Equation

$v_1 = G_1\ (i_g,\ v_g,\ \Theta_g)$

$$v_1 = [(v_g + g_{24}\, i_g \cos \Theta_g + g_{25}\, i_g \sin \Theta_g)^2 + (g_{25}\, i_g \cos \Theta_g - g_{24}\, i_g \sin \Theta_g)^2]^{1/2} \tag{4.27}$$

$$G_8 = -g_{26} \tag{4.28}$$

$$G_9 = \frac{g_{27}}{s^2 + s\,(p_5) + p_6} \tag{4.29}$$

$$v_{b4} = -g_{28} \tag{4.30}$$

Underexcited Reactive Ampere Limit System

$$v_{20} = G_{10}\,(i_g,\ v_g,\ \Theta_g) =$$

$$[(g_{29}\ i_g\ [g_{30} \cos \Theta_g + g_{31} \sin \Theta_g])^2 +$$

$$(g_{29}\ i_g\ [g_{30} \sin \Theta_g - g_{31} \cos \Theta_g] +$$

$$g_{32}\ v_g)^2]^{1/2} - [(g_{29}\ i_g [g_{30} \cos \Theta_g +$$

$$g_{31} \sin \Theta_g])^2 + [g_{29}\ i_g (g_{30} \sin \Theta_g -$$

$$g_{31} \cos \Theta_g) + g_{32}\ v_g + g_{33}\ v_g]^2]^{1/2} \tag{4.31}$$

T_4: upper limit = g_{34}; lower limit = g_{35} (4.32)

$$v_{b5} = -g_{36} \tag{4.33}$$

$$G_{13} = \frac{g_{37}\ s}{s + p_7} \tag{4.34}$$

T_5: upper limit = g_{38}; lower limit = $-g_{39}$ (4.35)

$$G_{11} = g_{40} \tag{4.36}$$

$$v_{b6} = g_{58} = 24\ (-1 + g_{40}) \tag{4.37}$$

$$G_{12} = \frac{g_{41}\ (s + p_8)}{s + p_9} \tag{4.38}$$

Exciter Minimum Voltage Limit System Expressions

$$G_{16} = g_{42} \tag{4.39}$$

$$v_{b8} = -g_{59} = 12\ (-1 + g_{42}) \tag{4.40}$$

$$T_6: \text{ upper limit} = g_{43};\ \text{lower limit} = -g_{44} \tag{4.41}$$

$$G_{17} = g_{45} \tag{4.42}$$

$$v_{b9} = g_{46} \tag{4.43}$$

(G_{14}, G_{15} and v_{b7} are also given for the automatic regulator as (4.19), (4.21) and (4.20) respectively.)

Phase Limit System Expressions

$$G_{20} = g_{47} \tag{4.44}$$

$$v_{b11} = -g_{48} \tag{4.45}$$

$$G_{21} = g_{49} \tag{4.46}$$

Manual Regulator System Expressions

$$G_{22} = \frac{-g_{50}\ (a_2 + g_{51})}{s + p_{10}} \tag{4.47}$$

$$v_{b12} = g_{61} = -g_{52}\ (a_2 + g_{51}) \tag{4.48}$$

T_7: upper limit = g_{53}; lower limit = g_{54} (4.49)

$$G_{23} = g_{55} \tag{4.50}$$

$$v_{b13} = g_{50} \tag{4.51}$$

TABLE 4.1

Control System Paramenters

g_0	1.0472	[1/volts]
g_1	π	[rad]
g_2	0	[rad]
g_3	202.173	[volts]
g_4	100	[1/sec]
p_0	150	[1/sec]
g_5	7.5	[volts]
a_1	500	[ohms]
g_6	5.036×10^{-5}	[1/ohms]
g_7	0.13295	-
g_8	2.731	-
g_9	0	[volts]
g_{10}	24	[volts]
g_{11}	0.278	-
p_1	20	[1/sec]
p_2	5.56	[1/sec]
g_{12}	∞	[volts]
g_{13}	24	[volts]
g_{14}	313.9	[volts]
g_{15}	16	[volts]
g_{16}	500	[1/sec
p_3	750	[1/sec]
g_{17}	1/3	-
g_{18}	99	[volts]

Table 4.1 - Continued

g_{19}	51/61	-
g_{20}	66	[volts]
g_{21}	4	[volts]
g_{22}	0.056	-
p_4	0.67	[1/sec]
g_{23}	5.59	-
g_{24}	*	-
g_{25}	*	-
g_{26}	2.21	[volts]
g_{27}	8.0074×10^6	$1/[sec^2]$
p_5	1.686×10^3	1/[sec]
p_6	6.076×10^5	$1/[sec^2]$
g_{28}	0.52	[volts]
g_{29}	†	-
g_{30}	8	[ohms]
g_{31}	4	[ohms]
g_{32}	†	-
g_{33}	†	-
g_{34}	10	[volts]
g_{35}	0	[volts]
g_{36}	24	[volts]
g_{37}	0.0769	[1/sec]
p_7	0.094	[1/sec]
g_{38}	0	[volts]

Table 4.1 - Continued

g_{39}	+24	[volts]
g_{40}	3.5	-
g_{41}	0.1071	-
p_8	1.603	[1/sec]
p_9	0.172	[1/sec]
g_{42}	0.1098	-
g_{43}	0	[volts]
g_{44}	+24	[volts]
g_{45}	3.1	-
g_{46}	50.4	[volts]
g_{47}	1/180	-
g_{48}	+12	[volts]
g_{49}	0.6	-
g_{50}	9.22	[volts/ohms-sec]
g_{51}	1.47[KΩ]	
g_{52}	3.479×10^4	[volts/ohms]
g_{53}	0	[volts]
g_{54}	+24	[volts]
g_{55}	3.1	-
g_{56}	50	[volts]
a_1	500 [adjustable between 0-500Ω]	
a_2	1.42 KΩ [adjustable between 0-5KΩ]	
p_{10}	903	[1/sec]
g_{57}	41.544	[volts]

Table 4.1 - Continued

g_{58}	60	[volts]
g_{59}	10.68	[volts]
g_{60}	110.16	[volts]
g_{61}	1	[volts]

---

* Parameters g_{24} and g_{25} belong to the Active-Reactive Current Compensator. (See Section 4.4) Parameters g_{24} and g_{25} are the resistance and reactance in per unit respectively between the Main Generator Terminal and the point that needs to be regulated.

† These parameters belong to the U.R.A.L. and are not given in the Alterrex manual. These parameters could be found as follows (refer to [4], Figure 18 entitled "Diagram and Vector Positions for Underexcited Reactive Ampere Limit"). Parameters g_{29}, g_{32} and g_{33} are found as follows:

$$g_{29} = \frac{i_g^b}{N_a},$$

where i_g^b is the base value of main generator terminal current and N_a the turns ratio of the current transformer connected in the armature of the main generator at phase b.

$g_{32} = M_1 \, v_g^b$, where v_g^b is the base value for the generator terminal voltage. M_1 is the fraction of generator terminal voltage measured from point (5) to M in B1VT of Figure 18 in Reference [4].

$g_{33} = M_2 \, v_g^b$, where M_2 is the fraction of v_g measured from (3) to (5) in B1VT.

Chapter V: COMPLETE MODEL OF THE ALTERREX EXCITATION CONTROL SYSTEM

5.1 Introduction

In this chapter the complete model for the excitation control system is given. The model is completed by using the self-excited exciter-alternator model given in Chapter III and adding the governing equations of the main generator. Thus the R-L load at the output of the model given in Chapter III is replaced by the field winding of the main generator. This model and the control system model (Chapter IV) constitute the complete model for the Alterrex excitation control system and is pictured schematically in Figure 5.1. The main generator is shown connected to an infinite bus, v_∞, through an inductive impedance, X_∞. The control system takes the exciter-alternator terminal voltage and current, v_e and i_1'' and the main generator terminal voltage and current v_g and i_g, and processes them to yield the value for the control input, the firing angle α.

The sample simulations presented in this chapter exclude the effect of the current boost system and the limiting systems, although these are included as part of the complete model. They simulate the case of the unloaded main generator and that of the generator connected to an infinite bus through an inductive impedance. The results of tests on this model for

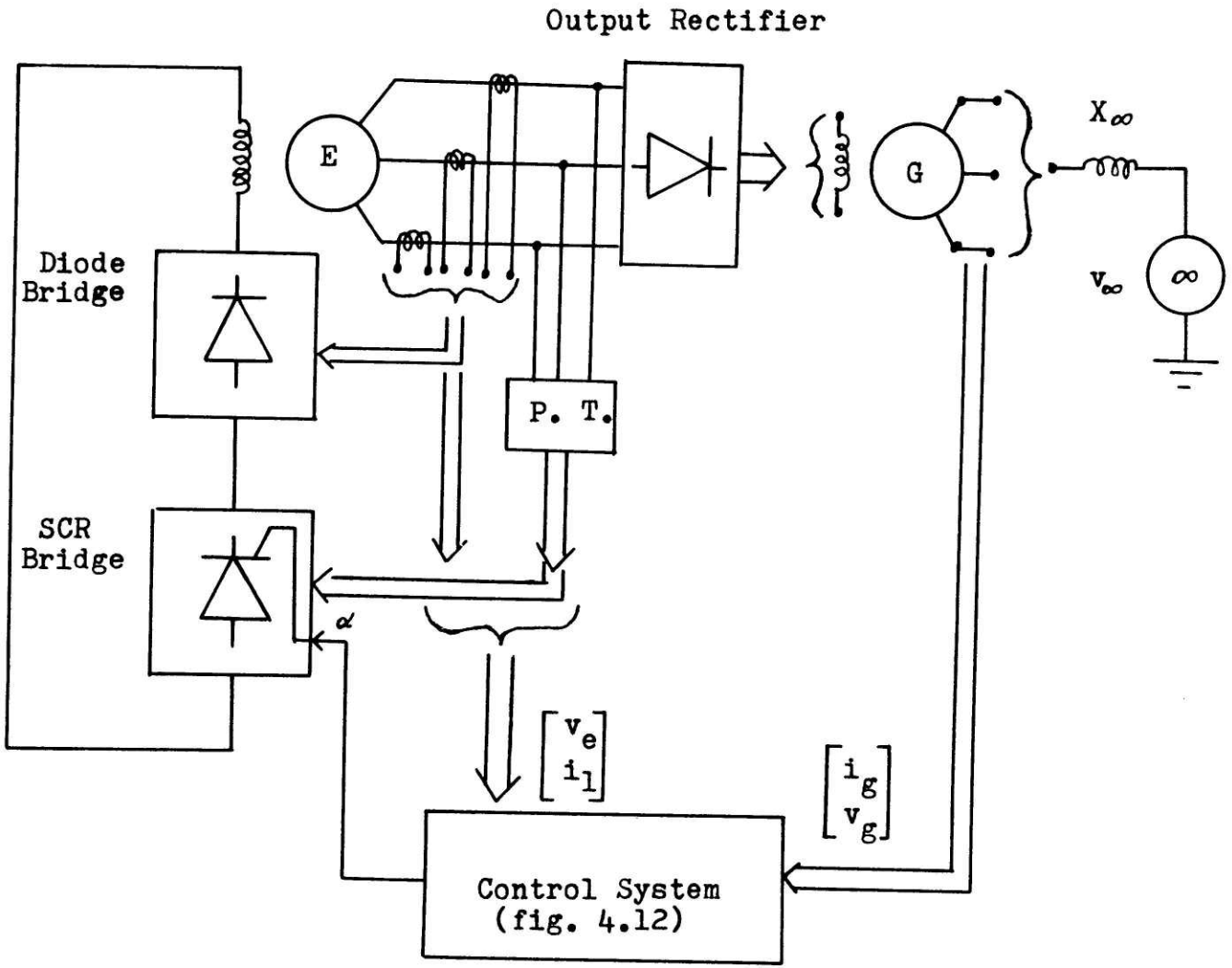

Figure 5.1 Schematic of the Model for the Alterrex excitation control system

these two cases are compared with the results of the type I model proposed by the IEEE committee on excitation systems [3].

5.2 Governing Equations for the Complete Model

5.2.1 Governing Equations for the Self-Excited Exciter-Alternator with Main Generator Connected to an Infinite Bus

The model for the self-excited exciter-alternator is defined by the model given in Chapter III for the self-excited exciter-alternator with current boost system but in this case feeding the field winding of the main generator. The main generator is connected to an infinite bus v_∞ through an inductive impedance X_∞. The model for the main generator is based on standard two-reaction theory for synchronous machines [1]. The parameters used can be found in Table 3.1 and in Table C.1 in Appendix C.

The model for the main generator includes damper windings and has a total of five states. The self-excited exciter-alternator with current boost system and damper windings has four states. Therefore there are a total of nine states for the self-excited exciter-alternator with the main generator model. In this thesis the turbine output will be modeled as a constant torque source.

5.2.2 The Control System Equations

The mathematical model for the control system is defined by the block diagram given in Figure 4.12 and the expressions

given at the end of Chapter IV in Section 4.7. The parameters used can be found in Table 4.1.

5.3 Solution Technique for the Self-Excited Exciter-Alternator with Main Generator and Automatic Regulator Problem

In this chapter the behavior of the Alterrex model is illustrated. In this section a method is developed to obtain the numerical solution of the self-excited exciter-alternator with main generator and the automatic regulator model. For the purposes of this section the limiting systems and current boost system effects are ignored. The Active-reactive current compensator has also been left out. This means that the input to the automatic regulator (v_1) is connected directly to the main generator terminals which therefore is regulating v_g.

The method presented here is an extension of the methods used in Chapters II and III. The method is given below step by step. The variables used have been defined in previous chapters and in Appendix C.

Step 1 - The first step consists of integrating the state equations given below. The necessary information to obtain these equations is given in Chapters II, III, IV and Reference [1] for the generator.

$$\frac{d\lambda_{fe}}{dt} = \omega_{eO} (-R_{fe} i_{fe} + v_{fe}) \qquad (5.1)$$

$$\frac{d\lambda_{kde}}{dt} = -\omega_{e0} R_{kde} i_{kde} \tag{5.2}$$

$$\frac{d\lambda_{kqe}}{dt} = -\omega_{e0} R_{kqe} i_{kqe} \tag{5.3}$$

$$\frac{d\lambda_{fg}}{dt} = \omega_{g0} (-R_{fg} i_{fg} + v_{fg}) \tag{5.4}$$

$$\frac{d\lambda_{kdg}}{dt} = -\omega_{g0} R_{kdg} i_{kdg} \tag{5.5}$$

$$\frac{d\lambda_{kqg}}{dt} = -\omega_{g0} R_{kqg} i_{kqg} \tag{5.6}$$

$$\dot{\delta}_g = \omega_g - \omega_{g0} \tag{5.7}$$

$$\dot{\omega}_g = \frac{-\omega_{g0}}{2H} (\lambda_{dg} i_{qg} + \lambda_{qg} i_{dg} - T_m) \tag{5.8}$$

$$\frac{dv_7}{dt} = -p_0 v_7 - (g_5 p_0 + g_4 g_3 v_g)(a_1 g_6 + g_7) \tag{5.9}$$

$$\frac{dv_{11}}{dt} = -p_2 v_{11} + g_{11}\left(g_8 \frac{dv_8}{dt} + p_1\left(g_{57} + g_8 v_8\right)\right) \tag{5.10}$$

$$\frac{dv_{30}}{dt} = -(v_{30} + g_{15}) p_3 - g_{16} g_{14} v_e \tag{5.11}$$

$$\frac{dv_{39}}{dt} = -p_4\, v_{39} + g_{22}\, \frac{dv_{38}}{dt} \qquad (5.12)$$

Equations (5.1) through (5.3) are the state equations for the exciter-alternator. Equations (5.4) through (5.8) are the state equations for the main generator. Finally Equations (5.9) through (5.12) are the state equations for the automatic regulator. Notice that the main generator variables are denoted using the same symbols used for the exciter-alternator with the exception that the subscript e is replaced by a g.

Step 2 - Step 1 yields the values for, λ_{fe}, λ_{kde}, λ_{kqe}, λ_{fg}, λ_{kdg}, λ_{kqg}, δ_g, ω_g, v_7, v_{11}, v_{30} and v_{39} at $t = t_0 + \Delta T$. The quantity v_∞ is also known. Step 2 consists of a procedure to find the value of main generator field current, i_{fg}, and α using the information available. Once this is found then the problem becomes analogous to the problem solved in Chapter III. This makes sense physically since the only external effects affecting the behavior of the self-excited exciter-alternator are the loading conditions and the input variable α, i.e. the firing angle of the SCR bridge. Once these variables are found the variables for the self-excited exciter-alternator can be obtained independently of everything else.

The main generator is connected to an infinite bus through an inductive impedance X_∞. It is possible to redefine the problem by adding X_∞ to the leakage inductance of the main

generator. In this case the problem is transformed to a problem with a new machine connected directly to an infinite bus. However the voltage regulator must be modeled so as to regulate the actual generator terminal voltage. After the variables for the new machine are obtained it is always possible to get v_g. What follows is the procedure to find the current i_{fg} and the variable α. First the expressions needed to find the variable i_{fg} are listed below. These equations can be derived from the governing equations of the main generator. They are given in this thesis without derivation.

$$i_{qg}\,(t_0 + \Delta T) = \left(\frac{X_{kqg}\left(C_4 - \frac{C_6\,C_1}{C_3}\right)}{C_6\,X_{mqg}/C_3} - \lambda_{kqg} \right) \Bigg/ \left(X_{mqg} + \frac{\left(C_5 - \frac{C_6\,C_2}{C_3}\right) X_{kqg}}{C_6\,X_{mqg}/C_3} \right) \tag{5.13}$$

$$i_{kqg}\,(t_0 + \Delta T) = \left(C_4 - \left(C_5 - \frac{C_6\,C_2}{C_3}\right) i_{qg} - \frac{C_6\,C_1}{C_3} \right) \Bigg/ \left(C_6\,X_{mqg}/C_3 \right) \tag{5.14}$$

$$i_{kdg}\,(t_0 + \Delta T) = \frac{C_1}{C_3} - \frac{C_2}{C_3}\, i_{qg} + \frac{X_{mqg}}{C_3}\, i_{kqg} \tag{5.15}$$

$$i_{dg}\ (t_0 + \Delta T) = \left[v_\infty \cos \delta_g \left(\frac{\omega_{g0}}{\omega_g}\right) - \left(\frac{X_{mdg}}{X_{ffg}}\right) \lambda_{fg} + R_{ag}\left(\frac{\omega_{g0}}{\omega_g}\right) i_{qg} + \right.$$

$$\left. - \left(X_{mdg} - \frac{X_{mdg}^2}{X_{ffg}}\right) i_{kdg} \right] \Bigg/ \left(-X_{dg} + \frac{X_{mdg}^2}{X_{ffg}}\right) \qquad (5.16)$$

$$i_{fg}\ (t_0 + \Delta T) = \left[\lambda_{fg} + X_{mdg}\ i_{dg} - X_{mdg}\ i_{kdg} \right] \Big/ X_{ffg} \qquad (5.17)$$

The variables C_1 through C_6 are given in Appendix C. The variables i_{qg}, i_{kqg}, i_{kdg}, i_{dg} and i_{fg} can be found at time $t_0 + \Delta T$ using Equations (5.13) through (5.17) respectively.

The value of α is found as follows (refer to Figure 4.12 in Chapter IV). Variables v_{11} and v_{39} are known from Step 1. Variable v_{12} can be obtained then by applying the nonlinearity T_2 to v_{11}. Variable v_{13} is obtained then by adding v_{39} to v_{12}. Using the model for amplifier 2, i.e. expressions G_7 and T_3, the value for v_{15} can be obtained. Knowing v_{15} the variable v_R can be obtained after adding v_{b3} to v_{15} (notice that for this case v_{16}, v_{36} and v_R are all equal). Therefore using the model for the phase angle system, i.e. expression T_8 and G_{24} the value for α can be found. The variables for the self-excited exciter-alternator can be found independently of the rest of the system. This can be done by using Steps 2, 3, 4, 5 and 6 of the solution technique given in Section 3.3.2 of

Chapter III. Notice that i_L of Chapter III is now i_{fg}. The reader should at this point refer to the solution technique presented in Chapter III. At the end of Step 6 in Chapter III it is said to go back to Step 1. This is not done so here. Instead at the end of Step 6 in Chapter III the procedure is continued as follows.

Step 3 - Before returning to Step 1 the variables v_{fg}, λ_{dg}, λ_{qg}, v_g, v_8 and v_{38} must be obtained. Also convenient expressions for $\frac{d\, v_8}{dt}$ and $\frac{d\, v_{38}}{dt}$ must be obtained. Furthermore if the saturation of the main generator has also been modeled, a new value of X_{mdg} must be calculated for $t_0 + \Delta T$.

The variable v_{fg} is the average voltage at the output of the rectifier of the exciter-alternator. This also happens to be indentical to v_L of Chapter III which is calculated in the solution technique of Chapter III (Step 6). The variables λ_{dg} and λ_{qg} can be found from the governing equations of the main generator [1]. The variable v_g is found using the transmission line reactance X_∞ and the current through it. Variable v_8 can be found from v_7 using T_1. If v_7 is between the limits set by T_1 then $\frac{d\, v_8}{dt}$ is equal to $\frac{d\, v_7}{dt}$ which means it is also given by the right side of Equation (5.9).

The variable v_{38} can be found from v_{30} using G_{18} and v_{b10}. After determining the value of the function G_{18}, the term $\frac{d\ v_{38}}{dt}$ can be set equal to G_{18} times $\frac{d\ v_{30}}{dt}$.

Finally X_{mde} can be found using the following expression chosen to model the saturation of the main generator. This expression fits the data for $i \leq 0.95$ p.u.

$$X_{mdg} = b_0 + b_1 i + b_2 i^2 + b_3 i^3 + b_4 i^4 \qquad (5.18)$$

$$\text{where, } i = i_{ffg} + i_{kdg} - i_{dg} \qquad (5.19)$$

Constants b_0 through b_4 are given in Table C.1 in Appendix C. The manufacturer's data for the main generator (AEPs Big Sandy Unit 2) is also given in Appendix C. Notice that values for X_{dg} and X_{ffg} must also be calculated using X_{mdg}. Now it is possible to go back to Step 1 and repeat the whole procedure to obtain new variables for $t_0 + 2\Delta T$.

The steady-state values for the case where the main generator is unloaded can be obtained fairly easily because for a given value of v_g the corresponding value of field current and voltage can be obtained using the saturated value of X_{mdg}. Then using the procedure described in Chapter III to obtain the steady-state conditions for the self-excited exciter-alternator it is possible to obtain the steady-state values of the exciter-alternator that are consistent with the

generator field voltage and field current. Then the adjustable parameters of the control system should be adjusted to satisfy these conditions.

The steady-state values for any other conditions can be obtained numerically using the method described in this chapter. The method should be initialized with a set of consistent initial conditions so as to avoid convergence problems, a desired input torque T_m and the external and the elements X_∞ and v_∞.

5.4 Demonstration of the Model for the Self-Excited Exciter-Alternator with Main Generator and Automatic Regulator

It is possible to implement the numerical method of solution described in the previous section using a digital computer. This was done here as a demonstration of the capabilities of the model for simulating the real system. These tests were made to test the self-excited exciter-alternator with the main generator and the automatic regulator. The current boost system and limiting control systems are not included.

5.4.1 Tests on the Model

Two different types of tests are performed on the model. One test consists of changing the reference setting of the control system with the main generator open circuited. The second test consists of introducing a fault somewhere in the system with the main generator loaded.

The first test is done by setting X_{∞} to a very high value as to simulate the open circuited conditions. The steady-state values are given in Table 4.1. The automatic regulator adjustment a_1 is initially adjusted to maintain 1.0 p.u. main generator output voltage. This value is given in Table 4.1. The automatic regulator adjustment a_1 is then changed so as to simulate the effect of a step input in the reference voltage of the automatic regulator. This causes the system to go to a new steady-state position after moving through a transient. The results of this test are shown in Figures 5.2 through 5.6 .

Notice that the generator terminal voltage has a rise time of about 0.5 seconds. It overshoots 14 percent with the peak of the overshoot at about 0.8 seconds and it settles in about 1.5 seconds. The parameters of the automatic regulator are adjusted to obtain a fast rise time and also a short settling time for the response, however, no attempt was made to find a set of values which yield the absolute fastest response.

It was observed that the time constant of the lead-lag network shown in the automatic regulator loop of Figure 4.11 had a strong effect on the rise time. Therefore the parameters of the lead lag network are adjusted to produce a short rise time in the response. It was also noticed that adjusting the exciter rate feedback time constant has a strong effect on the damping of the dynamic response of the system; it also has a smaller effect on the rise time. Therefore the time constant

of the rate feedback is adjusted to reduce the settling time and eliminate oscillations as much as possible without offsetting the rise time of the response by much. The parameters for the control system are given in Table 4.1.

It is interesting to observe from the plots of the results that the step input in the automatic regulator adjustment causes the control input α, plotted in Figure 5.3, to go to zero almost immediately. At this value the firing angle system saturates (see Figure 4.12). The control input stays at this value for about 0.25 seconds. This forces the exciter terminal voltage shown in Figure 5.4 to reach peak voltage at about 0.3 seconds.

It is interesting to observe the effect of the nonlinear rate feedback. From the plot of v_{30} shown in Figure 5.5 it is possible to deduce that the nonlinear rate feedback loop changes gain at about 0.2 seconds and at 0.5 seconds, i.e. when v_{30} = 99 volts. At point 0.2 seconds the rate feedback loop changes from a higher gain to a lower gain, resulting in less damping. This can be seen by the fact that signal v_{39} shown in Figure 5.6 decreases at a lower rate after 0.2 seconds. At 0.5 seconds the value of v_{30} becomes high enough so that the rate feedback loop regains a higher value for the gain. This is also the time at which the generator terminal voltage crosses the desired steady-state value and continues to overshoot. It seems as if the effect of the nonlinear gain in the feedback loop is to decrease the rise time while damping the tail of the transient response effectively.

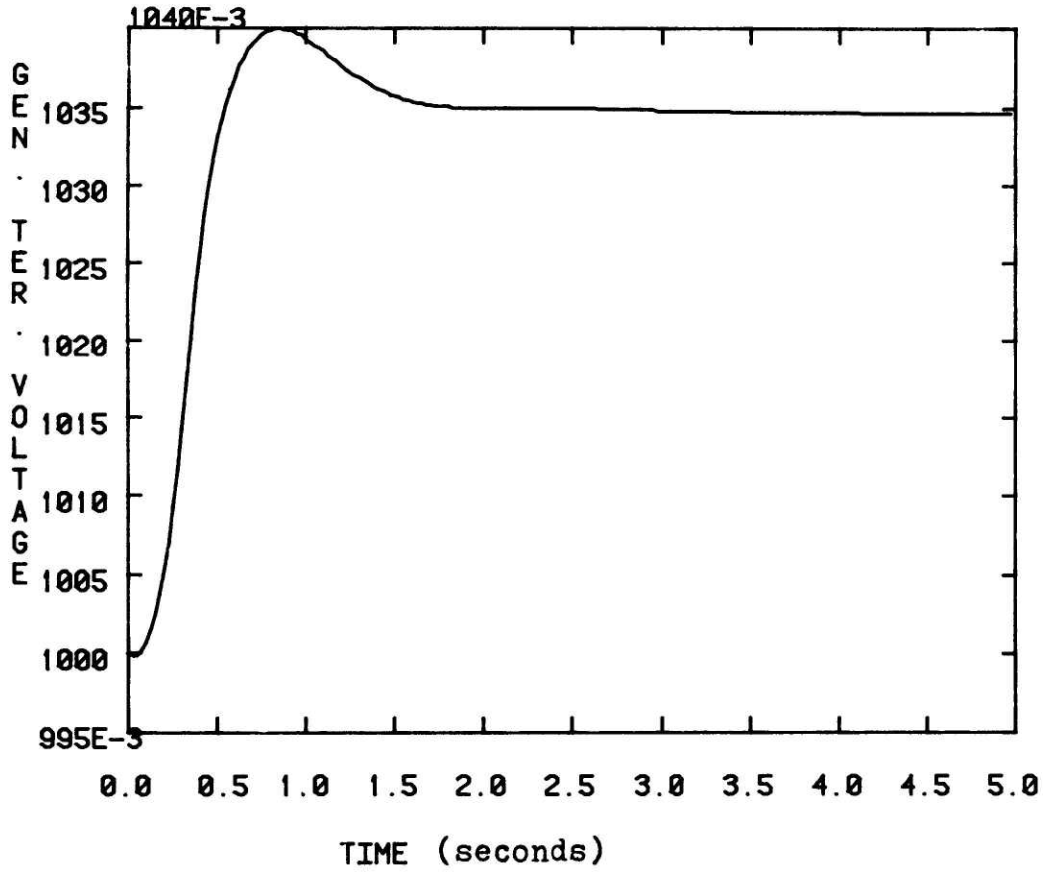

Figure 5.2 Computer plot of the generator terminal voltage for a step change in a_1

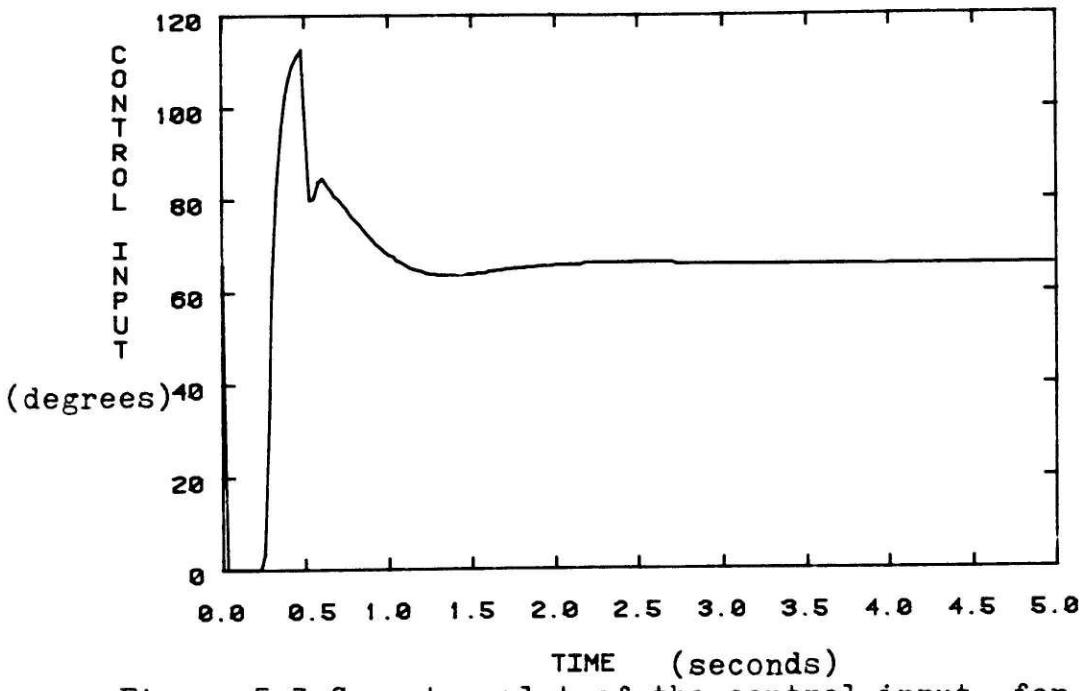

Figure 5.3 Computer plot of the control input for a step change in a_1

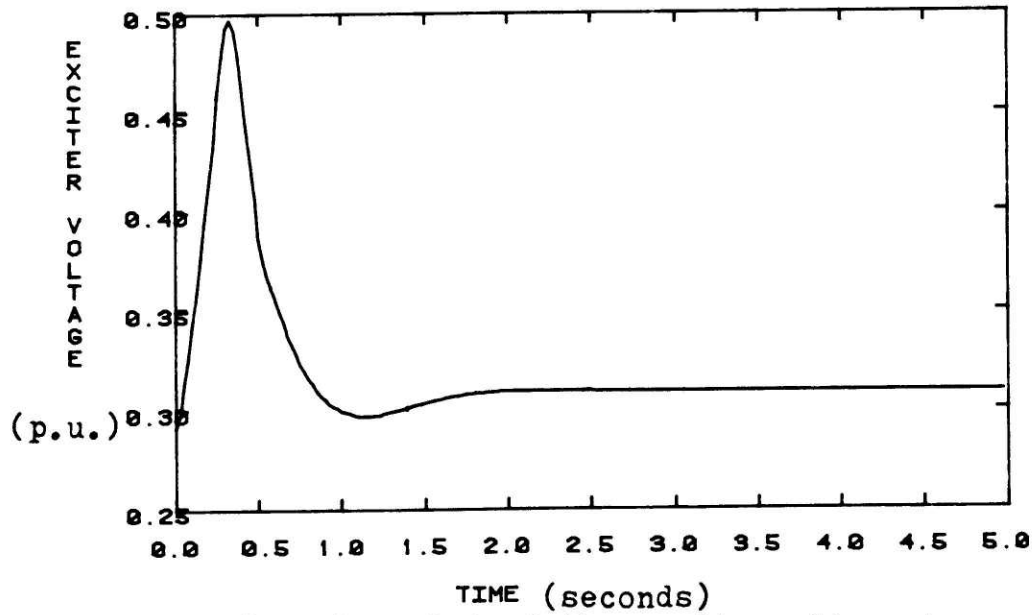

Figure 5.4 Computer plot of the exciter-alternator terminal voltage for a step change in a_1

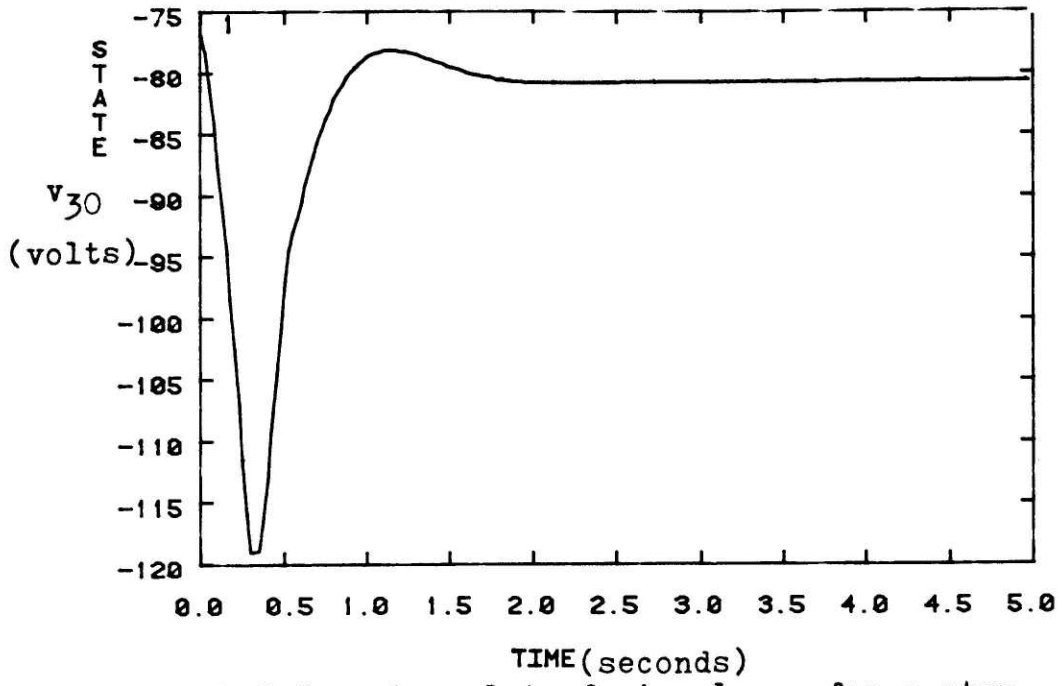

Figure 5.5 Computer plot of signal v_{30} for a step change in a_1

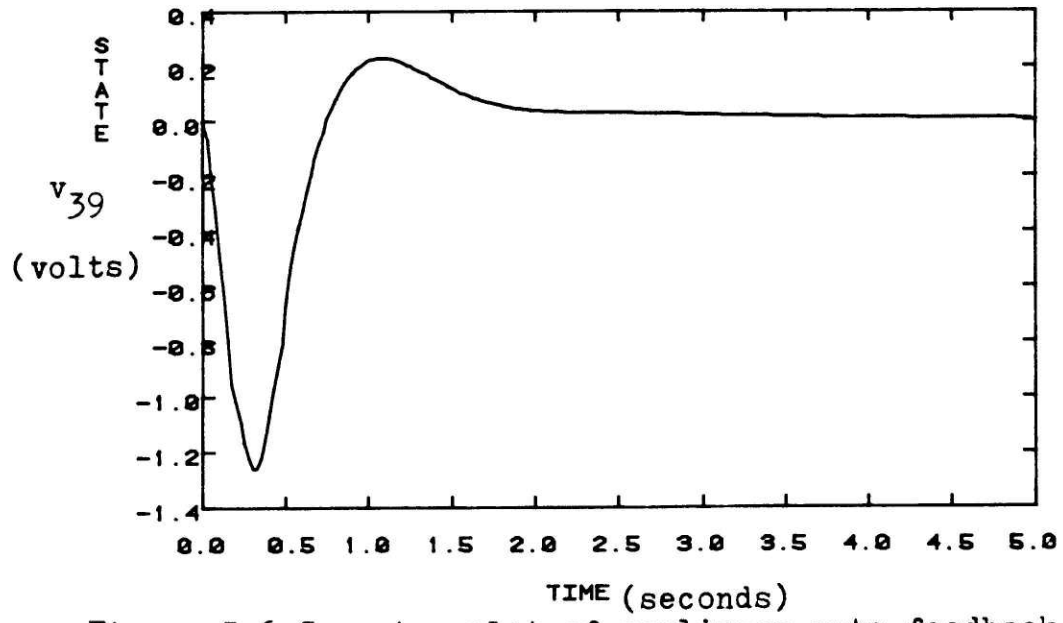

Figure 5.6 Computer plot of nonlinear rate feedback signal v_{39}

The next test performed on the model is done with the main generator connected to an infinite bus through an impedance X_∞. The steady-state values and the values for X_∞ and v_∞ are given in Table C.3. The test consists of a fault at the infinite bus cleared in 6 cycles. This test is performed on the generator both without and with the exciter model in order to observe the effect of the exciter on the dynamic behavior of the generator. The results of these tests are shown in Figures 5.7 through 5.12.

The generator terminal voltage for the case without and with exciter are shown in Figures 5.7 and 5.9 respectively. Comparing these two voltages it can be observed that there exists a slight difference between the two. The figures show that the exciter does improve the terminal voltage regulation, the voltage appearing to return to its steady-state value more rapidly.

It is also evident that the excitation system has an effect on the behavior of the load angle as shown in Figures 5.8 and 5.10 for the cases without and with exciter-alternator respectively. The difference in behavior between the two cases appears to be that the exciter initially raises field current in an attempt to maintain main generator terminal voltage, hence resulting in a negative effect on the rotor angle. This can be seen by comparing Figures 5.11 and 5.12 for the case with and without exciter-alternator respectively. It also appears to somewhat improve damping following the first swing as seen by Figures 5.8 and 5.10. As a result of this

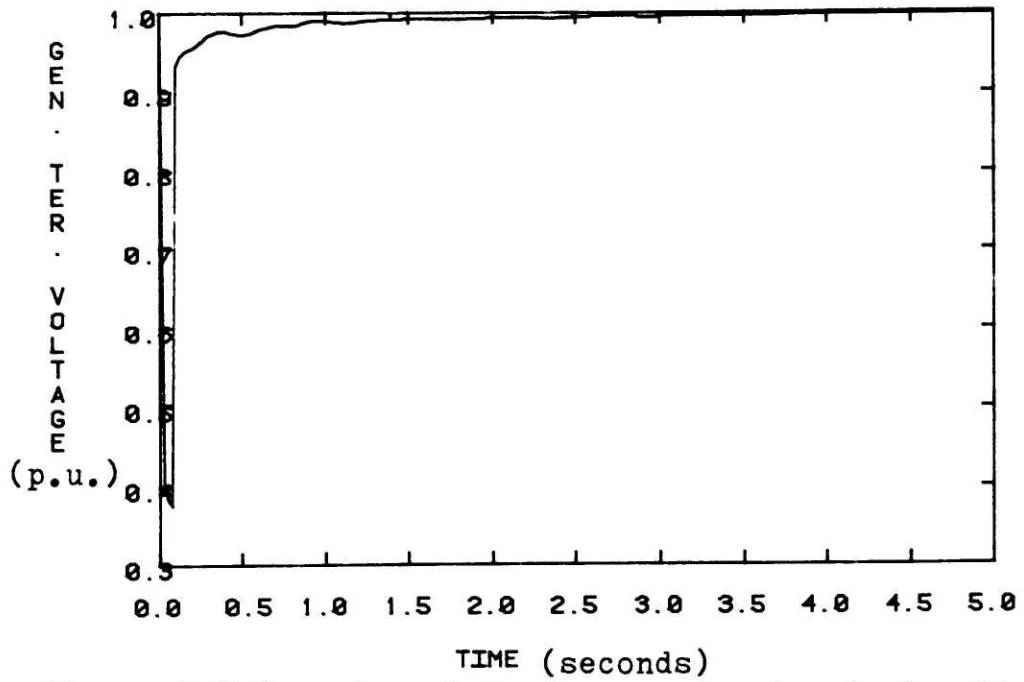

Figure 5.7 Computer plot of generator terminal voltage for fault-test without excitation control system

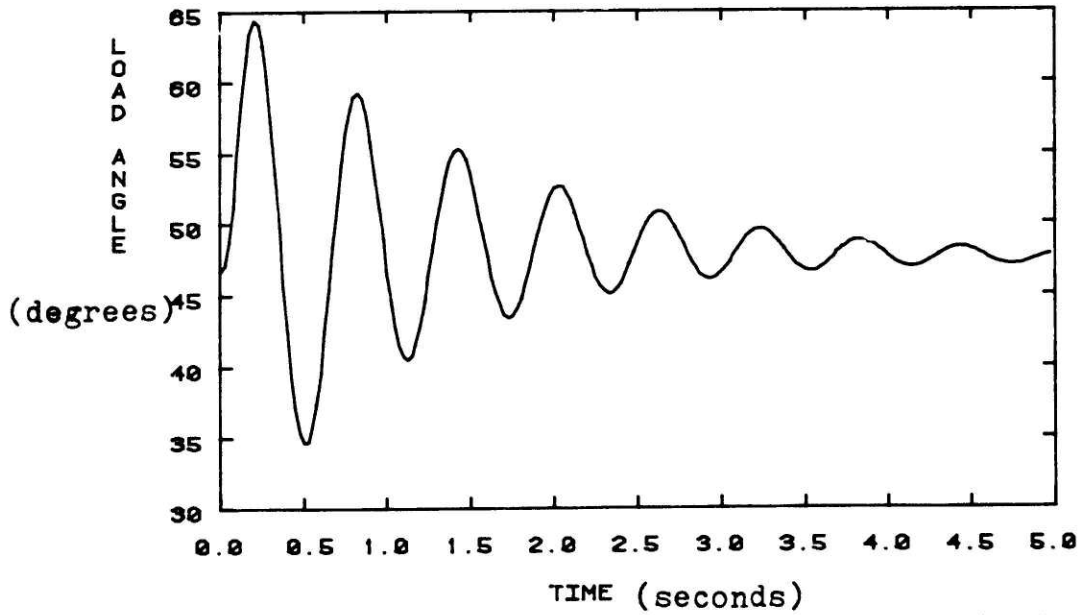

Figure 5.8 Computer plot of load angle for fault-test without excitation control system

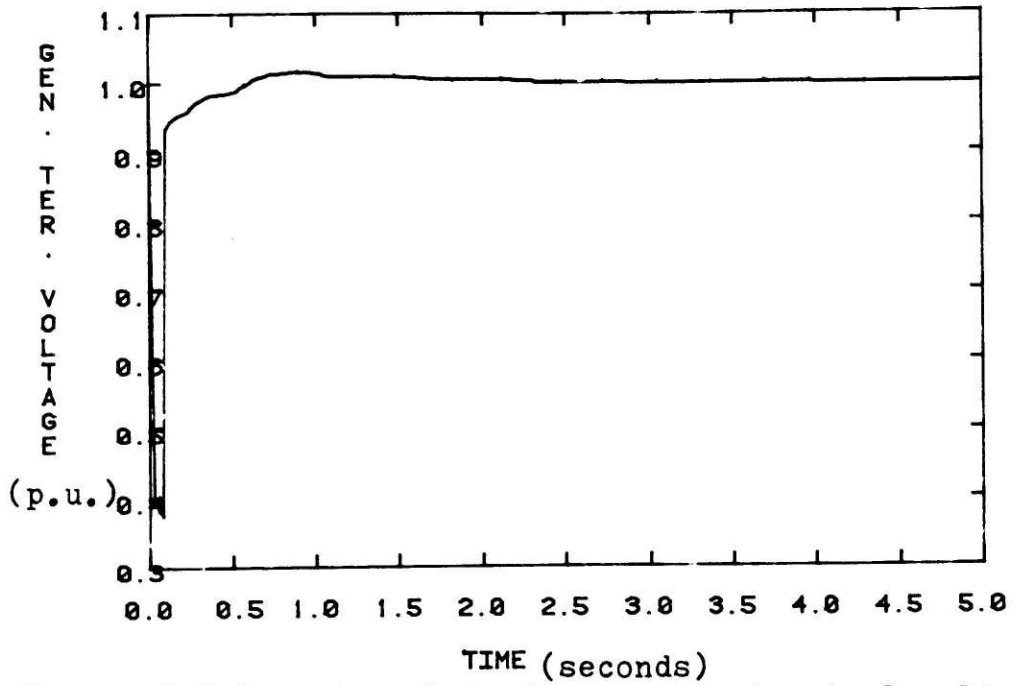

Figure 5.9 Computer plot of generator terminal voltage for fault-test with excitation control system

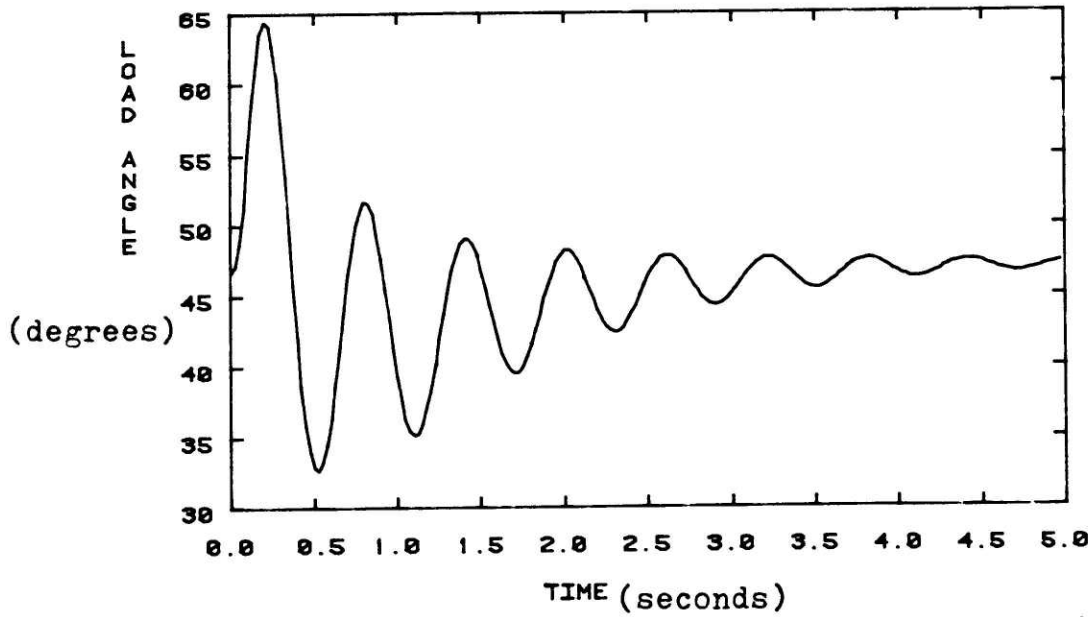

Figure 5.10 Computer plot of load angle for fault-test with excitation control system

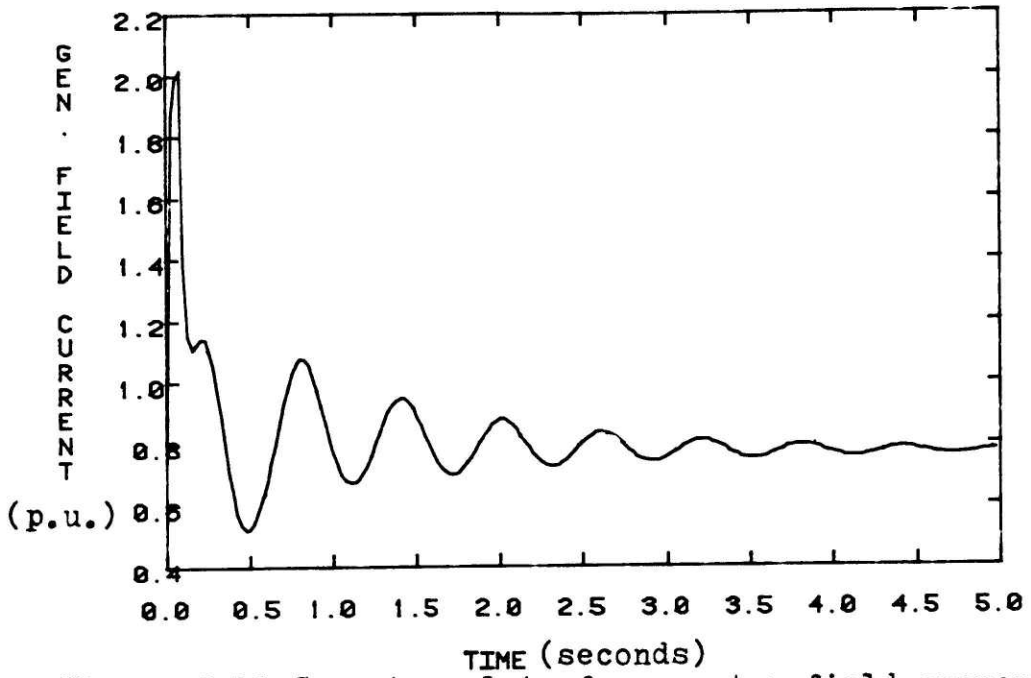

Figure 5.11 Computer plot of generator field current for fault-test with excitation control system

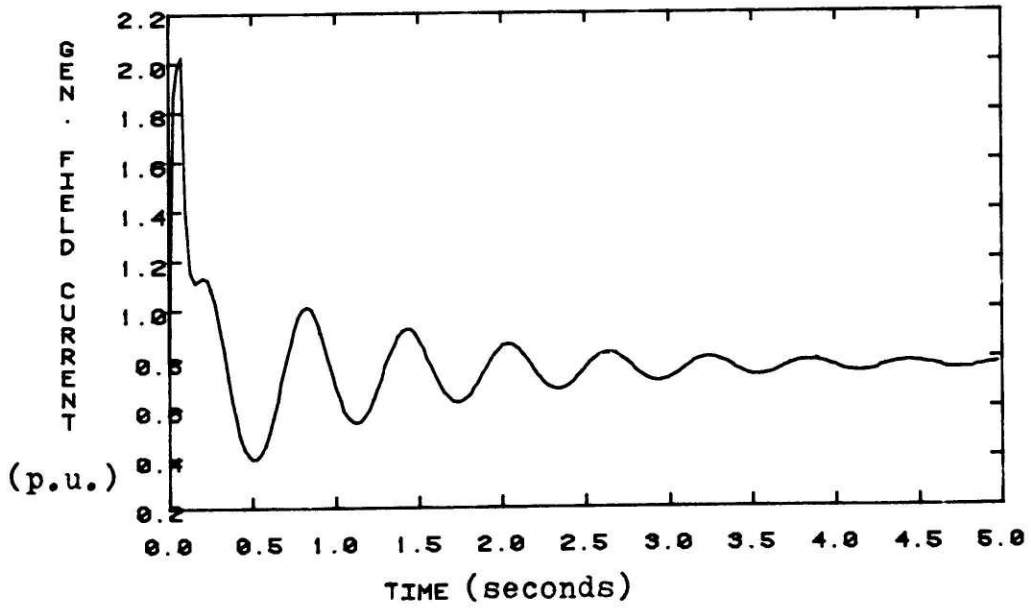

Figure 5.12 Computer plot of generator field current for fault-test without excitation control system

simulation, it can be seen that the exciter-alternator seems to have a significant effect on the dynamic behavior of the generator.

5.4.2 Comparison with the IEEE Type I Model

In this section the simulations done in Section 5.4.1 are repeated using the IEEE type I model (3) using typical data not necessarily consistent with the parameter values used for the detailed simulations in Section 5.4.1. Therefore small differences in behavior could be expected. The block diagram for the type I model is given in Figure 1.3 in Chapter I. The parameters used here for the type I model are given in Table 5.1.

The reference voltage is changed suddenly in the IEEE type I model to repeat the first test done in Section 5.4.1. The result for the terminal voltage is given in Figure 5.13. Comparing Figure 5.13 with the response obtained in Section 5.4.1 shown in Figure 5.2, it shows that both responses have essentially the same charateristics. The response in Section 5.4.1 however seems to be much better damped while retaining the same rise time characteristics. It seems reasonable to expect that this difference is due to the fact that the model proposed in this thesis accounts for the effect of nonlinear rate feedback while the IEEE type I model does not.

The fault test on the IEEE type I model is also repeated for the cases where the system is without and with exciter-alternator. The results are shown in Figures 5.14

through Figure 5.17. These results show that both models have captured the essential characteristics of the dynamic behavior. There is however a stronger effect on the swing of the rotor angle according to the model presented in this thesis than according to the IEEE type I model. For example Figure 5.10 shows that the simulation using the model presented in this thesis predicts a larger effect of the rotor angle than does the type I model.

The tests done above were intended to be an illustration of the utility of the model presented in this thesis and not as an exhaustive testing procedure. In fact, since no documented procedure can be found for the derivation of type I parameter values from the known physical construction of the generator, it is not possible to do more than the general sort of comparison tests presented here. However, the results do verify that the Alterrex model developed in this thesis behave consistently with expected behavior. Further verification must await comparison testing with an actual Alterrex system.

TABLE 5.1

Parameters For The IEEE Type I Model

T_R	0
K_A	400
T_A	0.05
V_{Rmax}	3.5
V_{Rmin}	-3.5
K_f	0.04
T_f	1.0
K_E	-0.17
T_E	0.95
V_S	$E_{fd} \cdot f(E_{fd})$
S_E	$Ae^{(BE_{fd})}$
A	2.65×10^{-3}
B	1.31

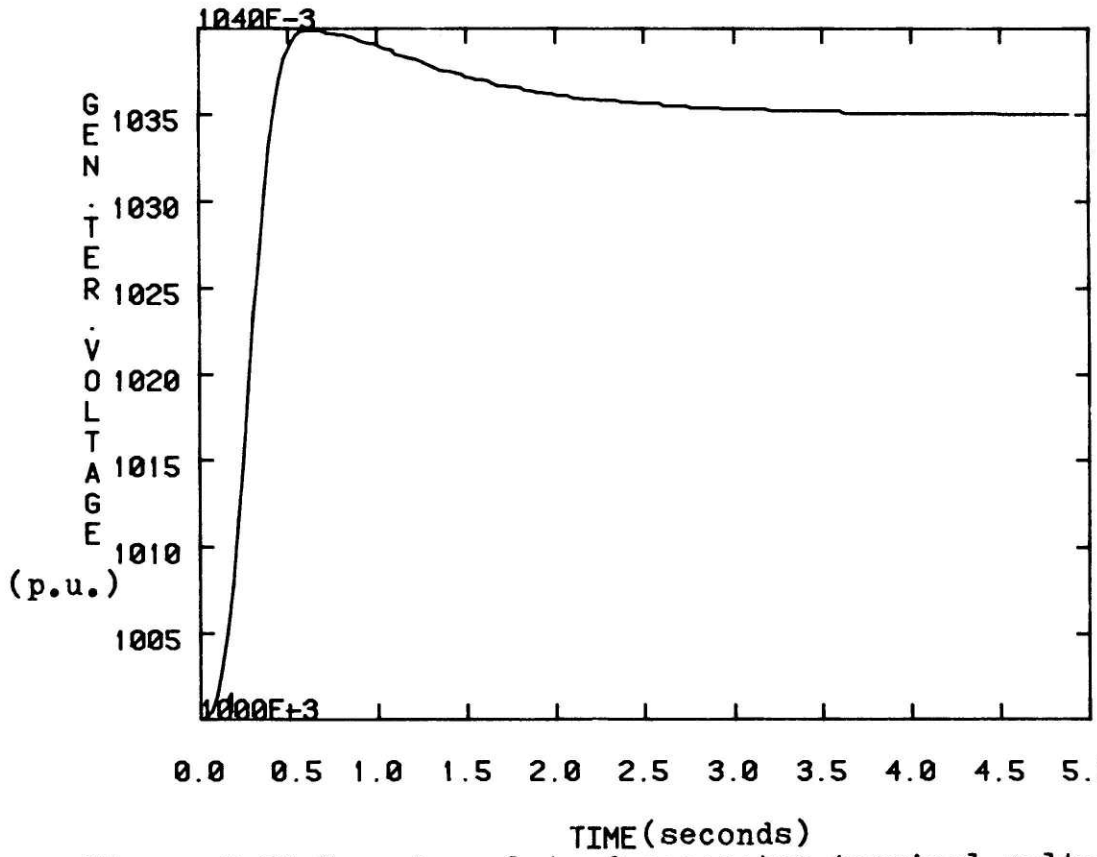

Figure 5.13 Computer plot of generator terminal voltage for step-test using type I model

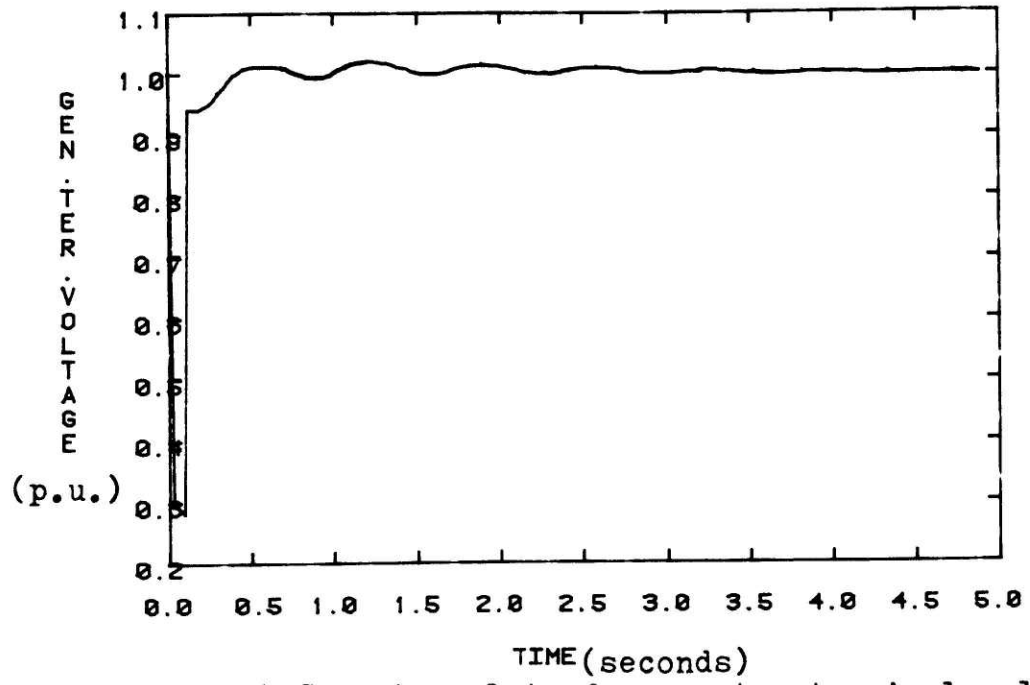

Figure 5.14 Computer plot of generator terminal voltage for fault-test using type I model

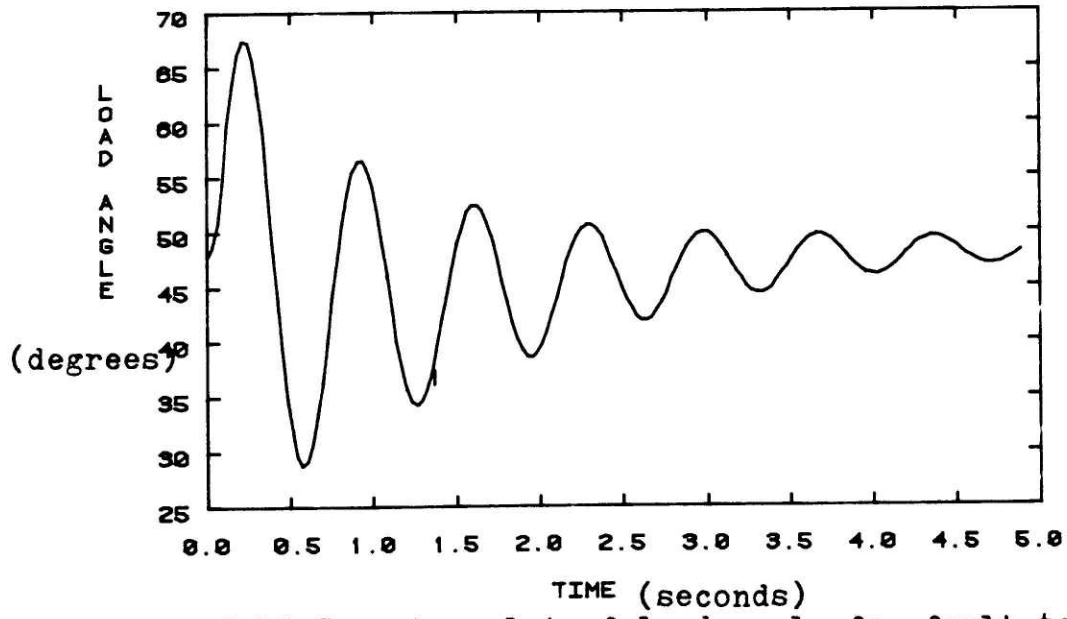

Figure 5.15 Computer plot of load angle for fault-test using type I model

Chapter VI: CONCLUSION AND SUGGESTED FURTHER WORK

6.1 Summary and Conclusion

A detailed model for the Alterrex excitation control system has been developed. The model has been developed by considering the physical principles governing the behavior of this system. The model developed has a direct relationship with the actual physical system, which is a departure from traditional models developed for this system [3]. Therefore the parameters of the model developed in this thesis have been obtained from the actual physical parameters of this system. This is considered to be an advantage over previous models.

The complete model for the Alterrex is given in Chapter V. The main part of the model is considered to be the self-excited exciter-alternator, the main generator and the automatic regulator. The simulations done on this model show that it predicts the expected behavior of the actual system. The results are also compared to the results obtained using the IEEE type I model [3] with typical data. The comparison shows that although both models capture some of the essential characteristics of the system the model presented in this thesis does seem to predict effects that the IEEE model could never predict even if different parameters were chosen. An example of such an effect is the nonlinear rate feedback.

Although the complete model given is specifically designed for the Alterrex system, the modeling techniques developed here could be applied to a wide range of excitation control systems,

particularly those that use an exciter-alternator with output rectifier. Other problems apart from excitation systems but involving ac machinery with rectifiers could also be solved using the material presented in this thesis.

This thesis has dealt with two basic problems. These are: the problem of the separately-excited exciter-alternator for transient conditions and the problem of the self-excited exciter-alternator for steady-state and transient conditions presented in Chapters II and III and complemented by Appendicies A and B. They by themselves constitute the heart of this work.

The control system was also modeled in order to obtain the complete model for the Alterrex excitation control system. Although this model can be obtained from the actual schematics of the system in a straightforward manner by using basic circuit theory, it is a tedious and time consuming task.

Notice that Chapter IV gave detailed explanations of the behavior of the control system. These explanations are more detailed than those found in the Alterrex Manual [4].

6.2 Suggestions For Further Work

The work presented here could suggest further research in several different directions. One direction is to try to reduce the present model to a smaller and more modest one yet maintaining a correlation between the model parameters and the parameters of the actual system.

It is also necessary to simulate the current boost system and the limiting systems. Only after this is done and after the simulations show that they predict expected behavior should the parameters and models given for them be considered adequately verified.

Another possibility is to use the model presented here to design control strategies to control the system optimally. For example the parameters g_0 through g_{61}, p_0 through p_{10} and a_1, a_2 could be optimized according to some criterion.

Finally further work should be done to justify experimentally the given model. At this stage the model has given results that are consistent with the expected behavior. Further experimental evidence, at this time unobtainable, should show the superiority of the model presented here over other models.

APPENDIX A
Derivation of the Equations Used in Chapter II

In this appendix Equations (2.19) through (2.32) are derived. Also the linearized equations and related constants are given. This includes Equations (2.33), (2.34) and (2.35).

A.1 Steady-State Equations

Equation (2.19) is Equation (2.18) applied in the steady-state case. Equation (2.21) is obtained by finding the driving point impedance at the terminal of the exciter-alternator. This is obtained by using Equations: (2.15) with di_L/dt set to zero, (2.16) and (2.17) as follows:

$$\frac{v_e}{i_1} = \frac{v_L/[(2.33)\ T_1 \cos\beta]}{i_L/(T_2/0.78)} = \frac{R/[(2.33)\ T_1 \cos\beta]}{(T_2/0.78)} =$$

$$= \frac{RT_2}{(2.33)(0.78)\ T_1 \cos\beta} \qquad (A.1)$$

Equation (2.20) is derived as follows. Looking at the phasor diagram of Figure A.1 we notice that E'_{fde} can be written as follows:

$$E'_{fde}\angle 0 = v_e \angle -\delta_e + R_{ae}\, i_1 \angle -\delta_e - \theta_1 + jx_{qe}\, i_1 \angle -\theta_1 - \delta_e \qquad (A.2)$$

Now multiply both sides of (A.2) by $1\angle\delta_e$:

$$E'_{fde}\angle\delta_e = v_e \angle 0 + R_{ae}\, i_1 \angle -\theta_1 + jx_{qe}\, i_1 \angle -\theta_1 \qquad (A.3)$$

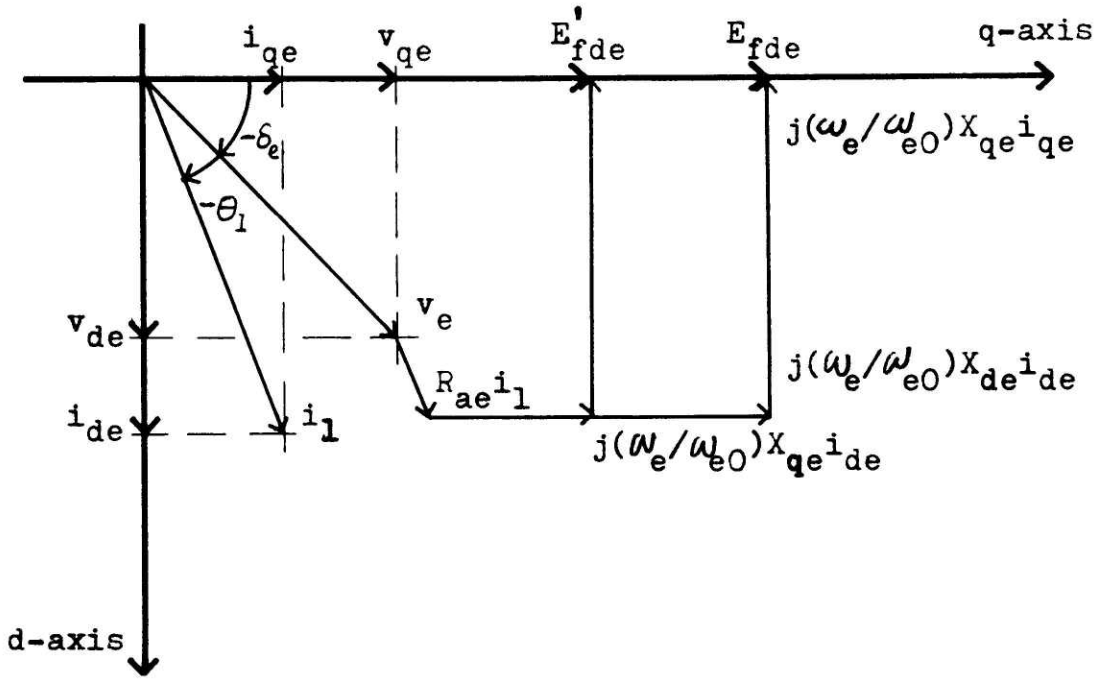

Figure A.1 Steady-State Phasor diagram for the exciter-alternator

or:

$$E'_{fde}\angle\underline{\delta_e} = (v_e + R_{ae}\, i_1 \cos\Theta_1 + x_{qe}\, i_1 \sin\Theta_1) +$$

$$+ j(-R_{ae}\, i_1 \sin\Theta_1 + X_{qe}\, i_1 \cos\Theta_1) \qquad (A.4)$$

From which Equation (2.20) follows trivially. Equation (2.22) follows from (2.12) with $\frac{d\lambda_{fe}}{dt}$ set to zero. Equation (2.24) follows from the definition of R_e as driving point impedance.

Equation (2.23) is derived as follows. Looking at the phasor diagram of Figure A.1 we see that it is possible to write for the steady-state:

$$E_{fde} \equiv X_{mde}\, i_{fe} = v_e \cos\delta_e + R_{ae}\, i_1 \cos(\delta_e + \Theta_1) +$$

$$+ x_{de}\, i_1 \sin(\delta_e + \Theta_1) \qquad (A.5)$$

And using (2.24) we can substitute for v_e and obtain

$$R_e i_{10} \cos\delta_{e0} + R_{ae}\, i_{10} \cos(\delta_{e0} + \Theta_1) +$$

$$+ X_{de}\, i_{10} \sin(\delta_{e0} + \Theta_{10}) = X_{mde}\, i_{fe0} \qquad (A.6)$$

From which (2.23) follows trivially.

A.2 Auxiliary Equations

Equation (2.25) is derived as follows. From Equations (2.1) and (2.2) it follows that,

$$\delta_e = \text{Tan}^{-1}\left(\frac{v_{de}}{v_{qe}}\right) \tag{A.7}$$

Now it is necessary to express v_{dc} and v_{qe} in terms of the states and δ_e. This is done by manipulating the equations as follows. First substitute (2.8) in (2.11). Then solve (2.9) by i_{kqe} and the result is substituted in the previous result. The result is an equation in terms of i_{qe}, i_{de} and λkqe. Using Equations (2.3), (2.4) and (2.17) it is possible to replace i_{qe} and i_{de} in terms of i_L and δ_e obtaining:

$$v_{de} = (\omega_e/\omega_{eO})\left(X_{qe} - \frac{X_{mqe}^2}{X_{kqe}}\right)\left(\frac{0.78\ i_L}{T_2}\right)\cos(\delta_e + \Theta_1) +$$

$$- R_{ae}\frac{(0.78\ i_L)}{T_2}\sin(\delta_e + \Theta_1) - (\omega_e/\omega_{eO})\frac{X_{mqe}}{X_{kqe}}X_{kqe} \tag{A.8}$$

Now the same sort of manipulations are done using Equations (2.5), (2.6), (2.7), (2.3), (2.4) and (2.17). Obtaining:

$$v_{qe} = (\omega_e/\omega_{eo})\left(K_3 + \frac{K_5^2}{K_7}\right)\left(\frac{i_L\ 0.78}{T_2}\right)\sin(\delta_e + \Theta_1) +$$

$$(\omega_e/\omega_{eo}) \left(K_4 + \frac{K_5 K_8}{K_7}\right) - R_{ae}\left(\frac{0.78\ i_L}{T_2}\right) \cos(\delta_e + \Theta_1) \qquad (A.9)$$

where,

$$K_1 = X_{qe} - \frac{X^2_{mqe}}{X_{kqe}} \qquad (A.10)$$

$$K_2 = \frac{X_{mqe}}{X_{kqe}} \qquad (A.11)$$

$$K_3 = - X_{de} + \frac{X^2_{mde}}{X_{ffe}} \qquad (A.12)$$

$$K_4 = \frac{X_{mde}}{X_{ffe}} \lambda_{fe} \qquad (A.13)$$

$$K_5 = X_{mde} - \frac{X^2_{mde}}{X_{ffe}} \qquad (A.14)$$

$$K_7 = X_{kde} - \frac{X^2_{mde}}{X_{ffe}} \qquad (A.15)$$

$$k_8 = \lambda_{kde} - \frac{X_{mde}}{X_{ffe}} \lambda_{fe} \qquad (A.16)$$

And from (A.7), (A.8) and (A.9) (2.25) follows trivially.

Equations (2.26), (2.27), (2.28), (2.30), (2.31) and (2.32) follow trivially from Equations (2.17), (2.18), (2.7), (2.6),

(2.9) and (2.16). Equations (2.29) can be derived as follows. Use Equation (2.1) and (2.2) to obtain:

$$v_e = \sqrt{v_{de}^2 + v_{qe}^2} \tag{A.17}$$

Then using (A.2) and (A.3) and substituting above Equation (2.29) is obtained.

A.3 Linearized Equations About Equilibrium Point

In general any nonlinear Equation with continuous partial derives of the form:

$$\underline{y} = \underline{f}\ (\underline{X}) \tag{A.18}$$

where,

$$\underline{y} = [y_1,\ y_2,\ y_3,\ldots,y_n]^T \tag{A.19}$$

$$\underline{f} = [f_1,\ f_2,\ f_3,\ldots,f_n]^T \tag{A.20}$$

$$\underline{x} = [x_1,\ x_2,\ x_3,\ldots,x_n]^T \tag{A.21}$$

can be linearized about an equilibrium point as follows:

$$\underline{\Delta y} = [J(\underline{x}) \Big|_{\underline{x_0}}] \ \underline{\Delta x} \tag{A.22}$$

where,

$$\underline{\Delta y} = \underline{y} - \underline{y_0} \tag{A.23}$$

$$\underline{\Delta x} = \underline{x} - \underline{x_0} \tag{A.24}$$

$\underline{y_0}$ and $\underline{x_0}$ are equilibrium values and,

$$J(\underline{x}) = \frac{\partial \underline{f}\ (\underline{x})}{\partial_{\underline{x}}} = \begin{bmatrix} \frac{\partial f_1(\underline{x})}{\partial x_1} & \frac{\partial f_1(\underline{x})}{\partial x_2} & \cdots & \frac{\partial f_1(\underline{x})}{\partial x_n} \\ \frac{\partial f_2\ (\underline{x})}{\partial x_1} & \frac{\partial f_2(\underline{x})}{\partial x_2} & \cdots & \frac{\partial f_2(\underline{x})}{\partial x_n} \\ \frac{\partial f_n(\underline{x})}{\partial x_1} & \frac{\partial f_n(\underline{x})}{\partial x_2} & \cdots & \frac{\partial f_n(\underline{x})}{\partial x_n} \end{bmatrix} \tag{A.25}$$

Applying this method the linearized equations and related constants can be obtained.

A.4 Linearization of Equations (2.1) Through (2.18) (Without Damper Windings).

$$\Delta\delta_e = N_1\ \Delta v_e + N_2\ \Delta i_1 \tag{A.26}$$

$$\Delta V_e = N_3\ \Delta i_1 + N_4 \frac{d\ \Delta i_1}{dt} \tag{A.27}$$

$$\Delta v_{fe} = N_5 \Delta i_{fe} + N_6 \frac{d \Delta i_{fe}}{dt} + N_7 \frac{d \Delta i_1}{dt} + N_8 \frac{d \Delta \delta e}{dt} \quad (A.28)$$

$$\Delta v_e = N_9 \Delta i_{fe} + N_{10} \Delta i_1 + N_{11} \Delta \delta e \quad (A.29)$$

Coefficients N_1 through N_{11} are given in terms of the parameters and the steady-state values.

$$N_1 = -\sin \delta_{e0} / (v_{e0} \cos \delta_{e0} + X_{mae} i_{10} \sin \delta_{e0}) \quad (A.30)$$

$$N_2 = X_{mae} \cos \delta_{e0} / (v_{e0} \cos \delta_{e0} + X_{mae} i_{10} \sin \delta_{e0}) \quad (A.31)$$

$$N_3 = R_e \quad (A.32)$$

$$N_4 = X_e = LT_2 / [0.78 (2.33) \omega_{e0} \cos (\beta_0) T_1] \quad (A.33)$$

$$N_5 = R_{fe} \quad (A.34)$$

$$N_6 = X_{ffe} / \omega_{e0} \quad (A.35)$$

$$N_7 = -X_{mde} \sin (\delta_{e0}) / \omega_{e0} \quad (A.36)$$

$$N_8 = -X_{mde} i_{10} \cos (\delta_{e0}) / \omega_{e0} \quad (A.37)$$

$$N_9 = (i_{feO} X^2_{mde} - i_{1O} \sin(\delta_{eO}) X^2_{mde})/v_{eO} \quad (A.38)$$

$$N_{10} = (i_{1O} \sin^2(\delta_{eO}) X^2_{mde} + i_{1O} \cos^2(\delta_{eO}) X^2_{mqe} +$$

$$- i_{feO} X^2_{mde} \sin(\delta_{eO}))/v_{eO} \quad (A.39)$$

$$N_{11} = (X^2_{mde} i^2_{1O} \cos(\delta_{eO}) \sin(\delta_{eO}) - X^2_{mde} i_{feO} i_{1O} \cos(\delta_{eO}) +$$

$$- X^2_{mqe} \cos(\delta_{eO}) \sin(\delta_{eO}) i^2_{1O})/v_{eO} \quad A.40)$$

Using these equations it is possible to obtain an equation of the following form:

$$f_f(t) = \omega_n^2 \Delta i_1 + 2\zeta\omega_n \frac{d\Delta i_1}{dt} + \frac{d^2\Delta i_1}{dt^2} \quad (A.41)$$

Notice that Equation (A.8) is a second order differential equation since only the field flux and the load current were considered to be states.

The coefficients for this equation are:

$$\omega^2_n = \left[\left(\frac{R_{fe}}{A} - \frac{R_{fe}\ CD}{A}\right)\frac{X_{mde}}{Z} + \left(\frac{R_{fe}\ CE}{A} - \frac{R_{fe}\ B}{A}\right)\right]\Big/ H \quad (A.42)$$

$$2\zeta\omega_n = \left[\left(\frac{R_{fe}}{A} - \frac{R_{fe}\,CD}{A}\right)X_e + \left(\frac{X_{ffe}}{\omega_{e0}\,A} - \left(\frac{X_{ffe}\,C}{\omega_{e0}\,A} - F\right)D\right)\frac{X_{mde}}{Z} + \right.$$

$$\left. + \left(\frac{X_{ffe}\,C}{\omega_{e0}\,A} - F\right)E - \left(\frac{X_{ffe}\,B}{\omega_{e0}\,A} + G\right)\right] \Big/ H \qquad (A.43)$$

$$H = \left(\frac{X_{ffe}}{\omega_{e0}\,A} - \left(\frac{X_{ffe}\,C}{\omega_{e0}\,A} - F\right)D\right)X_e \qquad (A.44)$$

$$A = X_{mde}\,Z\left(\frac{i_{fe0}}{i_{10}} - \frac{Z}{(1 + Z^2)^{1/2}}\right) \qquad (A.45)$$

$$B = X_{mde}\,Z\left(1 - \frac{i_{fe0}\,Z}{i_{10}\sqrt{1 + Z^2}}\right) \qquad (A.46)$$

$$C = \frac{X_{mde}\,Z\,i_{fe0}}{(1 + Z^2)^{1/2}} \qquad (A.47)$$

$$D = \frac{Z}{X_{mde}\,i_{10}\,(Z + 1/Z)} \qquad (A.48)$$

$$E = \frac{1}{i_{10}\,(Z + 1/Z)} \qquad (A.49)$$

$$F = \frac{X_{mde}\,i_{10}}{\omega_{e0}\,(1 + Z^2)^{1/2}} \qquad (A.50)$$

$$G = \frac{X_{mde}\, Z}{\omega_{eO}\,(1 + Z^2)^{1/2}} \qquad (A.51)$$

$$Z = X_{mde}/R_e \qquad (A.52)$$

Equation (2.33) and (2.34) are the solutions to the impulse response of Equation (A.41). Equation (2.35) is obtained by substituting $t = \frac{\pi/2}{\omega_n h}$ in Equation (2.33).

APPENDIX B

Derivation of the Equations Used in Chapter III

B.1 Current Boost System

A brief explanation of the operation of the current boost system is given in Section 3.2. The expressions modeling the behavior of the current boost system are also given in Section 3.2. The behavior of the current boost system can be divided into two modes of operation, Mode I for $i_{fe} < \frac{2i_L}{N_c}$ and Mode II for $i_{fe} \geq \frac{2i_L}{N_c}$. In this appendix, these modes of operation are investigated and the threshold value $i_{fe(th)} = \frac{2i_L}{N_c}$ is derived. Then using the saturation model of Figure 3.4 for the current transformers the governing equations for the current boost system are derived.

Let us begin by analyzing the system in Figure B.1 when the line to line currents at the secondary of the current transformers, i''_{ca}, i''_{cb}, and i''_{cc} are small compared to i_{fe}. The subscripts a, b, and c represent phases a, b, and c, respectively. In this case the six diodes of the current boost bridge are forward biased (Mode I) and the secondaries of the current transformers are short circuited through the diodes. The resistance R_c are thus inconsequential during Mode I of operation. Since the current transformers are short circuited, the transformers are operating unsaturated and simply stepping down the current passing through the

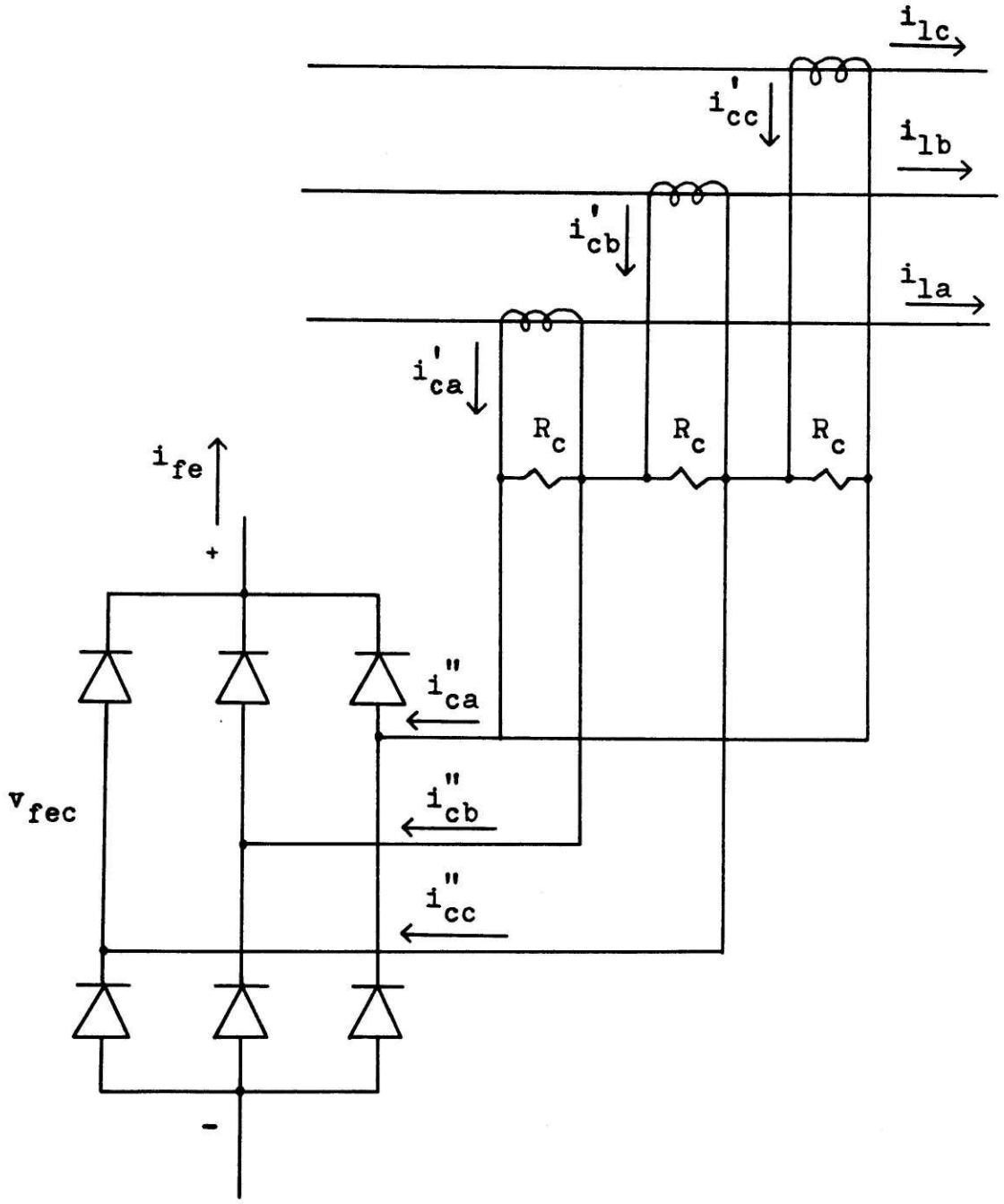

Figure B.1 Schematic of current boost system

primary by the factor N_c, i.e., the turns ratio of the current transformers.

Let us derive the current waveforms for this case. Notice that the current transformers have no direct effect on the rest of the system quantities during this mode of operation. The current through the field winding and the currents from the current transformers can be considered as time varying current sources. Figure B.1 can be drawn as Figure B.2. The symbols R_{b1} through R_{b6} stand for the 6 diodes, respectively. Using Kirchoff's current law for Figures B.1 and B.2 it is possible to obtain the current waveforms for the different branches of the current boost system. In doing this it is assumed that the armature currents were solely determined by the current drawn from the R-L load, i.e., the current i_1' due to the self-excitation loop is neglected. The waveforms obtained are shown in Figure B.3. Notice that the variable i_L is the magnitude of the load current which could be changing during transient conditions. The waveforms shown are: the line to line exciter-alternator terminal voltages v_{ab}, v_{ac}, v_{ba}, v_{ca}, v_{cb}, and v_{bc}, the exciter-alternator terminal currents i_{la}, i_{lb}, and i_{lc}, the phase currents of the secondary of the current transformers, i_{ca}', i_{cb}', and i_{cc}' and the line to line currents at the secondary of the current transformers, i_{ca}'', i_{cb}'', and i_{cc}''.

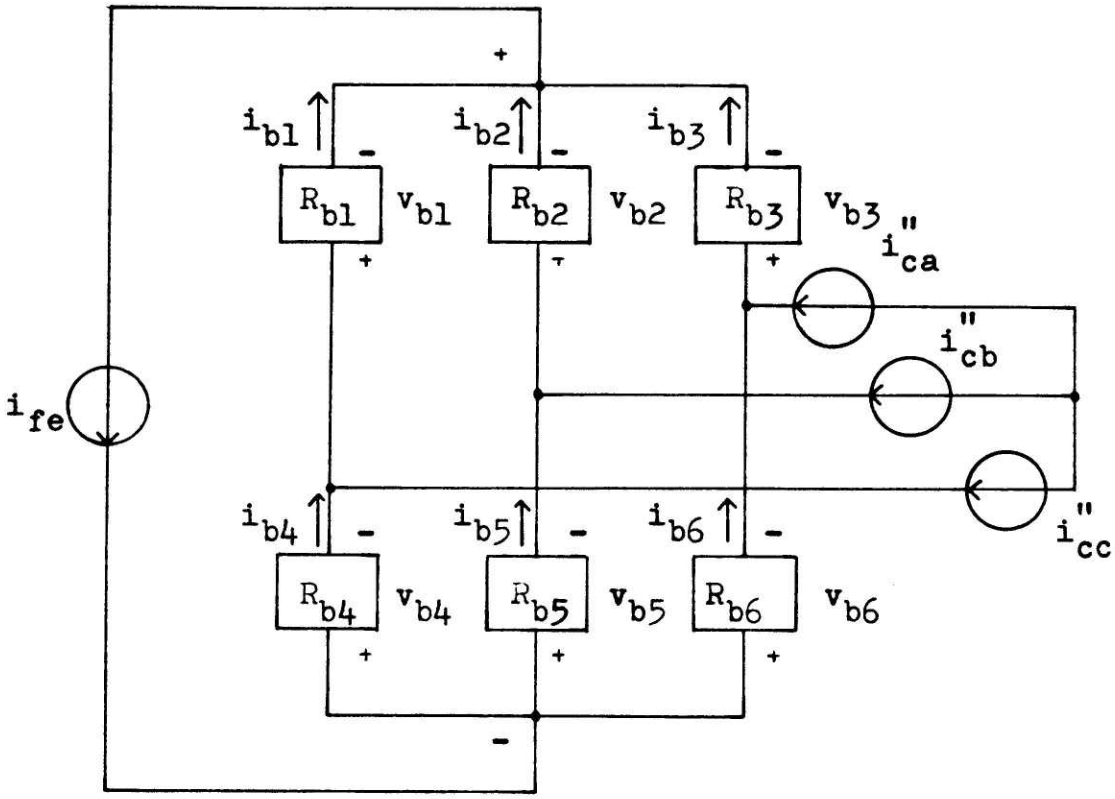

Figure B.2 Schematic of current boost system with time varying current sources

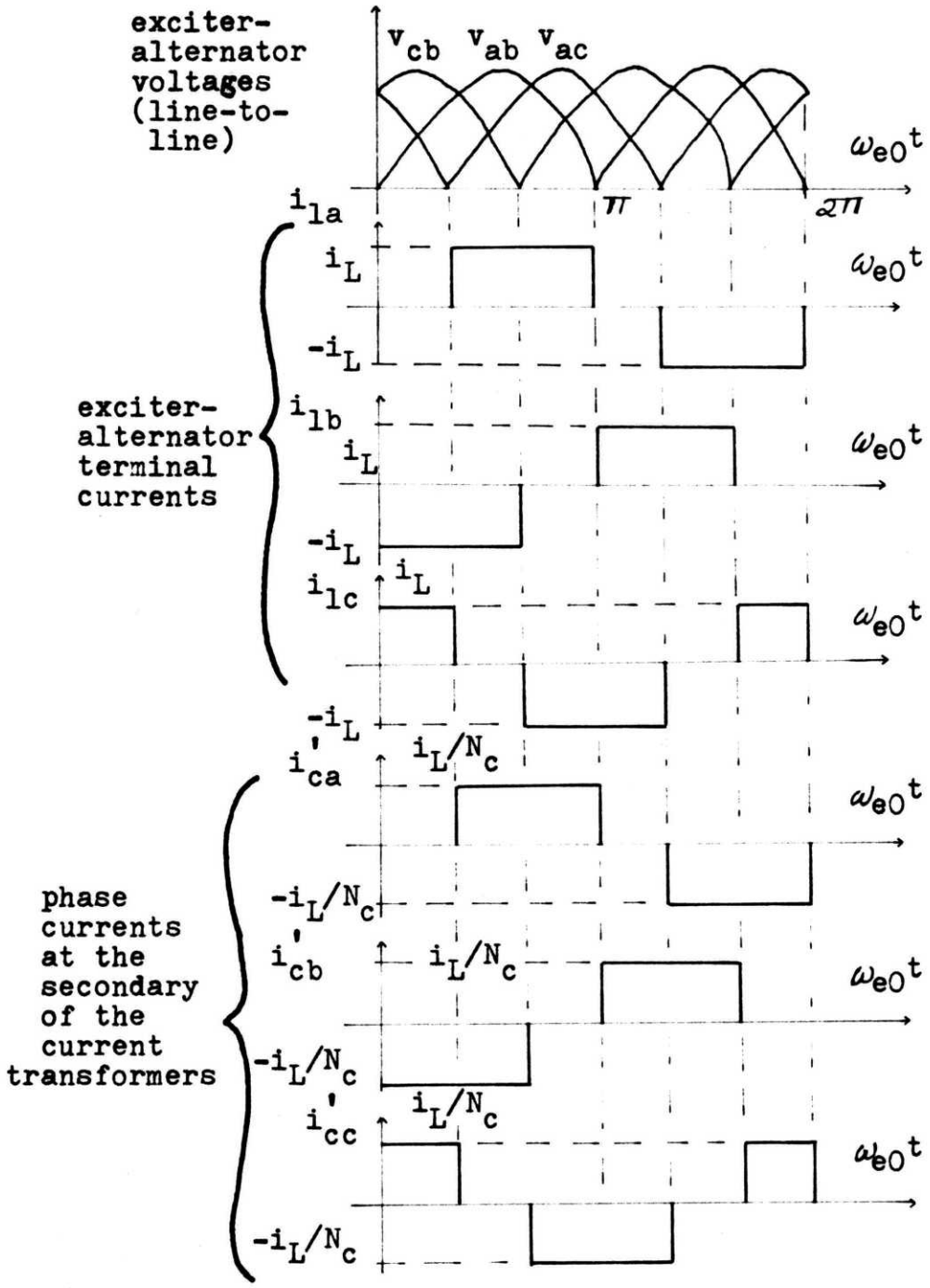

Figure B.3 Sketch of the current waveforms for the current boost system (continued)

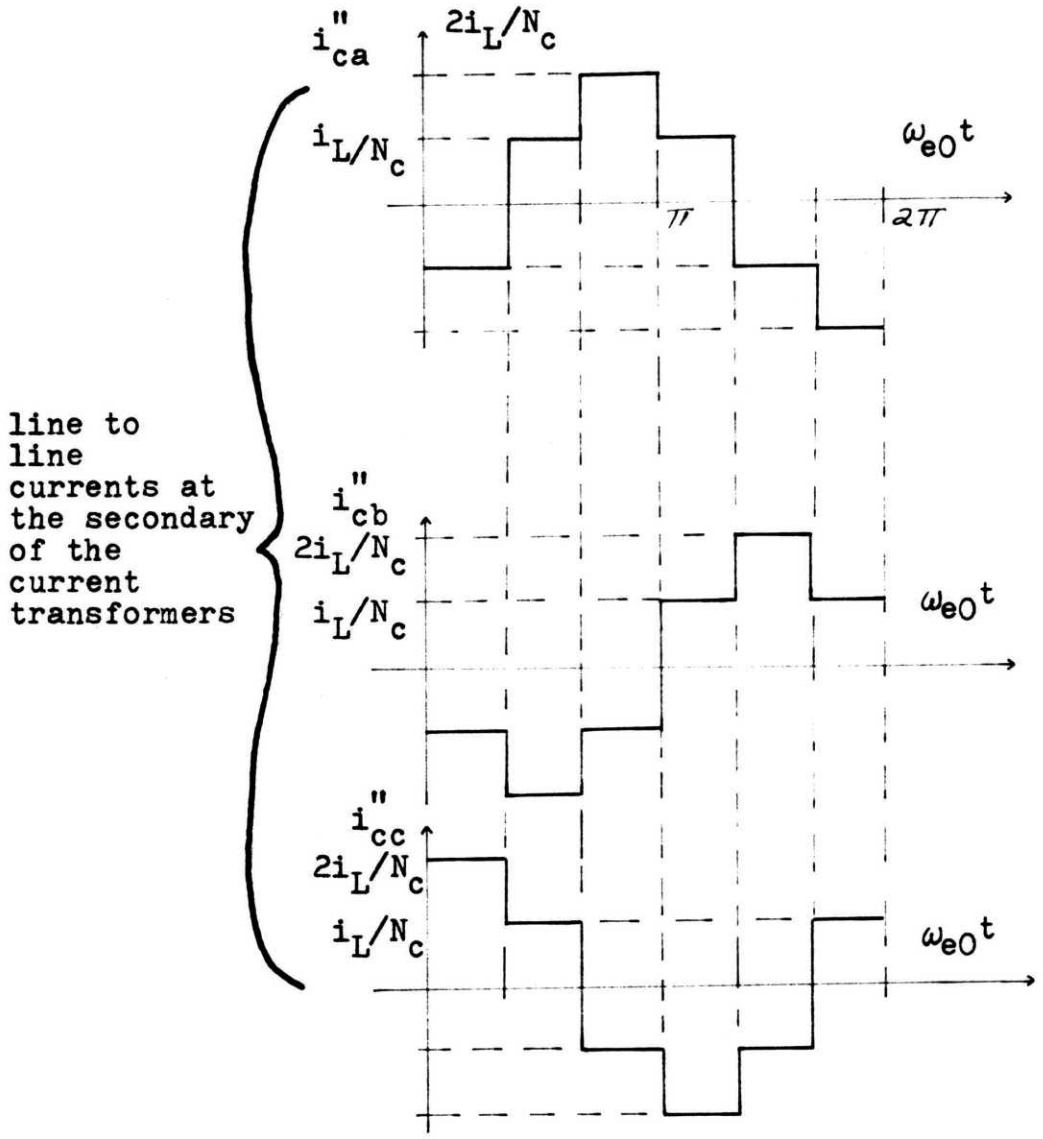

Figure B.3 Sketch of the current waveforms for the current boost system (continuation)

Now it is of interest to study the behavior of the current boost bridge for changes in the current i_L. The six diodes of the current boost bridge are represented as non-linear resistances R_{b1} through R_{b6}, with forward voltages across them v_{b1} through v_{b6} and forward currents through them i_{b1} through i_{b6}. The characteristics for the diodes can be modeled as follows:*

$$v_{bj} = R_s i_{bj} + \frac{kT}{q} \ln\left(\frac{i_{bj}}{I_s} + 1\right) \qquad (B.1)$$

The subscript j can be either **1**, 2, 3, 4, 5, or 6, i.e., corresponding to diodes 1, 2, 3, 4, 5, or 6, respectively. The quantities R_s, $\frac{kT}{q}$ and I_s are parameters of the diode. The variable v_{bj} is the forward voltage across the diode and i_{bj} is the current through the diode. We will consider the six diodes to be identical. It is possible to define the resistance R_{bj} for a diode j to be:

$$R_{bj} \triangleq \frac{v_{bj}}{i_{bj}} = R_s + \frac{\frac{kT}{q} \ln\left(\frac{i_{bj}}{I_s} + 1\right)}{i_{bj}} \qquad (B.2)$$

I_s is the reverse saturation current which is very small, therefore for i_{bj} very small the value of R_{bj} is very big and for all practical purposes is infinity. Also notice that

---

* See P. E. Gray [8].

when the current i_{bj} increases R_{bj} decreases. Assume that the current boost bridge is operating in Mode I and i''_{ca}, i''_{cb} and i''_{cc} are much smaller than i_{fe} or equivalently that $\frac{2i_L}{N_c}$ is much smaller than i_{fe} at all times. Then all the currents through the six diodes are due mostly to the current source i_{fe} (see Figure B.2). Therefore i_{fe} is forward biasing all the diodes which is equivalent to saying that the currents i_{bj}'s are relatively large and $R_{bj} \simeq R_s$ is a very small resistance value.

Now let us write the diode currents in terms of the time varying current sources of Figure B.3. Let us assume without loss of generality that all the events described hereon are taking place in the interval $0 \leq \omega_{e0} \leq \pi/3$ of Figure B.3.

In the case above the current i_{fe} is divided nearly equally among the three legs of the current boost bridge. Currents i''_{ca}, i''_{cb} and i''_{cc} also divide symmetrically, that is i''_{ca} will divide equally between R_{b3} and R_{b6} and then the current going through R_{b3} will divide equally between R_{b1} and R_{b2} and so on. As a result the currents can be written in terms of the current sources for the time interval of interest as:

$$\left.\begin{aligned} i_{b1} &= \frac{i_{fe}}{3} + \frac{i_L}{N_c} \\ i_{b2} &= \frac{i_{fe}}{3} - \frac{i_L}{2N_c} \\ i_{b3} &= \frac{i_{fe}}{3} - \frac{i_L}{2N_c} \\ i_{b4} &= \frac{i_{fe}}{3} - \frac{i_L}{N_c} \\ i_{b5} &= \frac{i_{fe}}{3} + \frac{i_L}{2N_c} \\ i_{b6} &= \frac{i_{fe}}{3} + \frac{i_L}{2N_c} \end{aligned}\right\} \qquad (B.3)$$

Assume now that the current $\frac{i_L}{N_c}$ starts to increase so that its effect becomes significant compared to $\frac{i_{fe}}{3}$. Notice that from the expressions above this implies that i_{b1}, i_{b5} and i_{b6} will increase and i_{b2}, i_{b3} and i_{b4} will decrease. However as soon as this starts to happen then the effect will be also to increase the resistances R_{b2}, R_{b3} and R_{b4} which can no longer be assumed to be equal to R_s. Resistances R_{b1}, R_{b5} and R_{b6} can still be assumed to be equal to R_s.

Notice that now currents will tend to redistribute according to the new values of the resistances. Now currents i''_{ca}, i''_{cb} and i''_{cc} will tend to take the path of

less resistance. Hence more current coming from i''_{cc} will tend to go through R_{b1} rather than R_{b4}. This implies that more current coming from i_{b1} must be divided between R_{b2} and R_{b3} which tends to increase R_{b2} and R_{b3} and decrease i_{b2} and i_{b3} even further. Since R_{b4} has increased, more current due to i_{fe} will tend to go through branches defined by the resistances $R_{b2}-R_{b5}$ and $R_{b3}-R_{b6}$ rather than $R_{b1}-R_{b4}$.

As this process continues to go on, that is as i_L increases relative to i_{fe} during the interval of interest it is possible to envision a limiting situation where most of the current due to i''_{cc} goes through R_{b1}; R_{b4} is now a very big resistance and hence it is plausible to assume that i_{fe} almost divides nearly equally between the branches defined by the resistances $R_{b2}-R_{b5}$ and R_{b3} and $R_{b3}-R_{b6}$. Also i_{b1} divides through R_{b2} and R_{b3}. This is because since i_{b4} is very small, very little current due to i''_{ca} and i''_{cb} will have to flow through i_{b5} and i_{b6} to balance the effect of the currents due to i_{b4}. As a result the currents through the diodes can be written approximately as:

$$\left.\begin{aligned} i_{b1} &\simeq \frac{2i_L}{N_c} \\ i_{b2} &\simeq \frac{i_{fe}}{2} - \frac{i_L}{N_c} \\ i_{b3} &\simeq \frac{i_{fe}}{2} - \frac{i_L}{N_c} \\ i_{b4} &\simeq 0 \\ i_{b5} &\simeq 0 \\ i_{b6} &\simeq 0 \end{aligned}\right\} \qquad (B.4)$$

Then as $\frac{i_L}{N_c} \rightarrow \frac{i_{fe}}{2}$ or equivalently when $i_{fe} \rightarrow \frac{2i_L}{N_c}$ we have the situation where the results above hold exactly as a result $R_{b4} \rightarrow \infty$, $R_{b2} \rightarrow \infty$ and $R_{b3} \rightarrow \infty$. This means that now for $i_{fe} \geq \frac{2i_L}{N_c}$ the system leaves Mode I and enters Mode II of operation. In fact notice that the topology obtained after setting R_{b3}, R_{b2} and R_{b4} equal to infinity and R_{b1}, R_{b5} and R_{b6} equal to 0 (R_s is very small) in Figure B.1 is the topology given in Figure 3.3. It can be shown that these results are obtained independently of the restriction $0 \leq \omega_{e0} \leq \pi/3$. Notice that as $\frac{i_L}{N_c}$ starts to decrease again the process reverses and for $i_{fe} < \frac{2i_L}{N_c}$ the current boost system leaves Mode II and enters Mode I.

It must be noted that we have ignored the gradual effect of the current boost bridge on the rest of the system as

some of the resistances representing the diodes of the current boost bridge grow larger. It has been assumed that the current boost system goes from a situation of no effect to a situation of effect on the rest of the system immediately. This is justified by the fact that the characteristics of the diode are exponential and therefore R_{bj} varies rapidly from a value of R_s to ∞.

We have shown that the threshold value $i_{fe(th)}$ that divides Mode I and Mode II of operation is $\frac{2i_L}{N_c}$. Now we will derive the governing equations for Mode II. The topology for Mode II is independent of the time interval considered and is shown in Figure 3.3. The current transformers have been modeled with a saturable mutual inductance as shown in Figure 3.4. Leakage inductances and winding resistances of the current transformers have been neglected. The current sources represent the exciter-alternator terminal currents flowing through the primary of the current transformers. Let us define:

$$i \triangleq \frac{2i_L}{N_c} - i_{fe} \tag{B.5}$$

This is also equation (3.19). Using Faraday's law for the current transformer it is possible to write the following expression for the transformer with voltage v_{fecl} across the secondary. The term $(i - v_{fecl}/R_c)$ is the current through the magnetizing inductance of the transformer.

$$\begin{cases} v_{fec1} = \dfrac{L_c}{\omega_{e0}} \dfrac{d(i-v_{fec1}/R_c)}{dt}, & i - \dfrac{v_{fec1}}{R_c} < i_m \\ v_{fec1} = 0, & i - \dfrac{v_{fec1}}{R_c} \geq i_m \end{cases} \tag{B.6}$$

Similarly for the lower half of Figure 3.3 it is possible to write

$$\begin{cases} v_{fec2} = \dfrac{L_c}{\omega_{e0}} \dfrac{d(\frac{i}{2} - v_{fec2}/R_c)}{dt}, & \dfrac{i}{2} - \dfrac{v_{fec2}}{R_c} < i_m \\ v_{fec2} = 0, & \dfrac{i}{2} - \dfrac{v_{fec2}}{R_c} \geq i_m \end{cases} \tag{B.7}$$

Notice that $v_{fc1} = 0$ and $v_{fc2} = 0$ for $i - \dfrac{v_{fec1}}{2} \geq i_m$ and $\dfrac{i}{2} - \dfrac{v_{fec2}}{R_c} \geq i_m$, respectively, is a consequence of the saturation of the current transformers. Expressions (B.7) and (B.8) can be manipulated using the fact that $v_{fec1} + v_{fec2} = v_{fec}$ to obtain (3.17). Inequalities at the extreme left of the equation (3.17) are added to the inequalities obtained from (B.7) and (B.8) to account for Mode I of operation. Equation (3.18) is obtained by manipulating the governing equations algebraically to obtain $\dfrac{di}{dt}$ as a function of the rate of change of the states λ_{fe}, λ_{kde}, λ_{kqe} and i_L. The variables Y_1 through Y_4 are given below

$$Y_1 = \left(M_1 + M_4\left(\frac{W_4}{1-W_3}\right)\right)^2 \tag{B.8}$$

$$Y_2 = \left(M_2 + M_4\left(\frac{W_5}{1-W_3}\right)\right)^2 \tag{B.9}$$

$$Y_3 = 2M_4\left(\frac{W_2}{1-W_3}\right) \tag{B.10}$$

$$Y_4 = \frac{2}{N_c}\left(M_3 + M_4\left(\frac{W_1}{1-W_3}\right)\right) \tag{B.11}$$

where,

$$M_1 = -\frac{1}{2}\left(\frac{1}{X_{ffe}} + \frac{X_{mde}^2}{K_7 X_{ffe}^2}\right) \tag{B.12}$$

$$M_2 = \frac{1}{2}\frac{X_{mde}}{K_7 X_{ffe}} \tag{B.13}$$

$$M_3 = 1 - \frac{1}{2}\left(\frac{X_{mde}}{X_{ffe}} - \frac{X_{mde}K_5}{X_{ffe}K_7}\right)M_5 \sin \delta_e \tag{B.14}$$

$$M_4 = -\frac{1}{2}\left(\frac{X_{mde}}{X_{ffe}} - \frac{X_{mde}K_5}{X_{ffe}K_7}\right)M_5 \frac{i_L}{N_c} \cos \delta_e \tag{B.15}$$

$$M_5 = 0.78/T_4 \tag{B.16}$$

Constants K_5, K_7 are given in Appendix A by (A.14) and (A.15), respectively, W_1 through W_5 are given by

$$W_1 = \frac{v_{qe}}{v_e^2}(\omega_e/\omega_{e0})\left(X_{qe} - \frac{X_{mqe}^2}{X_{kqe}}\right)M_5 \cos \delta_e - \frac{v_{de}}{v_e^2}(\omega_e/\omega_{e0})\left(K_3 + \frac{K_5^2}{K_7}\right)M_5 \sin \delta_e \tag{B.17}$$

$$W_2 = -\frac{v_{qe}}{v_e^2}(\omega_e/\omega_{e0})\frac{X_{mqe}}{X_{kqe}} \tag{B.18}$$

$$W_3 = -\frac{v_{qe}}{v_e^2}(\omega_e/\omega_{e0})\left(X_{qe} - \frac{X_{mqe}^2}{X_{kqe}}\right)\left(M_5 \frac{i_L}{N_c} \sin \delta_e\right)$$

$$-\frac{v_{de}}{v_e^2}(\omega_e/\omega_{e0})M_5 \frac{i_L}{N_c} \cos \delta_e\left(K_3 + \frac{K_5^2}{K_7}\right) \qquad (B.19)$$

$$W_4 = -\frac{v_{de}}{v_e^2}(\omega_e/\omega_{e0})\left(\frac{X_{mde}}{X_{ffe}} - \frac{K_5}{K_7}\frac{X_{mde}}{X_{ffe}}\right) \qquad (B.20)$$

$$W_5 = -\frac{v_{de}}{v_e^2}(\omega_e/\omega_{e0})\frac{K_5}{K_7} \qquad (B.21)$$

Constant K_3 is given in Appendix A by (A.12)

B.2 Steady-State Equations

The equations necessary to solve for the steady-state are listed below.* These equations and equations (3.21), (3.22) and (3.23) are sufficient to find the steady-state. Notice that in the steady-state the damper winding currents are zero.

$$R_e = \frac{T_4 R}{2.33 T_3 (0.78)} \qquad (B.22)$$

$$\hat{Z}_f = Z_f/\underline{\alpha} \qquad (B.23)$$

$$Z_f = \frac{R_{fe} T_6}{2.33 T_5 \cos \alpha (0.78)} \qquad (B.24)$$

---

* Hatted variables mean phasor or complex variables.

$$\hat{Z}_p = Z_p \underline{/\alpha+\gamma} \tag{B.25}$$

$$Z_p \triangleq \frac{v_e}{i_1} = \sqrt{(Z_f+X_p \sin\alpha)^2 + (X_p \cos\alpha)^2} \tag{B.26}$$

$$\hat{Z}_e = Z_e \underline{/\theta_1} \tag{B.27}$$

$$Z_e = \frac{\sqrt{(AC+BD)^2 + (BC-AD)^2}}{C^2 + D^2} \tag{B.28}$$

$$\theta_1 = \tan^{-1}[(BC-AD)/(AC+BD)] \tag{B.29}$$

$$A = R_e Z_f \cos\alpha \tag{B.30}$$

$$B = R_e X_p + R_e Z_f \sin\alpha \tag{B.31}$$

$$C = R_e + Z_f \cos\alpha \tag{B.32}$$

$$D = Z_f \sin\alpha + X_p \tag{B.33}$$

$$\delta_e = \tan^{-1}\left[\frac{X_{qe}\cos\theta_1 - R_{ae}\sin\theta_1}{Z_e + R_{ae}\cos\theta_1 + X_{qe}\sin\theta_1}\right] \tag{B.34}$$

First I will explain how to obtain these equations and equations (3.21), (3.22) and (3.23) from the basic governing equations in Chapter III. After that I will describe how to obtain the steady-state values using these equations and equation (3.1).

Equation (B.22) is obtained by calculating the driving point impedance at the input of the output rectifier. What this gives us is the equivalent impedance presented during steady-state by the load resistance as seen through the output rectifier. Something similar is done in the case of the separately-excited exciter-alternator and the reader is referred to Appendix A.

The complete quantity $\hat{Z}_f$ represents the impedance seen at the input of the SCR bridge looking towards the field winding of the exciter-alternator. The angle of the impedance being equal to α follows from the definition of driving point impedance, i.e.,

$$\frac{\hat{v}_e'}{\hat{i}_1'} = \frac{v_e'}{i_1'} \underline{/\theta_1'}$$

since θ_1' is the phase angle between v_e' and i_1' and θ_1' is from (3.12) equal to α. The magnitude of $\hat{Z}_f$, Z_f, is obtained as for R_e as shown in Appendix A.

The driving point impedance $\hat{Z}_p$ given by (B.25) and (B.26) is derived as follows:

$$\hat{Z}_p \triangleq \frac{\hat{v}_e}{\hat{i}_1'} \underline{/\alpha+\gamma} \qquad \text{(B.35)}$$

The angle $\alpha+\gamma$ follows from the fact that this is the phase angle between v_e and i_1' as shown in the phasor diagram given

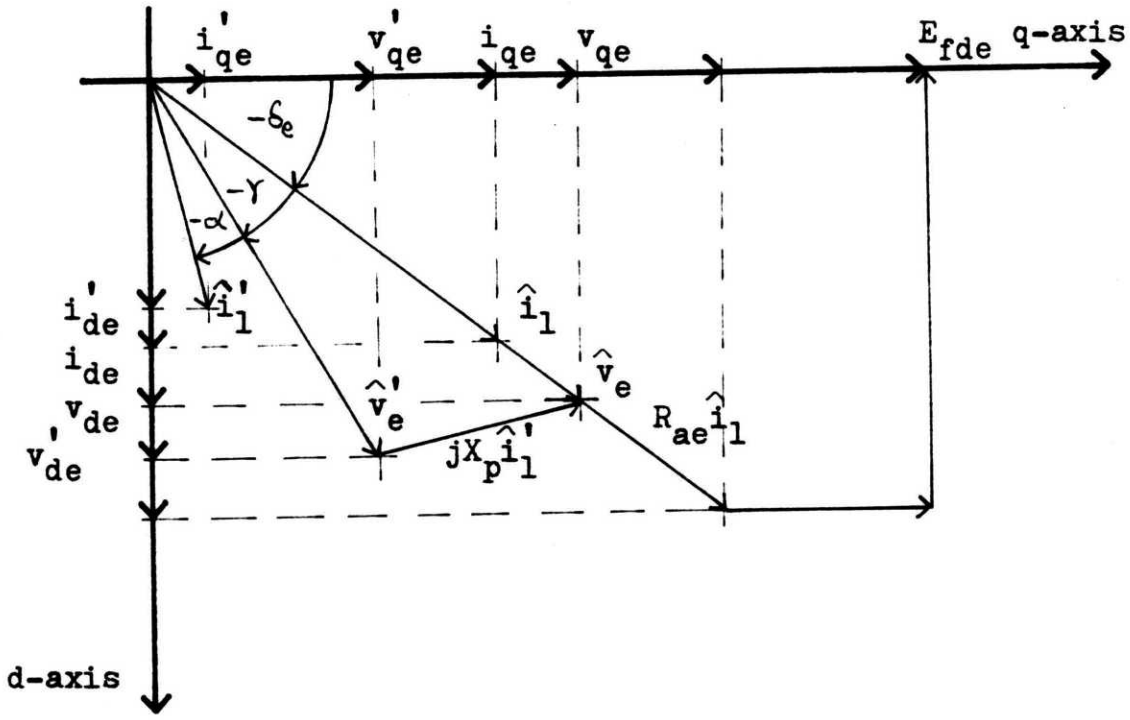

Figure B.4 Steady-state phasor diagram for self-excited exciter-alternator

in Figure B.4. The magnitude of $\hat{Z}_p$, Z_p is derived as follows. Equation (3.8) and (3.9) in phasor form can be written as

$$v_e\angle{-\delta_e} = v_e'\angle{-\delta_e-\gamma} + jX_p i_1'\angle{-\delta_e-\gamma-\alpha} \tag{B.36}$$

Now multiply (B.36) by $1\angle{\delta_e+\gamma}$ obtaining:

$$v_e\angle{\gamma} = v_e' + jX_p i_j'\angle{-\alpha} \tag{B.37}$$

or

$$v_e\angle{\gamma} = \left(v_e'+X_p i_1'\sin\alpha\right) + j(X_p i_1'\cos\alpha) \tag{B.38}$$

Equating magnitudes it follows that:

$$v_e = \sqrt{\left(v_e'+X_p i_1'\sin\alpha\right)^2 + \left(X_p i_1'\cos\alpha\right)^2} \tag{B.39}$$

Using the definition of Z_f as driving point impedance $\left(Z_f = \frac{v_e'}{i_j'}\right)$ it is possible to substitute v_e' in (B.39) for $z_f i_1'$. The variable i_1' can then be factored from (B.39) and after dividing both sides by i_1' (B.26) is obtained.

The complex quantity $\hat{Z}_e$ represents the driving point impedance that is observed by the exciter-alternator at its terminals $(\hat{v}_e/i_1')$. Since the exciter-alternator is loaded by both the R-L load and the excitation loop going to the field winding in parallel, it follows that $\hat{Z}_e$ is the parallel combination of R_e and $\hat{Z}_p$. Doing this yields equations (B.28) and (B.29).

Equation (B.34) follows from a derivation similar to that of (2.20) as derived in Appendix A. In this case R_e should be replaced by Z_e.

Equation (3.22) is derived as follows. From the definition of Z_p and Z_e it follows that

$$i_1 Z_e = i_1' Z_p \tag{B.40}$$

Using (3.11), i_1' can be expressed in terms of i_{fe}. This expression is substituted in (B.14) and the resulting expression is solved for i_{fe}

$$i_{fe} = i_1\left(\frac{Z_e(T_6/0.78)}{Z_p}\right) \tag{B.41}$$

Then using (B.41) and (2.3) the quantity $(i_{fe} - i_{de})$ can be written as follows.

$$i_{fe} - i_{de} = i_1\left(\frac{Z_e(T_6/0.78)}{Z_p} - \sin(\delta_e+\theta_1)\right) \tag{B.42}$$

Equation (3.22) follows trivially. Equation (3.23) follows trivially from the definition of Z_e as the driving point impedance.

Equation (3.21) for X_{mdeo} is found by manipulating the governing equations to obtain an expression in terms of the direct axis mutual inductance X_{mde}. From (2.1) and (2.2) it follows that

$$v_e^2 = v_{de}^2 + v_{qe}^2 \tag{B.43}$$

If (2.5) and (2.8) are substituted in (2.10) and (2.11), respectively, and the resulting expressions are

substituted in (B.43) with (ω_e/ω_{e0}) set equal to 1 it follows that

$$v_e^2 = \left(X_{qe}i_{qe}-R_{ae}i_{de}\right)^2 + \left(-X_{de}i_{de}+X_{mde}i_{fe}-R_{ae}i_{qe}\right)^2 \qquad (B.44)$$

Substituting $X_{de} = X_{ae} + X_{mde}$ in (B.44) and solving the resulting expression for X_{mde} it is possible to obtain the following expression

$$X_{mde} = \frac{\sqrt{v_e^2 - \left(-R_{ae}i_{de}+X_{qe}i_{qe}\right)^2} + X_{ae}i_{de} + R_{ae}i_{qe}}{i_{fe} - i_{de}} \qquad (B.45)$$

If expression (3.23) is substituted for v_e and (2.3) and (2.4) are substituted for i_{de} and i_{qe}, respectively, in the numerator of expression (B.45) it is possible to factor out the variable i_1 from the numerator. Then by substituting (B.42) for the denominator in (B.45) equation (3.21) is obtained after the variable i_1 is cancelled from the numerator and denominator.

The steady-state values can be found as described in Section 3.3.1 knowing the quantities Z_e, δ_e, θ_1 and Z_p. First it is necessary to find R_e and Z_f using (B.1) and (B.3), respectively. Then Z_f and other parameters are used to find Z_p using (B.26). With Z_p, Z_f and R_e and other exciter-alternator parameters found from Tables 2.2 and 3.2, it is possible to find Z_e and θ_1. Then δ_e can be obtained using (B.13). With

these quantities and equations (3.21), (3.22) and (3.23) the steady-state condition can be found.

B.3 Auxiliary Equations

The equations used in Section 3.3.2 to help obtaining the transient solution numerically are called auxuliary equations. What follows is a brief explanation of how to obtain these equations.

Equation (3.29) can be derived using (3.13) and (3.14) in phasor form (see phasor diagram in Figure B.4). It follows that

$$i'_1\underline{/-\gamma-\delta_e-\alpha} + i''_1\underline{/-\delta_e} = i_1\underline{/-\theta_1-\delta_e} \qquad (B.46)$$

Multiply (B.46) by $1/\underline{\delta_e}$ to obtain

$$i'_1\underline{/-\gamma-\alpha} + i''_1\underline{/0^\circ} = i_1\underline{/-\theta_1} \qquad (B.47)$$

Equating magnitudes, real and imaginary parts of this equation, it is possible to obtain (3.29) and (3.30). Equations (3.31) through (3.34) are derived for Chapter II in Appendix A. Equation (3.35) is derived from (3.11). Equation (3.36) follows from (B.39). Equation (3.37) can be obtained from (B.37). Equations (3.42) through (3.46) are obtained from the governing equations applied for t equal to $t_0 + \Delta_T$.

B.4 Linearization of the Governing Equations (Without Damper Windings, Potential Transformer and Current Boost Bridge)

In this section the linearized equations for the self excited exciter-alternator used in Section 3.4 are given.

$$\Delta v_e = \Delta i_1(s_1) + \Delta\delta_e(s_2) + \Delta i_1'(s_3) + \Delta X_{mde}(s_4) \tag{B.48}$$

$$\Delta i_1 = \Delta i_1'(s_{12}) - \Delta\alpha(s_{13}) + \Delta i_1''(s_{14}) \tag{B.49}$$

$$\Delta\delta_e(s_{19}) + \Delta i_1(s_{20}) + \Delta v_e(s_{22}) = 0 \tag{B.50}$$

$$\Delta v_e = R_e\Delta i_1'' + L_e \frac{d\Delta i_1''}{dt} \tag{B.51}$$

$$-\Delta\alpha = -(s_{23})\Delta v_e + (s_{24})\Delta i_1' + (s_{25}) \frac{d\Delta i_1'}{dt} + (s_{26}) \frac{d\Delta X_{mde}}{dt} - (s_{27}) \frac{d\Delta\delta_e}{dt} - (s_{28}) \frac{d\Delta i_1}{dt} \tag{B.52}$$

$$\Delta X_{mde} = (s_{29})\Delta i_1' - (s_{30})\Delta i_1 - (s_{31})\Delta\delta_e \tag{B.53}$$

Manipulating these equations an equation of the following form can be obtained

$$-\Delta\alpha(Z_o) = \Delta i_1''\omega_n^2 + 2\zeta\omega_n \frac{d\Delta i_1''}{dt} + \frac{d^2\Delta i_1''}{dt^2} \tag{B.54}$$

Notice that equation (B.54) is second order because only the field flux and the load current are considered states.

The constant coefficients for equations (B.48) through (B.54) are given below:

$$s_1 = ((R_{ae}\sin(\theta_{10}+\delta_{e0}) - X_{qe}\cos(\theta_{10}+\delta_{e0}))(R_{ae}i_{10}\sin(\theta_{10}+\delta_{e0}) - X_{qe}i_{10}\cos(\delta_{e0}+\theta_{10})) + (-R_{ae}\cos(\delta_{e0}+\theta_{10}) - X_{de0}\sin(\delta_{e0}+\theta_{10})) \cdot ((T_6/0.78)X_{mde0}i'_{10} - X_{de0}i_{10}\sin(\delta_{e0}+\theta_{10}) - R_{ae}i_{10}\cos(\delta_{e0}+\theta_{10})))/v_{e0} \quad (B.55)$$

$$s_2 = ((R_{ae}i_{10}\cos(\theta_{10}+\delta_{e0}) + X_{qe}i_{10}\sin(\delta_{e0}+\theta_{10}))(R_{ae}i_{10}\sin(\theta_{10}+\delta_{e0}) - X_{qe}i_{10}\cos(\delta_{e0}+\theta_{10})) + (-X_{de0}i_{10}\cos(\delta_{e0}+\theta_{10}) + R_{ae}i_{10}\sin(\delta_{e0}+\theta_{10})) \cdot ((T_6/0.78)X_{mde0}i'_{10} - X_{de0}i_{10}\sin(\delta_{e0}+\theta_{10}) - R_{ae}i_{10}\cos(\delta_{e0}+\theta_{10})))/v_{e0} \quad (B.56)$$

$$s_3 = ((T_6/0.78)X_{mde0})((T_6/0.78)X_{mde0}i'_{10} - X_{de0}i'_{10}\sin(\delta_{e0}+i_{10}) - R_{ae}i_{10}\cos(\delta_{e0}+\theta_{10}))/v_{e0} \quad (B.57)$$

$$s_4 = (((T_6/0.78)i'_{10} - i_{10}\sin(\delta_{e0}+\theta_{10}))((T_6/0.78)X_{mde0}i'_{10} - X_{de0}i_{10}\sin(\delta_{e0}+\theta_{10}) - R_{ae}i_{10}\cos(\delta_{e0}+\theta_{10})))/v_{e0} \quad (B.58)$$

$$s_{12} = \left(i''_{10}\cos(\alpha_0)+i'_{10}\right)/i_{10} \quad (B.59)$$

$$s_{13} = \left(i''_{10}i'_{10}\sin(\alpha_0)\right)/i_{10} \quad (B.60)$$

$$s_{14} = \left(i''_{10}+i'_{10}\cos(\alpha_0)\right)/i_{10} \quad (B.61)$$

$$s_{19} = \cos \delta_{e0}(v_{e0}+R_{ae}i_{10}\cos \theta_{10}+X_{qe}i_{10}\sin \theta_{10}) + \sin \delta_{e0}(-R_{ae}i_{10}\sin \theta_{10}+X_{qe}i_{10}\cos \theta_{10}) \quad (B.62)$$

$$s_{20} = \sin \delta_{e0}(R_{ae}\cos \theta_{10}+X_{qe}\sin \theta_{10}) + \cos \delta_{e0}(-X_{qe}\cos \theta_{10}+R_{ae}\sin \theta_{10}) \quad (B.63)$$

$$s_{22} = \sin \delta_{e0} \quad (B.64)$$

$$R_e = \frac{T_4 R}{2.33T_3(0.78)} \quad (B.65)$$

$$L_e = \frac{T_4 L}{2.33T_3(0.78)\omega_{e0}} \quad (B.66)$$

$$s_{23} = \frac{\cos \alpha_o}{\sin \alpha_0(v_{e0})} \quad (B.67)$$

$$s_{24} = \frac{R_{fe}(T_6/0.78)}{(2.33)T_5(\sin \alpha_0)v_{e0}} \quad (B.68)$$

$$s_{25} = \frac{X_{ffe0}(T_6/0.78)}{\omega_{e0}(2.33)T_5(\sin \alpha_0)v_{e0}} \quad (B.69)$$

$$s_{26} = \frac{(T_6/0.78)i'_{10} - i_{10}\sin(\delta_{e0}+\theta_{10})}{\omega_{e0}(2.33)T_5(\sin \alpha_0)v_{e0}} \quad (B.70)$$

$$s_{27} = \frac{i_{10}X_{mde0}\cos(\delta_{e0}+\theta_{10})}{\omega_{e0}(2.33)T_5(\sin \alpha_0)v_{e0}} \quad (B.71)$$

$$s_{28} = \frac{X_{mde0}\sin(\delta_{e0}+\theta_{10})}{\omega_{e0}(2.33)T_5 v_{e0}\sin \alpha_0} \quad (B.72)$$

$$s_{29} = (T_4/0.78)(C_1+2C_2(i_{fe0}-i_{de0}) + 3C_3(i_{fe0}-i_{de0})^2) \tag{B.73}$$

$$s_{30} = (C_1+2C_2(i_{fe0}-i_{de0}) + 3C_3(i_{fe0}-i_{de0})^2)\sin(\delta_{e0}+\theta_{10}) \tag{B.74}$$

$$s_{31} = (C_1+2C_2(i_{fe0}-i_{de0}) + 3C_3(i_{fe0}-i_{de0})^2)i_{10}\cos(\delta_{e0}+\theta_{10}) \tag{B.75}$$

where C_1 through C_3 are given in Table 3.2.

$$\omega_n^2 = \frac{R_e P_3 + P_5}{P_4 L_e} \tag{B.76}$$

$$2\zeta\omega_n = \frac{L_e P_3 + P_4 R_e + P_6}{P_4 L_e} \tag{B.77}$$

$$Z_o = \frac{P_1}{P_4 L_e} \tag{B.78}$$

$$N = s_1 - s_{30}s_4 - (s_2-s_{31}s_4)\frac{s_{20}}{s_{19}} + (s_3+s_{29}s_4)/s_{12} \tag{B.79}$$

$$P_1 = 1 + \frac{s_{24}s_{13}}{s_{12}} - \frac{((s_3+s_{29}s_4)(s_{13}/s_{12})(s_{24}/s_{12})}{N} \tag{B.80}$$

$$P_2 = \frac{s_{13}}{s_{12}}(s_{25}+s_{26}s_{29}) - \Big((s_{25}+s_{26}s_{29})/s_{12} + (s_{27}+s_{26}s_{31})\frac{s_{20}}{s_{19}} - (s_{28}+s_{26}s_{30})\Big)\Big((s_3+s_{29}s_4)\frac{s_{13}}{s_{12}}\Big)/(N) \tag{B.81}$$

$$P_3 = -s_{23} + (s_{24}/s_{12})(1 + (s_2-s_{31}s_4)(s_{22}/s_{19}))/(N) \tag{B.82}$$

$$P_4 = (s_{26}s_{31}+s_{27})\frac{s_{22}}{s_{19}} + \Big((s_{25}+s_{26}s_{29})/s_{12} + (s_{27}+s_{26}s_{31})\frac{s_{20}}{s_{19}} - (s_{28}+s_{26}s_{30})\Big)\Big(1 + (s_2-s_{31}s_4)\frac{s_{22}}{s_{19}}\Big)/(N) \qquad (B.83)$$

$$P_5 = \frac{(s_{24}/s_{12})(s_3+s_{29}s_4)(s_{14}/s_{12})}{(N)} - \frac{s_{24}s_{14}}{s_{12}} \qquad (B.84)$$

$$P_6 = \Big((s_{25}+s_{26}s_{29})/s_{12} + (s_{27}+s_{26}s_{31})\frac{s_{20}}{s_{19}} - (s_{28}+s_{26}s_{30})\Big) \cdot \Big((s_3+s_{29}s_4)\frac{s_{14}}{s_{12}}\Big)/(N) - \frac{s_{14}}{s_{12}}(s_{25}+s_{26}s_{29}) \qquad (B.85)$$

Variables with subscript 0 represent steady-state values and are obtained using the method of 3.3.1.

APPENDIX C

Data and Expressions Used in Chapter V

C.1 TABLES

TABLE C.1

Parameters for the Main Generator

X_{ag}	0.18	p.u.
R_{ag}	0.00448	p.u.
X_{mdg}	2.04	p.u.
X_{mqg}	1.64	p.u.
X_{kqg}	1.97	p.u.
X_{kdg}	2.1153	p.u.
R_{kdg}	0.0141	p.u.
R_{kqg}	0.00746	p.u.
R_{fg}	0.94×10^{-3}	p.u.
X_{ffg}	2.129	p.u.
V_g^b	26	KV
KVA[6]	907000	KVA
Field Resistance	0.0963Ω	@ 125C°
ω_{g0}	377.0	rad/sec
b_0	2.04	---
b_1	-0.34	---
b_2	1.665	---
b_3	-5.12	---
b_4	2.987	---
H	3.14	seconds

TABLE C.2

Parameters for Step-Test

λ_{fe0}	0.379	p.u.
λ_{kde0}	0.268	p.u.
λ_{kqe0}	-0.129	p.u.
λ_{fg0}	1.0505	p.u.
λ_{kdg0}	1.0	p.u.
λ_{kqg0}	0.0	p.u.
δ_{g0}	0.0	p.u.
$\dot{\delta}_{g0}$	0.0	rad/sec
v_7	-22.493	volts
v_{11}	-19.902	volts
v_{30}	-77.024	volts
v_{39}	-0.173×10^{-2}	volts
α_0	1.15304	rad
v_{e0}	0.29162	p.u.
v_{g0}	1.0	p.u.
i_{fg0}	0.57	p.u.
i_{fe0}	0.656	p.u.
i_{g0}	0.0	p.u.
i_{l0}	0.3081	p.u.
δ_{e0}	0.5881	rad
i_{kde0}	0.0	p.u.
i_{kdg0}	0.0	p.u.
v_{fe0}	0.5379×10^{-3}	p.u.

TABLE C.3

Parameters for Fault-Test

λ_{fe0}	0.5175	p.u.
λ_{kde0}	0.3654	p.u.
λ_{kqe0}	-0.1756	p.u.
λ_{fg0}	0.8877	p.u.
λ_{kdg0}	0.8186	p.u.
λ_{kqg0}	-05922	p.u.
δ_{g0}	0.8151	rad
$\dot{\delta}_{g0}$	0.0	rad/sec
v_7	-0.225×10^{2}	volts
v_{11}	-19.904	volts
v_{30}	-99.23	volts
v_{39}	0.0	volts
α_0	1.1534	rad
v_{e0}	0.3977	p.u.
v_{g0}	0.9998	p.u.
i_{fg0}	0.7772	p.u.
i_{fe0}	0.8946	p.u.
i_{g0}	0.4996	p.u.
i_{10}	0.42024	p.u.
δ_{e0}	0.5883	rad
i_{kde0}	0.0	p.u.
i_{kdg0}	0.0	p.u.
v_{fe0}	0.73339×10^{-3}	p.u.
X_∞	0.3	p.u.
v_∞	1.0	p.u.

C.2 Variables C_1 Through C_6 for the Auxiliary Equations Used in Chapter V

$$C_1 = v_{dg}\left(\frac{\omega_{g0}}{\omega_g}\right) + \frac{R_{ag}\left(\frac{\omega_{g0}}{\omega_g}\right)^2 v_{qg} - R_{ag}\left(\frac{\omega_{g0}}{\omega_g}\right)\frac{X_{mdg}}{X_{ffg}}\lambda_{fg}}{\left(-X_{dg} + \frac{X_{mdg}^2}{X_{ffg}}\right)} \quad (C.1)$$

$$C_2 = \frac{-R_{ag}^2\left(\frac{\omega_{g0}}{\omega_g}\right)^2}{-X_{dg} + \frac{X_{mdg}^2}{X_{ffg}}} + X_{qg} \quad (C.2)$$

$$C_3 = \frac{R_{ag}\left(\frac{\omega_{g0}}{\omega_g}\right)\left(X_{mdg} - \frac{X_{mdg}^2}{X_{ffg}}\right)}{\left(-X_{dg} + \frac{X_{mdg}^2}{X_{ffg}}\right)} \quad (C.3)$$

$$C_4 = \lambda_{kdg} - \frac{X_{mdg}}{X_{ffg}}\lambda_{fg} - \frac{\left(-X_{mdg} + \frac{X_{mdg}^2}{X_{ffg}}\right)\left(\frac{\omega_{g0}}{\omega_g}\right)v_{qg}}{\left(-X_{dg} + \frac{X_{mdg}^2}{X_{ffg}}\right)}$$

$$+ \frac{\left(-X_{mdg} + \frac{X_{mdg}^2}{X_{ffg}}\right)\frac{X_{mdg}}{X_{ffg}}\lambda_{fg}}{\left(-X_{dg} + \frac{X_{mdg}^2}{X_{ffg}}\right)} \quad (C.4)$$

$$C_5 = \frac{\left(-X_{mdg} + \frac{X_{mdg}^2}{X_{ffg}}\right) R_{ag} \left(\frac{\omega_{g0}}{\omega_g}\right)}{\left(-X_{dg} + \frac{X_{mdg}^2}{X_{ffg}}\right)} \qquad (C.5)$$

$$C_6 = \frac{\left(-X_{mdg} + \frac{X_{mdg}^2}{X_{ffg}}\right)^2}{\left(-X_{dg} + \frac{X_{mdg}^2}{X_{ffg}}\right)} + \left(X_{kdg} - \frac{X_{mdg}^2}{X_{ffg}}\right) \qquad (C.6)$$

REFERENCES

1. B. Adkins and R. G. Harley, "The General Theory of Alternating Current Machines," London: Chapman and Hall Ltd., 1975

2. P. M. Anderson and A. A. Fouad, "Power System Control and Stability," Iowa: The Iowa State University Press, 1977.

3. IEEE Committee Report, "Computer Representation of Excitation Systems," IEEE Transactions, PAS-87, 1968, pp. 1460-64.

4. Manual of the Alterrex Excitation Control System, General Electric Company.

5. S. B. Dewan and A. Straughen, "Power Semiconductor Circuits," New York: John Wiley, 1975.

6. A. E. Fitzgerald, C. Kingsley, Jr., and A. Kusko, "Electric Machinery," New York: McGraw-Hill, 1971.

7. A. S. Langsdorf, "Principles of Direct-Current Machines," New York: McGraw-Hill, 1959.

8. P. E. Gray and C. L. Searle, "Electronic Principles Physics, Models, and Circuits," New York: John Wiley, 1969.